Waste Resources Utilization as Stable Supports for Sintering Resistant CaO-Based Sorbents for Calcium Looping CO_2 Capture in Cement Industry

Ismail Salah Ahmed Mohamed

Thesis to obtain the Master of Science Degree in

Energy Engineering and Management

Supervisors: Dr. Paula Alexandra Lourenço Teixeira

Prof. Carla Isabel Costa Pinheiro

Examination Committee

Chairperson: Prof. Francisco Manuel da Silva Lemos

Supervisor: Dr. Paula Alexandra Lourenço Teixeira

Member of the Committee: Dr. Auguste Rodrigues Fernandes

November 2018

Abstract

Utilization of calcium looping technology in cement industry for CO_2 capture in aim to reduce the 6 % anthropogenic CO_2 emissions produced by cement plants is faced with a major drawback; sintering, which cause a decay in sorbent reactivity with increasing number of CO_2 capture cycles. This work aims to investigate the possibility of using waste-derived materials as a support for CaO sorbents which are utilized for CCS with the advantage of cost reduction and circular economy fulfillment by recycling spent sorbents as raw material for cement production.

In the scope of this research, a natural $CaCO_3$ was supported with coal fly ash (CFA) and spent fluid catalytic cracking catalyst (SFCC) using different mixing ratios. The CO_2 carrying capacity of sorbents was evaluated in a thermogravimetric analyzer, a fixed bed unit and by in-situ XRD. Sorbents went under three calcination atmospheres and a CO_2 content of 25 % during carbonation. Fresh and used sorbents were characterized by N_2 adsorption, SEM, and XRD to determine their textural and morphological properties and mineralogical composition.

Results obtained showed that addition of CFA and SFCC to natural $CaCO_3$ improved its CaO conversion by reducing particles agglomeration and maintaining available surface area, also showing that among tested mixing ratios, the blends with 90 % of CaO had the highest CO_2 capture capacity. CO_2 calcination atmosphere proved to have an adverse effect on sorbent capture capacity by increasing sintering, while steam addition proved to enhance carrying capacity by improving product layer diffusion.

Keywords: Calcium looping, CO_2 capture, CaO conversion , sintering, waste-derived supports, fixed bed

Resumo

A indústria cimenteira emite 6% do CO_2 de origem antropogénica, a incorporação do Ciclo do Cálcio nesta indústria pretende reduzir estas emissões. Contudo esta tecnologia depara-se com um obstáculo, a sinterização que é responsável pela perda de reatividade dos adsorventes com o aumento do número de ciclos. Este trabalho investiga a utilização de materiais derivados de resíduos, como suporte de adsorventes a base de CaO, com a vantagem da redução dos custos e enquadramento no conceito de economia circular, através da reutilização de adsorventes usados como matérias primas para a produção de cimento.

No âmbito desta investigação, um $CaCO_3$ natural foi suportado com diferentes quantidades de cinzas volantes de carvão (CFA) e catalisadores usados de fluid catalytic cracking (SFCC). A capacidade de captura do CO_2 pelos adsorventes foi testada num analisador termogravimetrico, uma unidade de leito fixo, e por XRD in-situ. Efetuaram-se ensaios de captura em três atmosferas de calcinação e com 25% de CO2 durante a carbonatação. Os adsorventes frescos e usados foram caracterizados por adsorção de N2, SEM e XRD, de modo a determinar as suas propriedades texturais, morfológicas e a composição mineralógica.

Os resultados obtidos mostraram que a adição de CFA e SFCC ao $CaCO_3$ natural melhorou a conversão do CaO, reduzindo a aglomeração de partículas e mantendo a área superficial disponível. Além disso, mostrou que a mistura com 90 % de CaO foi a que apresentou maior capacidade de captura. A calcinação em atmosfera de CO_2 mostrou ter um efeito adverso na capacidade de captura do adsorvente devido ao aumento da sinterização, enquanto que a adição de vapor melhorou a capacidade de captura devido a alterações na camada de difusão do produto.

Keywords: Ciclo do cálcio, captura de CO_2, conversão de CaO, sinterização, suportes derivados de resíduos, leito fixo

Table of Contents

List of figures

List of Tables

List of Abbreviations

CCS	Carbon Capture and Storage
CFA	Coal Fly Ash
CFB	Circulating Fluidized Bed
GHG	Greenhouse Gases
SEM	Scanning Electron Microscopy
SFCC	Spent Fluid Catalytic Cracking catalyst
TGA	Thermogravimetric Analysis
WMP	Waste Marble Powder
XRD	X-Ray Powder Diffraction

1. INTRODUCTION

In a fast population propagation world, the energy demand is vastly increasing to meet the economical and living quality development. Such increasing demand was coped with an increase in consumption of conventional sources of energy, i.e. coal, petroleum, and natural gas (Figure 1.1). Extensive consumption of these conventional fuels led to fast growth in Greenhouse Gases (GHG) emissions with its effect being observed in the climate change including increase in frequency of floods, droughts, hurricanes, melting of ice glaciers, and increasing sea water level. Specifically, anthropogenic CO_2 emissions majorly generated from the combustion of fossil fuels, cement and steel industries was found to be related to the increase in the globe surface mean temperature. Reduction of greenhouse gases (GHG) emissions has been a major concern for scientists, researchers, and even policy makers in the developed countries.

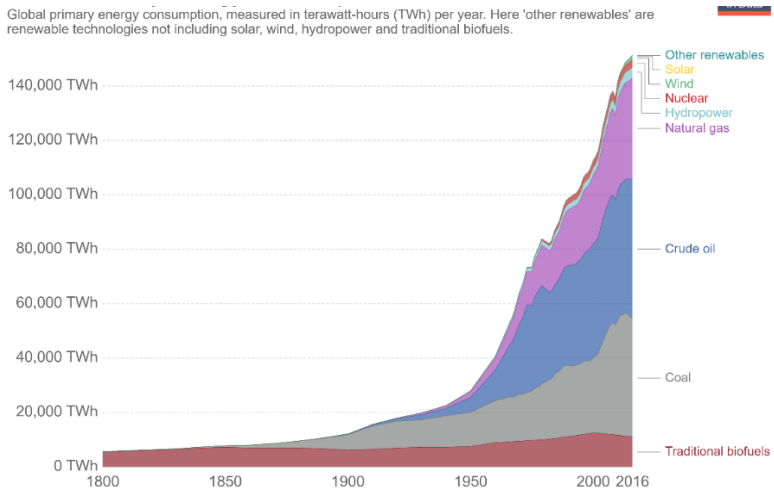

Figure 1.1: Global Primary Energy Consumption, World [1]

An early awareness of the hazardous nature of the GHG emissions and its subsequent climate change effect led to the Kyoto protocol treaty signed in 1997 in connection with the United Nations Framework Convention on Climate Change (UNFCCC), in which its parties were obliged by setting internationally binding emission reduction targets, heavier burden was placed on developed countries as they were recognized to be basically responsible for the current higher levels of GHG [2]. The protocol has three mechanisms, which are international emissions trading, clean development mechanism (CDM), and joint implementation (JI) intended to achieve the objective of reducing six GHG emissions; Carbon dioxide (CO_2), Methane (CH_4), Nitrous oxide (N_2O), Hydrofluorocarbons (HFCs), Perfluorocarbons (PFCs), and Sulphur hexafluoride (SF_6) [3]. A new climate agreement referred to as the Paris Agreement was implemented in 2016 after 55 countries responsible for 55 % of GHG emissions met the conditions for ratification previously agreed on Doha amendment in 2015 [4]. The main aim of the Paris agreement was a long-term goal to maintain the increase of the global average temperature to well below 2 °C, with also countries providing their plans for a national climate actions for emissions reduction and confirming to report progressive implement of their targets [5].

On the climate change report some figures concerning the consequences of elevated GHG emissions were presented (Figure 1.2), where it has been observed that with rapid growth in global anthropogenic CO_2 emissions, accounted for fossil fuels combustion, cement industry and flaring, the average land and ocean surface temperature rose and the precipitation over the mid-latitude of northern hemisphere has increased, salinity increase in high saline regions due to evaporation and oppositely low salinity regions become fresher due to precipitation. Average sea level has rose by about 20 cm compared to 1900 level, due to loss in mass of ice in Greenland arctic sea-ice, as well as Antarctic ice sheets, also this rapid growth of CO_2 emissions was manifested in its high levels of concentration compared to other GHG [6].

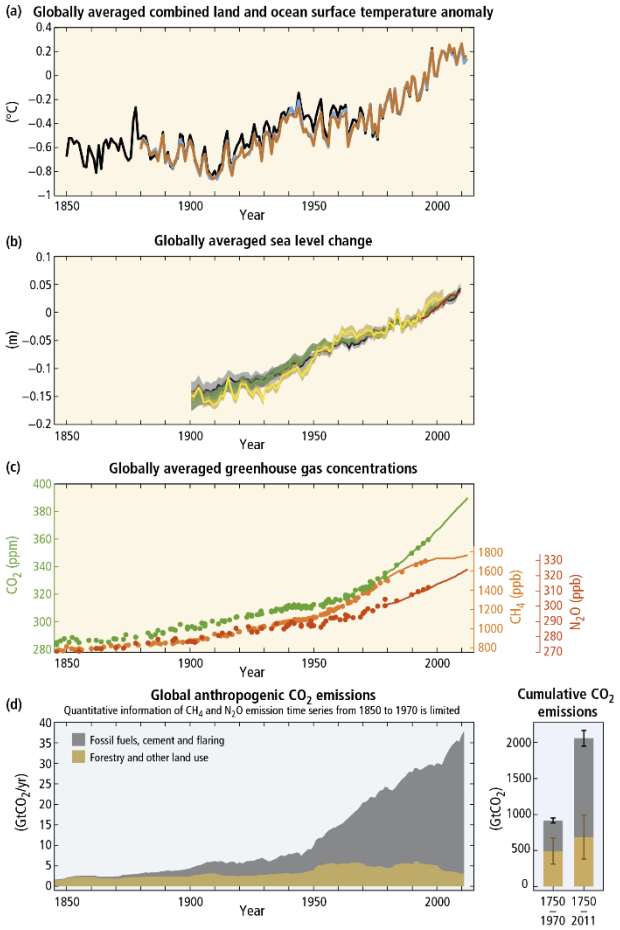

Figure 1.2: Complex relation between observations (a, b, c) and emissions (d) [6]

CO_2 emissions was the primary focus when it comes to GHG emissions mitigation concerns, not because of its global warming potential (GWP) (it measures the relative warming impact of one unit mass of a greenhouse gas relative to CO_2) when compared with other gases emissions since it has a lower value (Figure 1.3), yet because of the extensive production rate of CO_2 gas (Figure 1.4) as its emission is accounted for 76 % of global greenhouse gases emissions, which include 65 % CO_2 emissions from fossil fuels and industrial processes, and the rest is from forestry and land use [7].

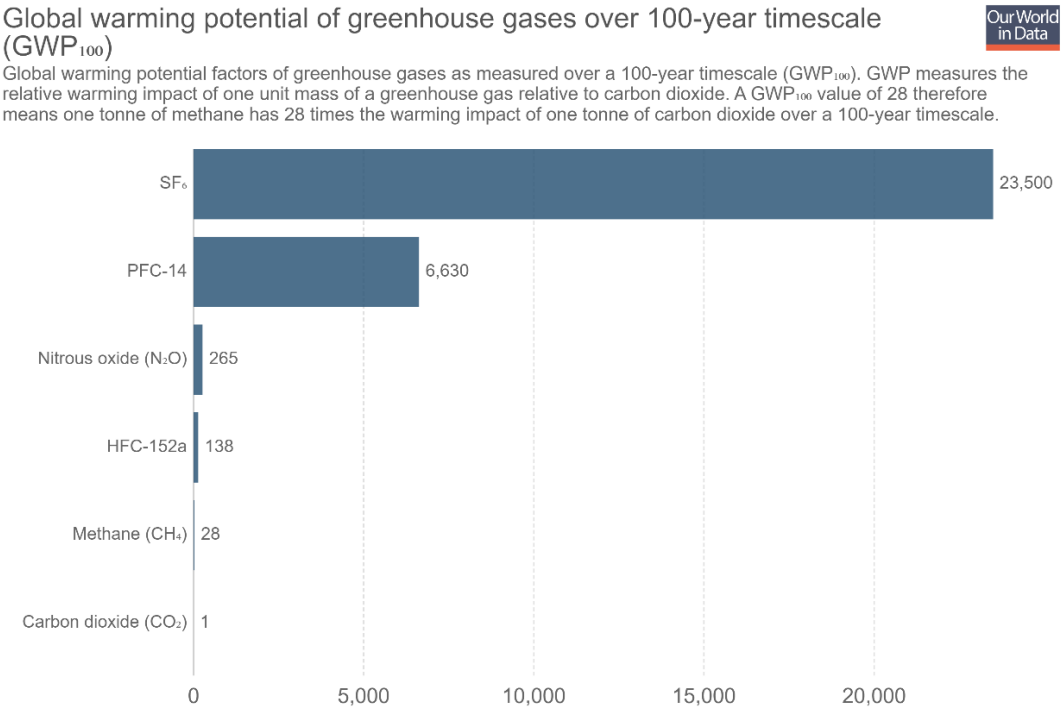

Figure 1.3: Global warming potential of greenhouse gases over 100-year timescale (GWP_{100}) [8]

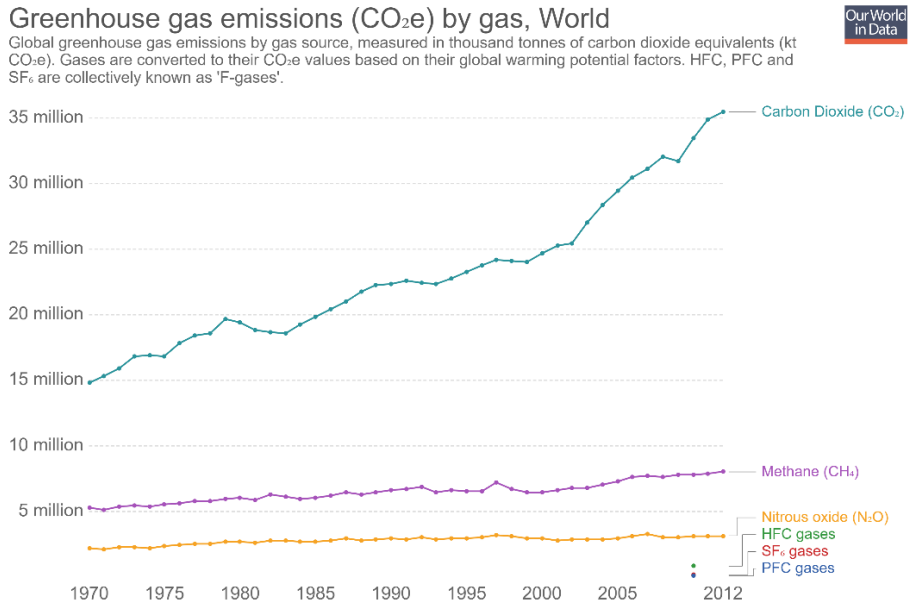

Figure 1.4: Greenhouse gas emissions (x1000 ton.CO_2e) by gas [8]

Research studies had focused on the development of methods that primarily aiming for CO_2 emissions reduction. Substantially, these technologies aim for more sustainable and renewable energy production, it focused mainly on three technology development aspects that was targeted for stationary CO_2 emissions sources, i.e. power and industry sectors, which are responsible for about 60 % of the total CO_2 emissions [9]; first was the transition to the clean renewable energy (solar and wind) with its zero CO_2 emission (generation-wise), second aspect was reducing the energy consumption by increasing of energy efficiency which can be achieved by improving production process, third aspect was

implementation of carbon capture and storage (CCS) technologies which represent a last line of defense for CO_2 emissions reduction by CO_2 capture. Additional two methods that has possibility for emissions reduction were also discussed, first one can be exemplified by switching to lower carbon content fuels (coal to natural gas or biomass) typically in transport and industry sectors, and the second method is the increase of production of nuclear energy yet putting into account it's hazardous nature and nuclear waste disposal difficulties. Figure 1.5 summarize the aggregate CO_2 reduction shares accounted by different technologies for varies energy sectors.

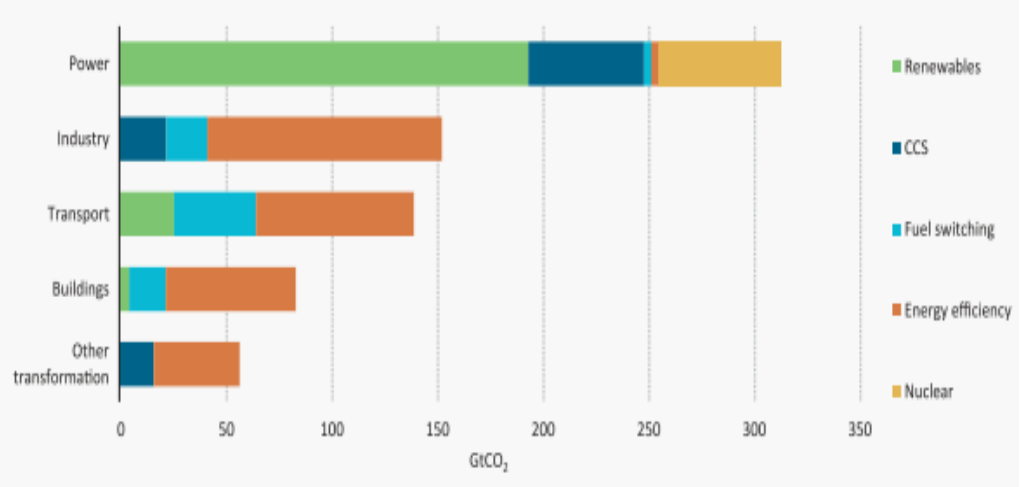

Figure 1.5: Cumulative CO_2 reduction shares by sector and technology to 2050 [10]

1.1 CARBON CAPTURE AND STORAGE TECHNOLOGIES

CCS appears to be a key technology for decarbonization suitable for stationary power and industrial plants, since it can be installed in new plants and the possibility of integration into existing plants through retrofitting. Basically, CCS process can be divided into three steps; separation and capture, transportation, and storage. CCS is considered as a very expensive and energy intensive technology, However, separation and capture process is deemed to be the most expensive as it's accounted for 70 - 90 % of CCS total cost and can reduce the net capacity of an electricity power-plant for instance by 20 % [11]. Fundamentally, CCS technologies has variety of types that has categorized in three main implementation approaches (Figure 1.6); Pre-combustion CO_2 capture where emission producing element are separated before fuel combustion, Oxy-fuel combustion in which pure oxygen is only used for combustion process, and Post-combustion CO_2 capture in which GHG are captured from the flue gases before release to the atmosphere.

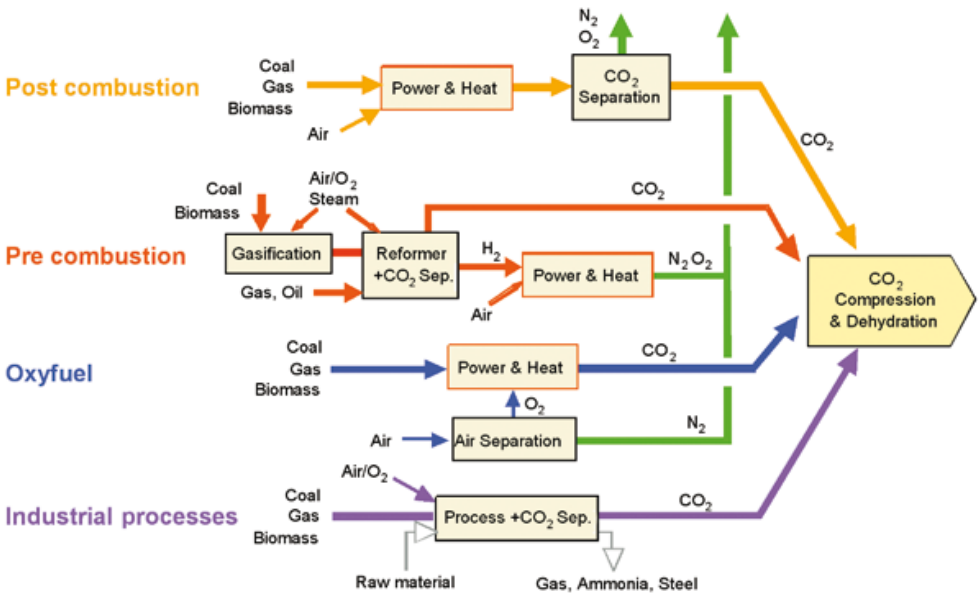

Figure 1.6: Types of CCS technologies [12]

1.1.1 Pre-combustion CO_2 capture technology

Pre-combustion CO_2 capture process focuses on the reformation of primary fuels into syngas which is a mixture of hydrogen and carbon monoxide by one of two methods: steam reforming (Eq. 1.1) where a stream of steam is added, and oxygen reforming (Eq. 1.2) which is also called 'partial oxidation' when using gaseous or liquid fuels, or 'gasification' when applied on solid fuels [12].

$$C_xH_y + xH_2O = xCO + \left(x + \frac{y}{2}\right)H_2 \quad \text{(Eq. 1.1)}$$

$$C_xH_y + \frac{x}{2}O_2 = xCO + \frac{y}{2}H_2 \quad \text{(Eq. 1.2)}$$

$$CO + H_2O = CO_2 + H_2 \quad \text{(Eq. 1.3)}$$

Using a water-gas shift reaction CO is converted into CO_2 through steam addition, resulting in a mixture of H_2 and CO_2 (Eq. 1.3). Afterwards CO_2 is separated, compressed, and transported to storage location while H_2 is combusted for electricity generation. (Figure 1.7) illustrates the steps of CO_2 production and capture process, where it's only to be explained that gas supply can either be air or oxygen. The pre-combustion process has same principle for all fuel type, however, an additional gas purification steps are required when using coal or oil feeds to remove ash, sulfur compounds, and other impurities.

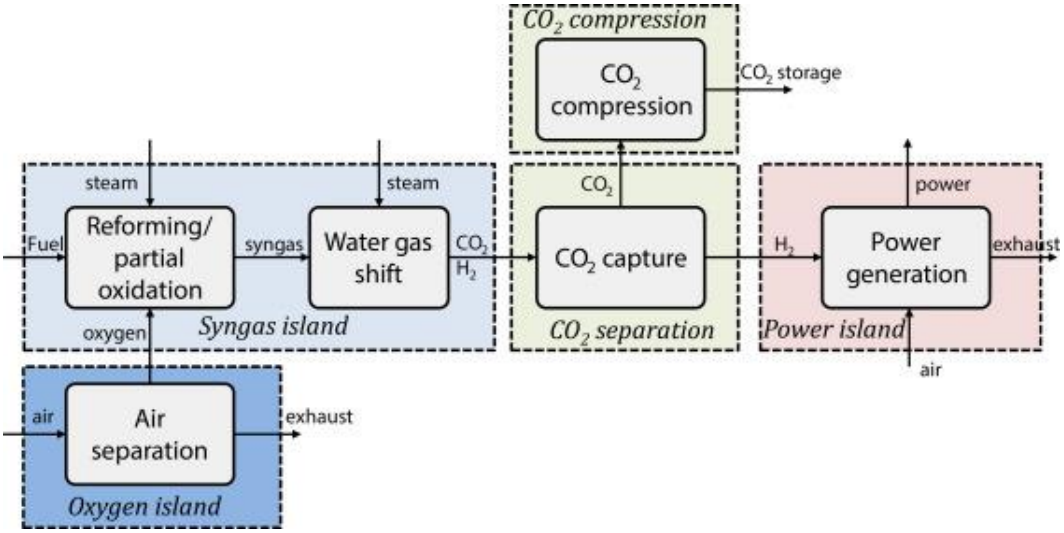

Figure 1.7: Schematic of Pre-combustion CO_2 capture [13]

1.1.2 Oxy-fuel combustion CO_2 capture technology

In oxy-fuel combustion the oxygen is separated from air prior to combustion process through an air separation unit (ASU), Oxygen can be used as pure component for combustion or it may be diluted in CO_2-rich recycled flue gas. This method aims to eliminate the presence of N_2 in the flue gas and subsequently prevent formation of prompt NO_x. Flue gas from oxy-fuel combustion mainly consist of water vapor (H_2O), carbon dioxide (CO_2), and the excess O_2 that didn't react which was supplied to ensure complete combustion of fuel. Figure 1.8 shows a simplified illustration of the oxy-fuel combustion for carbon capture.

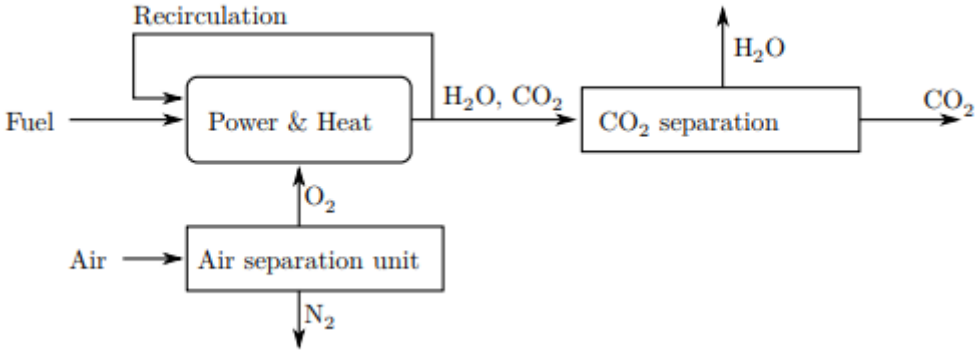

Figure 1.8: Schematic of oxy-fuel combustion CO_2 capture [14]

1.1.3 Post-combustion CO_2 capture technology

Post-combustion CO_2 capture technology focus on removing CO_2 emissions from flue gas stream, no changes to the combustion process is needed as capture process is regarded to the flue gas. This technology can be installed to new power and cement plants as well as retrofitting into old plants.

Post-combustion is believed to have the capacity for CO_2 emission cut in the future from stationary power and industrial plants. It has a wide range of technologies with different applicability and selectivity. As shown in Figure 1.9, such technologies have been divided into four groups; capture by absorption,

adsorption, cryogenic, and membranes. This sub-section would be concerned with describing some of these technologies that can be applied for CO_2 capture.

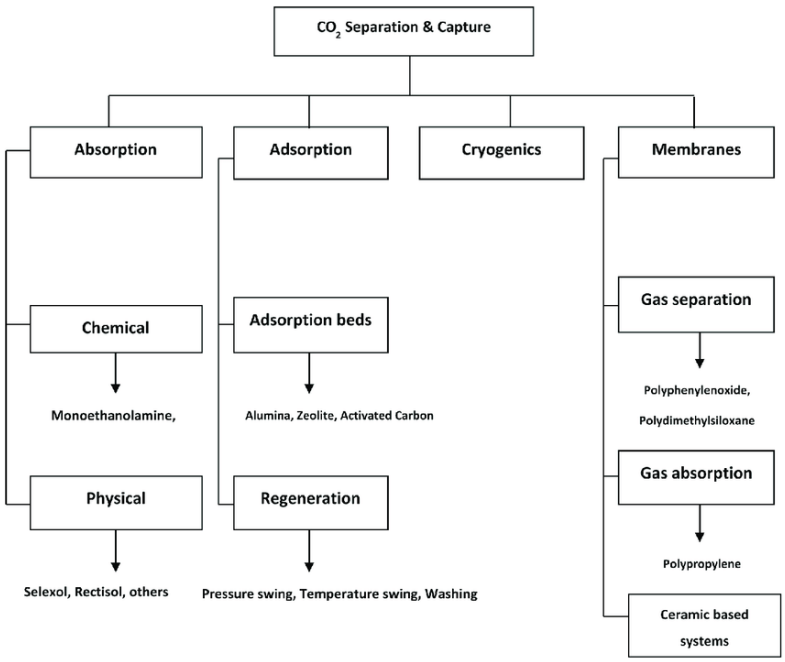

Figure 1.9: Post-combustion carbon capture technologies [15]

Absorption of CO_2 can be achieved through two methods: chemical or physical. In the chemical method an alkaline aqueous solvent, e.g. MEA (monoethanolamine), is exploited for its reversible nature of chemical reaction. Cooled flue gas is brought into contact with the solvent that has a selectivity for CO_2, then flue gas would undergo water wash to remove solvent droplets [12]. This solvent has high absorption capacity and operates at low pressures; however, it requires high energy supply for regeneration and large supply volume of absorber. Physical absorption uses solvents to absorb the targeted gas, and then it would be released through a pressure and/or temperature swing, selexol and rectisol are examples for used solvents. Physical absorption is characterized by low energy consumption, but it is reckoned for having low absorption capacity [16].

Membranes represent a good separation process when gas flow at high pressure and concentration, but on the flue gas stream the CO_2 has low partial pressure and such requires improving the membranes selectivity, as the principal of membranes is to profit from the pressure difference between membrane sides (Figure 1.10). It's yet to be developed technology to achieve the minimum capture capacity and purity of CO_2 required from a capture technology.

Cryogenic offers a wide range of pollutant removal beside CO_2 capture like hg, SO_x, NO_2, and HCl. It works by cooling down the flue gas stream to desublimation temperature (-100 to -135 °C) at which CO_2 solidifies then it's separated from light gases after which CO_2 is compressed to final pressures (100-200 atm). Cryogenic CO_2 capture is believed to lower the energy and cost expenses invested in other capture technologies involving ASU and solvents by 30 %, beside its potential of cooling water saving where processed gases can be used to cool the flue gases stream through a heat exchanger, and possible energy storage in form of pressurized gaseous stream [17].

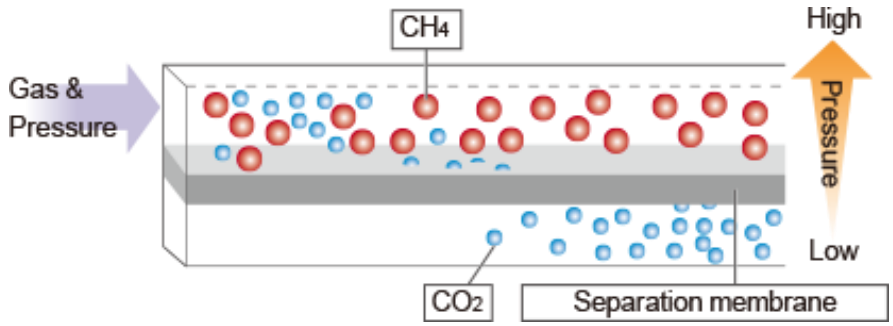

Figure 1.10: Gas separation membrane [18]

Adsorption separation is accomplished by physical or chemical method, just like absorption. In physical method pressure swing adsorption (PSA) and temperature swing adsorption (TSA) can be used where it benefits from solid sorbent's (e.g. molecular sieves and active carbons) ability to adsorb a gas by change in pressure and temperature, respectively. TSA attracts less attention as longer cycle times arising from the slow process of increasing and decreasing sorbent's temperature is adhered to this technology when compared to PSA. Chemical adsorption is characterized by its stronger bonds between adsorbate and adsorbent and more selective towards adsorbed gases.

1.2 MOTIVATION AND RESEARCH OBJECTIVES

CaO-based sorbents are visualized as promising technology for CO_2 emissions capture, due to the high carrying capacity provided by natural sorbents like limestone, dolomites, and WMP, as well as their abundant resources in nature. Both features make it possible to achieve the low-cost aim of CCS technologies development. Major drawback that has been the center of research studies is the reactivity decay of the sorbents carrying capacity along repetitive calcination and carbonation cycles.

Natural calcium carbonate is an important entry in cement production, and the process of calcinating the $CaCO_3$ to produce CaO in kilns is accounted for 60 % of CO_2 produced from cement plant, this opens the opportunity to use such CaO to capture plant emitted CO_2 to achieve a targeted circular economy. One of the enhancement methods to sorbents performance being investigated is the utilization of waste material as structural support and sintering inhibitor, which is also used in cement production. This thesis aims to test the effect of using wastes as a support on a local natural CaO-based sorbent for CO_2 capture by calcium Looping process.

The objectives targeted for this work are the following:

- Test the change in carrying capacity of sorbent when using different mixing ratios of CaO/waste support
- Test the effect of using three CaO precursor (natural and commercial sorbents) and two types of wastes-derived materials (CFA and SFCC)
- Test the sorbent's performance under application of different supporting methods (dry mixing and wet impregnation)
- Test the behavior of the sorbent under different atmospheres, by changes in both pre-calcination atmosphere (sorbent activation) and calcination-carbonation atmosphere and under steam atmosphere

2. LITERATURE REVIEW

This chapter will mainly discuss calcium looping technology for power and industrial plants CO_2 capture, as it present a promising potential applicability in cement industry which is deemed for 6 % of the total CO_2 emission from stationary sources [12]. Along with issues that represent a barrier to implementation of calcium looping.

2.1 CALCIUM LOOPING FOR CO_2 CAPTURE CYCLE

Calcium looping is considered as a chemical adsorption method, it is regarded as one of the promising CCS methods due to many reasons; 1) high carrying capacity that allows to capture CO_2 from large emitting plants as it can be implemented to power plants and cement and steel industrial plants, 2) abundance of calcium looping precursors in nature like limestone and dolomites, and 3) cost cut-off key feature that is sought after in CCS technology development due to its capacity and regenerative possibility and natural availability.

Chemical looping method uses a metal oxide to transfer O_2 from air to fuel. In more specific case calcium looping is used to capture CO_2 from the flue gas with a calcium-based sorbent (CaO) in a reactor known as the carbonator and then reaction is reversed in another reactor called the calciner in which a pure CO_2 stream is produced [19], Figure 2.1 shows the calcination and carbonation cycle for CO_2 capture.

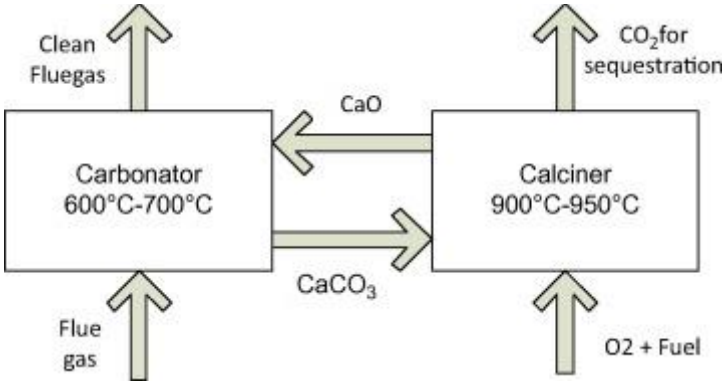

Figure 2.1: Calcium looping calcination-carbonation cycle [20]

The calcination reaction (Eq. 2.1) at the calciner occurs at a temperature around 900 °C and $CaCO_3$ is decomposed releasing CO_2 captured by the CaO which would be recycled to the carbonator, this regeneration reaction is endothermic. The atmosphere of calcination is a key aspect due the fact that for efficient compression and sequestration the CO_2 purity should be higher than 99 %, therefore calcination atmosphere should be a pure CO_2 or easy separable gas mixture with CO_2. Another reason is that temperature and atmosphere of calcination affect the sorbent morphology, i.e. specific surface area, total pore volume and structure where lower temperature and partial pressure are preferable to keep sorbent's reactivity, however, reaction condition should be maintained in a way for reaction to take place.

$$CaCO_{3_{(s)}} \rightarrow CaO_{(s)} + CO_{2_{(g)}} \qquad \Delta H_{900°C,1\,bar} = +165\ \frac{KJ}{mol} \qquad \text{(Eq. 2.1)}$$

The carbonation reaction (Eq. 2.2) is an exothermic reaction which occurs at temperature between 650 °C - 700 °C, where CO_2 is captured by CaO sorbent to form $CaCO_3$ which in return is sent back to the calciner, and the cycle is continued. Carbonation reaction occurs in two stages (Figure 2.2), a fast controlled stage that is dominant in the early cycles, and a slow diffusion limited stage which dominates after many cycle, due to loss of reactivity by pore blockage which increase time of CO_2 diffusion through $CaCO_3$ particles formed previously in the first stage.

$$CaO_{(s)} + CO_{2_{(g)}} \rightarrow CaCO_{3_{(s)}} \qquad \Delta H_{700°C,1\,bar} = -170\ \frac{KJ}{mol} \qquad \text{(Eq. 2.2)}$$

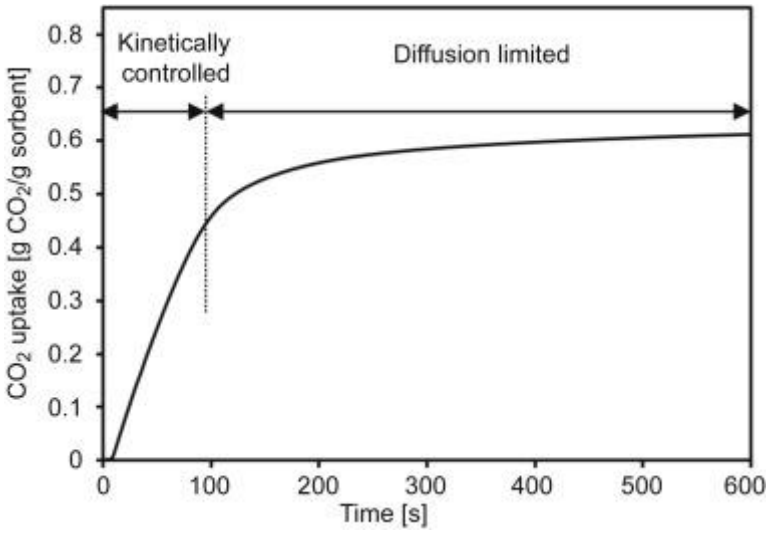

Figure 2.2: carbonation reaction stages [21]

The calcination and carbonation reaction are both dependent on temperature, and it is to be noticed that temperature is related to the carbon dioxide vapor pressure, Figure 2.3 shows the relation between CO_2 vapor pressure and temperature. It brings attention to the importance of the reaction atmosphere especially when it goes towards calcination reaction, dependence of temperature on the CO_2 pressure was described by the following equation [22]:

$$log_{10} P_{eq}(atm) = 7.079 - \frac{8308}{T\,(K)} \qquad \text{(Eq. 2.3)}$$

Carbonation reaction can be conducted in such lower temperature (600 °C-700 °C) with relatively low CO_2 partial pressure which corresponds to their percentage in the flue gas (e.g. 25 % in cement industry) as shown in figure below, while to force calcination reaction especially in pure CO_2 atmosphere, reaction temperature should be above 900 °C.

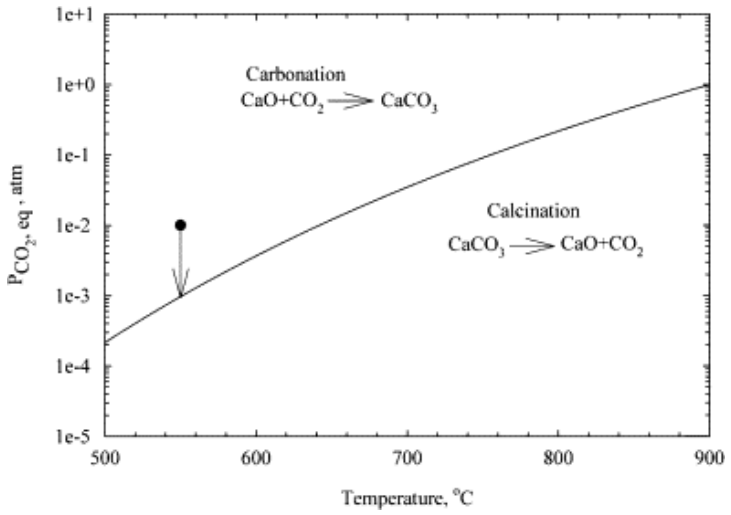

Figure 2.3: Equilibrium partial pressure of CO_2 from $CaCO_3$ decomposition [23]

2.2 CALCIUM LOOPING SORBENTS

Sorbents used for calcium looping can be natural, which assure the cost-effective feature required from a sorbent or a synthetic sorbent which achieve performance enhancement feature. Disregarding which type is used, there are key features that sorbents should fulfill to be considered as efficient and good candidate for large scale applications. The first property is sorbent's capture capacity which is an intrinsic property of a sorbent as it defines the amount of sorbent needed for capture process. Second, sorbent should have higher selectivity towards capturing CO_2, sometimes sorbents get poisoned by sulphur content of flue gas or fly ash which may affect selectivity and reactivity. This poisoning problem affects sorbent's effective regeneration process, where through regeneration sorbent reactivate to restore capture capacity, degradation surely reduces capacity and thus sorbent's life which requires a more frequent change of sorbent, and consequently increase expenses. On top of that sorbents should maintain mechanical resistance towards attrition as well as thermal stability along the cycles due to fact that in industrial application sorbent's calcination and carbonation reaction would be conducted in two separated reactors that requires shifting sorbents between them, unlike experimental testing where sorbents are tested in TGA, fixed bed, or fluidized bed.

Natural sorbents like limestone ($CaCO_3$), dolomite ($CaMg(CO_3)_2$) and waste marble powder (WMP) excel in carrying capacity property, also they are the best candidates since they are abundant and cheap. Implementing them in cement industry drew valued benefits as after using them as CO_2 capture sorbents, they can be recycled as limestone and dolomite represent raw material for cement production. Natural sorbent fails in maintaining their attrition resistance due to their fragile structure and repetitive exposure to high temperature of calcination, and this has been a research hotspot in chasing after exploring methods to overcome such drawbacks.

On the other hand, synthetic sorbents present better performance over cycles as they have altered structure and thermal resistance. different materials were utilized through impregnation to provide a stable framework that would work as structure support and thus inhibits sintering of CaO like calcium

aluminate and titanium ethoxide. Also, sol-gel technique applied in combining an inorganic active material and organic template revealed promising results, were a CaO-based sorbent was supported by Al_2O_3 using carbon-gel template to synthesize a micro and nanostructure that had around 85 % CaO conversion after 30 cycles [24], another study [25] using a sol-gel prepared sorbent reported a conversion around 74 %. Although synthetic sorbents provide more reactive and sintering resistant sorbent, the main issue is that they are still expensive compared to natural sorbents.

2.2.1 Performance and decay of sorbents

Major problem that halts the breakthrough of calcium looping technology is sorbent's sintering which is presented as the factor that drive sorbent's performance down and accounted for decay of sorbent along the calcination-carbonation cycles. Sintering is caused by high temperature and presence of impurities in reaction atmosphere, as of fragile structure attributed for unsupported CaO-based sorbent high temperature heating leads to loss of morphology as the sorbent melts and grain growth takes place.

Sintering can occur during both calcination and carbonation stages, mainly the rate of deactivation increases during calcination at higher temperature and a bimodal pore size distribution is created, from small pores that appear from CO_2 release and bigger pores from surface energy minimization [20]. Reactivity decay occurrence during carbonation rises from the closure of small pores due to carbonate formation that fails to reopen subsequently by calcination [26].

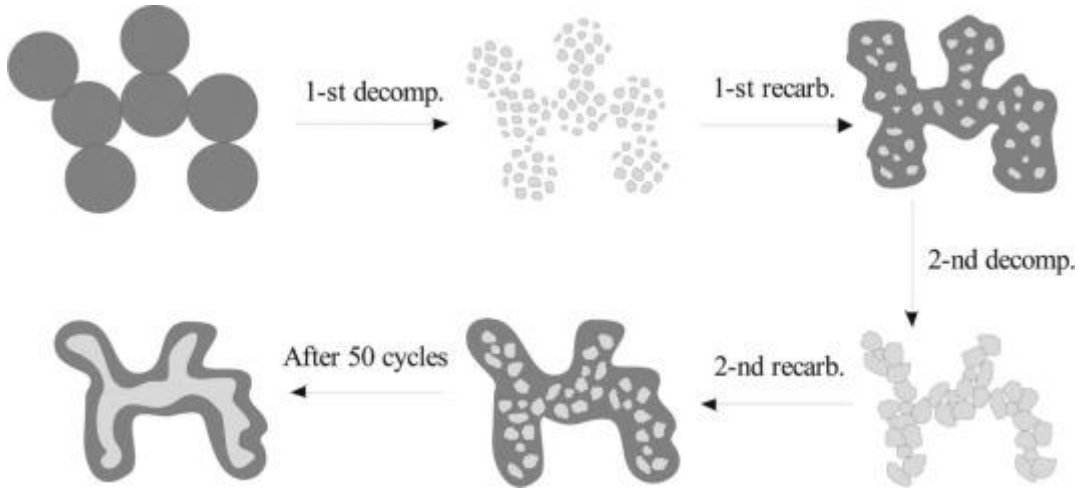

Figure 2.4: Schematic of CaO-based sorbent transformation over calcination-carbonation cycles [27]

The structural transformation of the sorbent along calcination-carbonation cycles is illustrated by (Figure 2.4), after first decomposition a highly porous and reactive CaO is created, followed by a re-carbonation that is not fully complete due to pores loss from blockage of grain growth due to carbonate formation. As the cycles continue the pore blockage increases leading to loss of surface area and more isolated pores and thus decay in the sorbent reactivity. This process continues along large number of cycles ending in a poor reactive sorbent recovery.

Several explanations can be drawn from Figure 2.5, it depicts the decay that occur to the sorbent along 50 cycles, this shows the severe effect of sintering that after about 25 cycles sorbents were only able

to capture less than 10 % of its total weight, compared to around 30 % on the first cycle, this is a typical performance of an unsupported natural sorbent. Kinetics of sorbent's reaction is an important factor in determining sorbent carrying capacity. Basically, as referred in section 2.1, carbonation reaction takes place through two stages: first, a fast carbonation stage, a kinetically controlled reaction in which CO_2 reacts with CaO exposed surface, formation of higher particle size $CaCO_3$ leads to pore blockage before total carbonation of all CaO this why even on first cycle weight retrieval wasn't achieved. A second stage with a slow carbonation, which is also known as diffusion limited reaction where newly formed layer of $CaCO_3$ block behind pores with CaO that CO_2 has to diffuse through smaller pores to reach there, this stage is normally require longer times and has lower contribution to CaO conversion, around 76 % of CaO conversion is accounted for first carbonation stage while second carbonation stage can raise CaO conversion to about 96 % [28] . Moving along cycles shows that now the second stage carbonation starts even earlier as it's a sign for sintering.

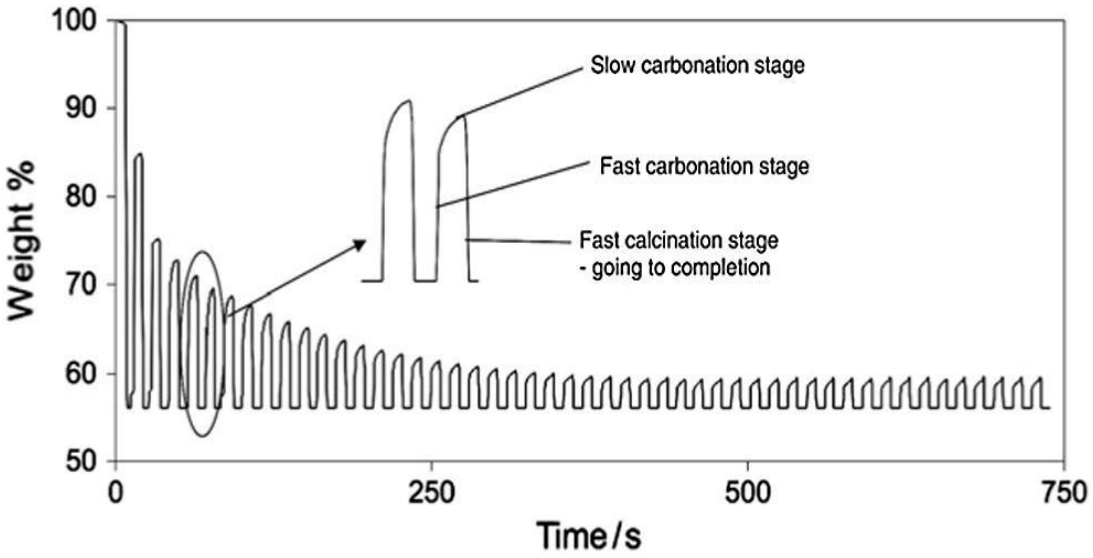

Figure 2.5:CaO carrying capacity along calcination-carbonation time [20]

Attrition is the accumulated fragmentation of the particles due to overburden of thermal and mechanical stresses, thermal stress causes the primary fragmentation that occurs during calcination reaction and affected by over-pressure induced by CO_2 release. Mechanical stress is due to interaction between particles and reactor in fluidized bed for instance. Factors like gas velocity, size and configuration of the plants are fundamental to attrition. Normally, attrition is considered an investigation must when it comes to exploring new sorbents, also in application on CO_2 capture in pilot scale plants.

2.2.2 Enhancement on sorbent's performance and atmosphere effect

Researchers started working in new methods for preparing sorbents or apply some modification to natural sorbents that would eventually lead to higher and long-lasting carrying capacity. Improvements on the sorbent's surface area and pores availability were the major focus. Enhanced sorbents techniques present a midpoint solution between natural sorbent with their reactivity decay challenges and adaptation of complex methods for synthetic sorbents preparation which is attributed to be

comparatively costly. Enhancement techniques include thermal pretreatment, reactivation by hydration, doping and other methods.

Reactivation of sorbents by hydration can be applied to both fresh sorbents as pre-treatment and spent sorbents as a way for periodically improving of sorbent reactivity, it can be achieved by using water, water vapor, or steam. However, it requires addition of a third vessel for hydration process as the partial pressure operating in calciner and carbonator doesn't allow the hydration to occur (Figure 2.6). A study showed that after 15 cycles the capture capacity of a limestone reduced by about 32 %, however, after hydration (Figure 2.7) the sorbent retained around 53 % of capture capacity under the following 15 calcination-carbonation cycles [29]. Use of hydration as a pre-treatment can be considered as using a new sorbent, where in this case Calcium Hydroxide ($Ca(OH)_2$) is the sorbent. A study proved that this treated sorbent improved the CaO conversion by 52 % after 20 cycle [30], yet calcium hydroxide is deemed to be extremely fragile and is not suited for fluidized bed applications.

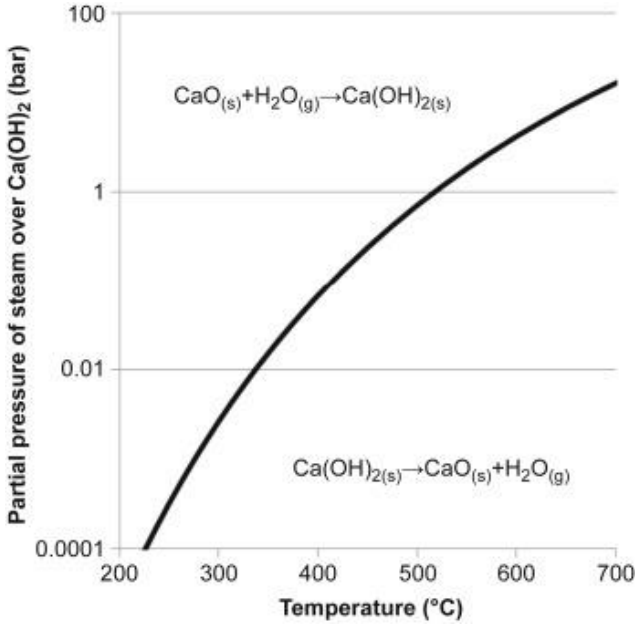

Figure 2.6: equilibrium vapor pressure of steam over $Ca(OH)_2$ vs temperature [31]

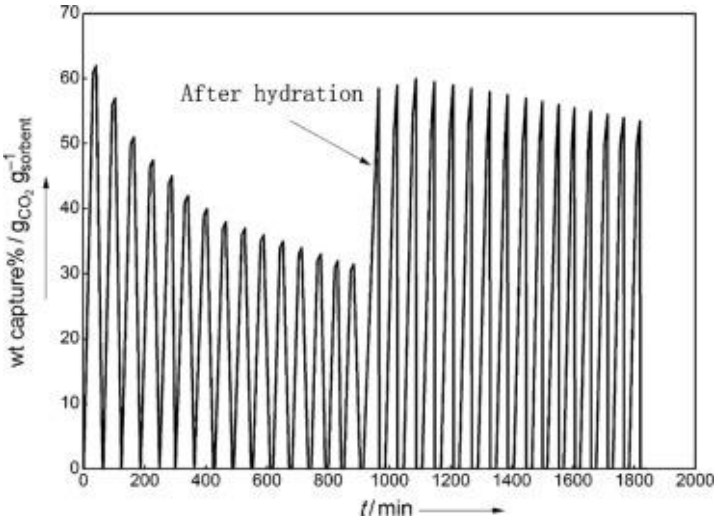

Figure 2.7: hydration effect on decay rate of CO_2 carrying capacity of CaO sorbent [20]

Grinding and repalletizing is presented as reactivation method, this method involves utilization of water for pellets binding. Increased porosity and exposure of inner core CaO to the surface, as well as use of water to increase hydration was discussed before as a factor of increasing carrying capacity, these are considered a double benefit of this reactivation technique. It has also been investigated in a study of using limestone reactivation by palletization for SO_2 capture that wet binding excel on dry binding by 20 % - 30 % of required energy saving, however, formation of cementitious materials is considered problematic as it's prone to solidification [32]. In an investigation of repalletization effect on CO_2 capture, a study used a mixture of calcined limestone and 10 % calcium aluminate cement as a binder, formed pellets were cycled for 300 cycles at 850 °C under 100 % CO_2 calcination and 100 % N_2 carbonation then removed for grinding, mixed with water, and forming further pellets, TGA tests on these spent sorbent showed a similar results of 33 % - 34 % CaO conversion after 30 cycles when compared to fresh pellets [33]. On a second study presented by the same authors, material from a pilot-scale dual-fluidized bed were pelletized in three pellets type; 1) with no cement binder, 2) with 10 % calcium aluminate cement, 3) cement-free core with a cement-containing mixture. Results comparison showed an improvement for treated sorbents over the spent sorbent (Figure 2.8), yet not the same conversion expressed by fresh limestone due to sulphation during cycles [34].

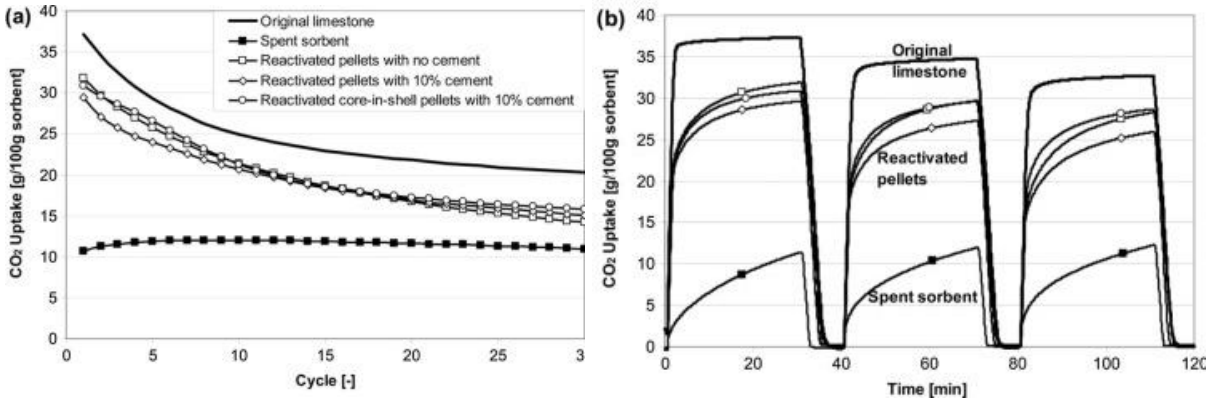

Figure 2.8: (a) CO_2 capture capacity during 30 cycles and (b) conversion profiles during the first three cycles [34]

Doping materials were used by researcher to reduce the rate of sorbent decay. A wide range of dopants which are metal salts proved to be efficient. Doping is carried out through three methods: quantitative wet impregnation (QWI), wet impregnation (WI), and dry mixing (DM). Both QWI and WI involve pouring a solution of the dopant in the sorbent then after mixing and sealing for amount of time, they are dried. In DM, undissolved dopant is directly mixed with the sorbent. Studies mainly used wet impregnation, with the use of sodium chloride (NaCl) the conversion of CaO was preserved at 40 % after 13 cycles while sodium carbonate (Na_2CO_3) showed no improvement compared to undoped sorbent (Figure 2.9). Research also demonstrated that this enhancement was only observed while using TGA, but due to pore blockage both sorbents' capacity declined when tested in a fluidized bed [35]. Inorganic salts (like $MgCl_2$, $CaCl_2$) were also used and showed improvement on performance. On two studies presented by same researchers, it was concluded that doping with low solution concentration exhibited better performance [36], and the addition of steam raised the uptake three times compared to limestones without steam addition after running of 50 cycles [37]. Using simple salts or acids like HBr doping

present a potential inexpensive technology for long-term performance improvement, moreover, DM no energy-penalty advantage further reduces the method cost.

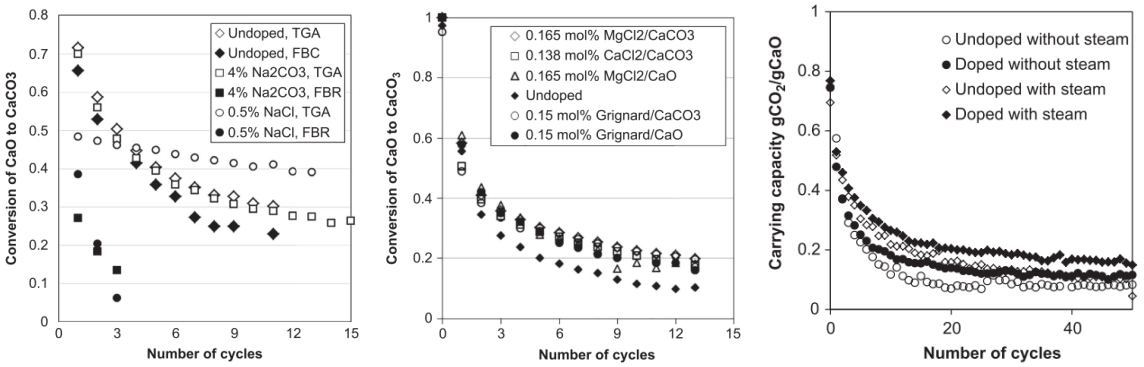

Figure 2.9: Effect of using various dopants [31]

Thermal pretreatment has been proved as a valid method for CaO conversion improvement, the theory presented demonstrate that a skeleton (Figure 2.10a) is formed after repeated calcination-carbonation cycles of agglomerated CaO which only behave as an outer surface of reactive CaO that define sorbent carrying capacity [27]. This was taken further in another study where samples were pretreated in temperature range of 800 °C – 1300 °C for various durations. Results obtained (Figure 2.10b) were from the best experiment conducted, after many cycles all pretreated sample maintained a better carrying capacity compared to the fresh sorbent [38]. Initially, sorbents had dropped capacity of conversion followed by a rise that preserved to be higher than the original sorbent. Higher pretreatment temperatures resulted in relatively low capture capacity that eventually kept elevating, while an addition of hydration process considerably increased the CaO conversion in early cycles, later dropped below the un-hydrated sorbent maybe due fragile nature of hydrated sorbents.

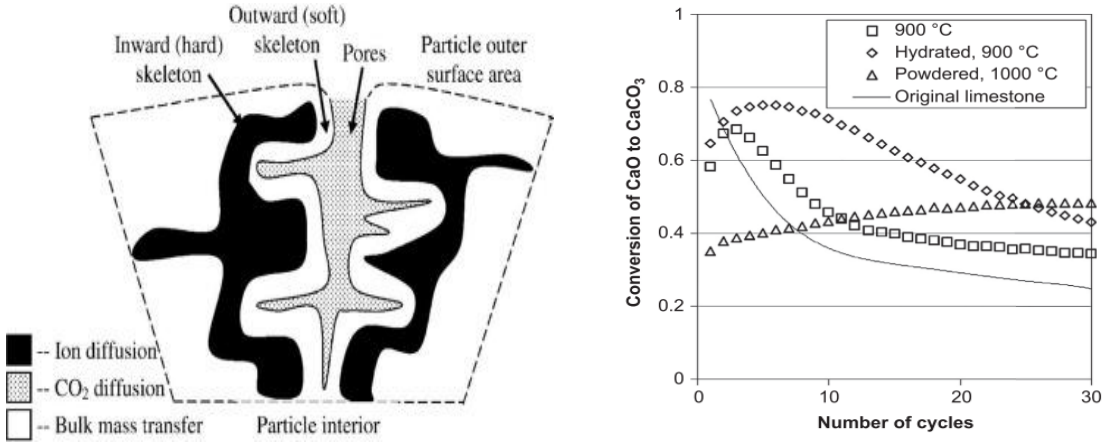

a) b)

Figure 2.10: a) Schematic representation of proposed pore-skeleton model [38], b) CaO conversion of pretreated samples [39]

Steam presence in the flue gas was not much investigated earlier as much as the focus attributed to the CO_2 and SO_2, in which it was concluded that capture of CO_2 by fresh CaO is lowered in the presence SO_2 and H_2S compared to these two gases absence [40][41]. Studies showed that presence of steam enhances calcination and carbonation reaction rate while it increases the rate of sintering. However, a

thesis study obtained that presence of steam enhanced the reactivity of a limestone sorbent as well as maximum reaction rates of calcination and carbonation. Steam presence during calcination reaction also enhanced sintering but in a way that created a pore structure that lead to maximization of the conversion [42]. The important thing to mention regarding Figure 2.11 presented, as on the experiment of this thesis work, steam was used during both calcination and carbonation reaction due to equipment installation limitation, unlike industrial application where steam is present during carbonation mostly. The carrying capacity are closer in case of utilizing steam in both calcination and carbonation and during carbonation only.

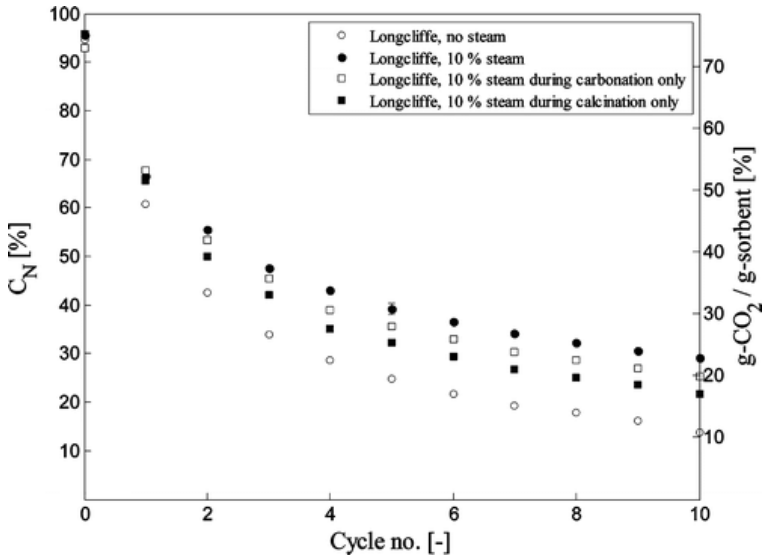

Figure 2.11: effect of steam addition on carrying capacity [42]

2.3 INDUSTRIAL APPLICATION OF CALCIUM LOOPING

Normally, developing technologies for industrial application starts from a basic research and a laboratory work. Technology readiness level (TRL) is scale of 9 levels used to determine the maturity of a technology, it was majorly common in energy production technology, and is currently used to describe the improvement realized and expected to be achieved within the CCS technologies. Each level gives a characterization of the progress in development of a technology, starting from basic principle and research (level 1) to the full-scale deployment of the technology. CCS calcium looping technology currently achieved level 6 on TRL where prototype system pilot scale has been demonstrated and are expected to reach level 8 in which system is completed and test qualified through demonstration in a plant environment by 2020, this case is for the ITRI HECLOT project.

The Industrial Technology Research institute (ITRI) has cooperated with Taiwan cement company (TCC) to install High-Efficiency Calcium Looping Technology (HECLOT) test facility at the TCC's cement plant primary aiming to reduce CO_2 emission from the plant. This project is considered the world largest test facility for calcium looping to be installed. The design of HECLOT was precedented by a bench-scale $3KW_{th}$ calcium looping test facility also developed by ITRI, it demonstrated a CO_2 capture capacity of above 85 % with a calcination efficiency of 90 % with rotary kiln calciner. The cement plant in which HECLOT was installed emits flue gas with 20 % - 25 % CO_2 content at 70 °C. Out of the 300

MW_{th} capacity of the whole plant, the test facility (Figure 2.12) captures 1 tonnes/hour of CO_2 from a 1.9 MW_{th} section that produces a flue gas stream of 3.1 tonnes/hour [43]. An update on the 2014 capture capacity of the project has stated that currently the capture capacity is above 90 % with an energy penalty reduction below 20 %, and a capture cost of less than 30$/tonne including heat integration instead of 40 $/tonne estimated previously. Plans are set to scale up the technology to an equivalent 30 MW_{th} test facility.

In a fluidized bed carbonator CO_2 is absorbed by the CaO to form $CaCO_3$ which is transferred to a rotary kiln calciner to release CO_2 by heating the sorbent using an oxy-fuel burner. Improvements are under investigation for this technology with addition of a steam hydration process to decrease temperature demand and enhance sorbent reactivity and cascade cyclones to reduce the energy penalty furthermore.

Figure 2.12: the 1.9 MW_{th} pilot plant in Heping, Taiwan [43]

Another pilot scale project was realized in 2009 in La Pereda, Spain, known as CaOling project. It's the biggest European and most ambitious project for CO_2 capture. The project consists of a 1.7 MW_{th} experimental facility installed in La Pereda 50MWe CFB power plant. This facility had been used for CO_2 and SO_2 capture achieving capture efficiencies over 90 % and 95 %, respectively. Facility tested different sorbents with different CO_2 volume fraction, SO_2 concentrations, and inventory of solids in the carbonator which lead a wide scope for CO_2 capture capacity (40 % - 95 %) at the time that SO_2 capture efficiency remained almost intact at the range (95 % - 100 %) [44].

The design (Figure 2.13) of the carbonator and calciner included two interconnected circulating fluidized bed (CFB) equipped with a cooling bayonet tubes that allow heat extraction to allow different temperature conditions. The calciner was operated under air or oxy-fuel combustion in which higher CO_2 capture were observed when using oxy-fuel combustion. On a developed technoeconomic feasibility study that this project demonstrated a competitive cost of 20-25€ per ton of CO_2 captured which can be further decreased with improvement on calcium looping scheme.

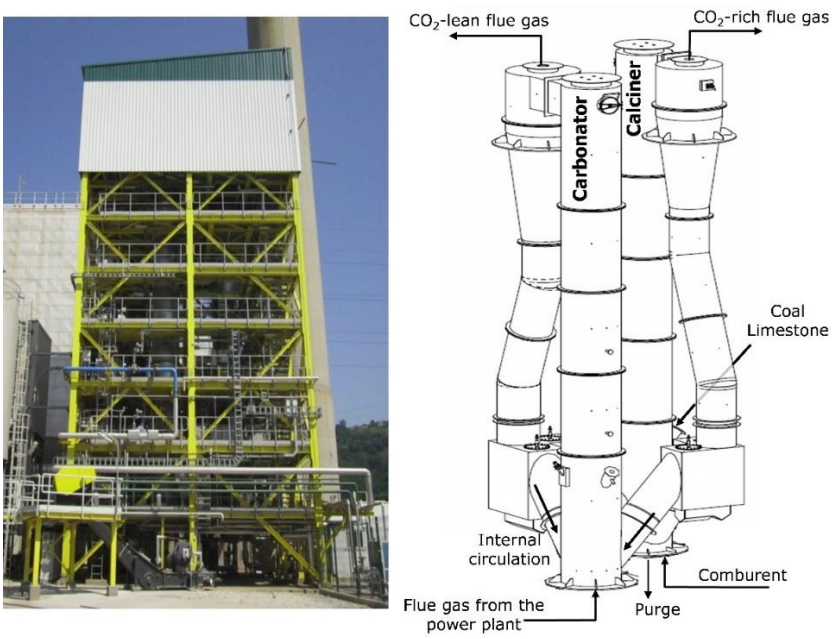

Figure 2.13: La Pereda 1.7 MW_{th} experimental facility [45]

A 200 KW_{th} pilot scale plant at institute of Combustion and Power Plant Technology (IFK), Germany, operating with two interconnected CFB that operates under a calcination temperature 890 °C - 930 °C and a carbonation temperature of 600 °C - 700 °C and 15 % CO_2 content in the flue gas have achieved above 90 % capture efficiency for when carbonation temperature was under 650 °C, and it's believed that with the synergy effect when this technology is combined with cement production can reach over 95 % of capture efficiency [46].

2.4 UTILIZATION OF WASTE IN INDUSTRY

In 2010, the amount of coal ash produced worldwide were estimated around 600 million tons annually, 500 million tones are coal fly ash representing 75 % - 80 % of total produced ash. These numbers are on the rise as the expansion in thermal power plants and other industrial factories around the world, resulting in a dilemma considering disposal of produced fly ash which particles are deemed to be highly contaminating as it captures traces of toxic elements condensed from flue gas. Back then the average world utilization of ash was merely 16 % of the total ash production, varying individually in a wide range between a minimum of 3 % and 57 % tops. Fly ash mainly consist of high percentage of silica 60 % - 65 %, alumina 25 % - 30 %, magnetite and hematite 6 % - 15 %, beside different elements like P, K, Ca, Mg and many others, this silica-alumina composition for fly ash gives it high thermal stability [47].

Coal fly ash utilization has become more common due to reasons such as increased landfill cost, and profit that is withdrawn from selling what was considered a waste before. Utilization of waste include but not limited to: structural fill, roadway and pavement embankments, light weight aggregate for construction materials, cement and concrete production, flue gas cleaning, and water, soil, and environment improvement.

Fly ash as flue gas cleaning method is used to remove SO_x, NO_x, and mercury present in the flue gas, as these compounds are considered health endangering elements with high toxicity. The alkaline nature

of fly ash beside its calcium, ferric and magnesium oxides with their pore size distribution and porosity are considered an efficient way for wastewater treatment from heavy metal content [47].

An emerging synergy from utilization of fly ash in cement production can be exploited, where both limestone and fly ash are considered as materials used for production of cement, bearing in mind the fact that 60 % of the CO_2 emissions from cement plant is generated by calcination of limestone ($CaCO_3$) to produce lime (CaO). Calcium looping CCS technology utilizes the $CaCO_3$ and CaO cycle to capture the CO_2 from flue gas and release it in a pure stream for sequestration. A substantial problem is that limestone reactivity decay has been considered a hinder for calcium looping largescale implementation. Coal fly ash (CFA) with its high-temperature stable silica-alumina components represent a possible thermal enhancement of sorbents, reducing the CaO agglomeration and sintering. On a study on the effect of CFA addition to CaO-based sorbent (Figure 2.14) it appeared that using different mixing ratio gave improvement on carrying capacity of CO_2, also it's noticed that decay rate almost stabilized along 30 cycles where it can be justified that CFA particle worked as a physical barrier preventing CaO from agglomeration [48]. Studies shows that utilization of different CaO precursors could lead to different results. This would be in the scope of work for this research.

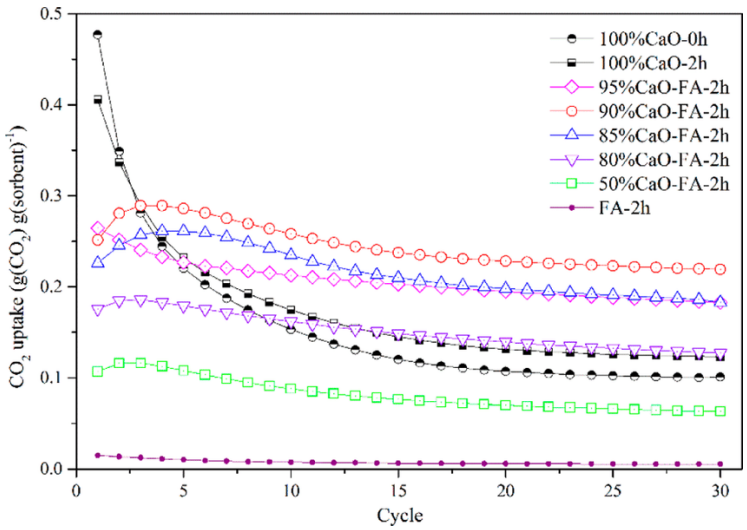

Figure 2.14: CO_2 carrying capacity with different CaO/FA ratios [48]

Another waste material considered as a valuable source that can be utilized is spent fluid catalytic cracking catalyst (SFCC), it's also used in cement industry since it presents several benefits just like CFA; environmental benefit as it minimize exploitation of natural resources and reduce disposal to the landfill, and economically low-cost input material as it's considered as a by-products [49]. SFCC catalysts are silica-alumina zeolites that can be mixed with hydrated lime producing a calcium silico-aluminate hydrates and used as cement additives or even partial replacement [50]. Beside cement industry, SFCC catalysts are well known for their use as asphalt fillers and red bricks production. Recent studies showed that SFCC can be utilized as an adsorbent for organics in hydraulic fracturing flow back and adsorbent for heavy metal.

Due to its similar chemical composition to CFA and utilization in cement industry, SFCC would also be investigated as a potential waste support for the CO_2 capture by calcium looping.

3. MATERIALS AND CHARACTERIZATION METHODS

3.1 SORBENTS AND WASTE-DERIVED SUPPORTS

Sorbents used for the research conducted for this master thesis consisted of two commercial sorbents; commercial calcium carbonate ($CaCO_3$), and a tetrahydrate calcium nitrate ($Ca(NO_3)_2.4H_2O$). and a natural calcium carbonate ($CaCO_3$) that contained more impurities.

The first sorbent to be tested was the commercial calcium carbonate ($CaCO_3$) – SIGMA-ALDRICH product with an assay of 98.5 % - 100.5 % with small traces of sulfide, chloride, iron, and others. This sorbent was mainly used as a reference to the natural sorbent, and it appears that the natural sorbent was the main target for studies because of its high purity. The natural calcium carbonate ($CaCO_3$) used is a good representative of a cement plant raw material which is a main component used for producing cement.

The tetrahydrate calcium nitrate ($Ca(NO_3)_2.4H_2O$) – SIGMA-ALDRICH product with an assay of > 99% was used as a third sorbent to test its performance of sorbent-support mixture under two methods of mixing: dry physical mixing, and wet impregnation of sorbent on support. The last one requires preparing a solution from sorbent to be impregnated on waste-derived support which won't be feasible for the calcium carbonate sorbent as it's known for them to have very low solubility.

Waste supports used were Coal Fly-Ash (CFA) and Spent Fluid Catalytic Cracking catalyst (SFCC), since they can provide two needed features for the sorbents embodied; which are the scope of this research. First, thermal and structural stability for the sorbent mixture as they mainly contain alumina and silica oxides (AlO_3, SiO_2), and second more over they are economically viable as they are waste derived supports.

The CFA was provided by a national cement plant and the SFCC was provided by a national oil industry.

3.2 THERMOGRAVIMETRIC ANALYSIS

Thermal Analysis can be referred to the study of the behavior of a sample (change in a property) according to its temperature change when the sample get heated or cooled under a controlled environment [51]. For the property of the weight/mass of the sample, thermogravimetric analysis TGA definition presented by the ICTAC (International Confederation of Thermal Analysis and Calorimetry) was stated as ‘’**a technique in which the mass of a substance is measured as a function of temperature whilst the substance is subjected to a controlled temperature programme**’’. Thermogravimetric data are usually plotted as the mass of the sample against time and/or temperature with its mass gain plotted in the upwards of ordinate and vice versa the mass loss is plotted downwards [52].

For the experiments conducted in accordance to this master thesis research the experimental unit used for thermogravimetric analysis was TG-DSC setsys Evo 16 - SETARAM analyzer (Figure 3.1).

Figure 3.1: TG-DSC setsys Evo 16 - SETARAM analyzer

3.3 NITROGEN ADSORPTION

The Nitrogen adsorption technique was used to characterize fresh and used sorbents to obtain some sorbent properties, i.e. specific surface area (S_{BET}), total pore volume (V_p), and pore size distribution (PSD) to see the effect of the CO_2 capture carbonation-calcination reactions on sorbents. Nitrogen adsorption technique uses gas adsorption manometry that help determining the adsorption isotherms of nitrogen at liquid nitrogen temperature (~77 K) were the amount of nitrogen adsorbed is measured by the change in gas pressure [53]. According to the difference in adsorption isotherms of porous materials this method is used to determine the type of pores from one of three categories that porous material has been classified into depending on their pores' internal width: micropores (< 2 nm), mesopores (between 2-50 nm), and macropores (> 50 nm). IUPAC (International Union of Pure and Applied Chemistry) classified the physisorption isotherms (Figure 3.2) into six types defined as follows:

1. **Reversible Type I isotherm**: is present with solids that have micropores with relatively small external surface like activated carbons, type I(a) is observed for microporous solids with narrow micropores (<~1nm), while type I(b) is for materials with boarder pore size distribution (< ~2.5 nm)
2. **Reversible Type II isotherm**: indicates either nonporous or macroporous material, this isotherm also can illustrate the presence of monolayer or multilayer adsorption at high relative pressures, if point B of the curve was sharp this corresponds to a completion of monolayer adsorption, but a more gradual curvature indicates overlapping monolayer and an onset multilayer adsorption.

3. **Type III isotherm**: monolayer formation cannot be identified, and there's weak interaction between adsorbed gas and solid adsorbent. Adsorbed molecules are clustered around favorable sites of a nonporous or macroporous solid surface.
4. **Type IV isotherm**: is a representation of mesopores presence. A mesopores with a higher width than a certain critical one would observe an isotherm of type IVa, while smaller width mesopores would give and isotherm of type IVb.
5. **Type V isotherm**: at high relative pressure would indicate micropores and mesopores, for example water adsorption on hydrophobic adsorbents, but at low relative pressure this isotherm behaves mostly like type III isotherms.
6. **Type VI isotherm**: represent a uniform nonporous surface that exhibit a layer-by-layer adsorption, capacity of adsorbed layer controls the height of the step.

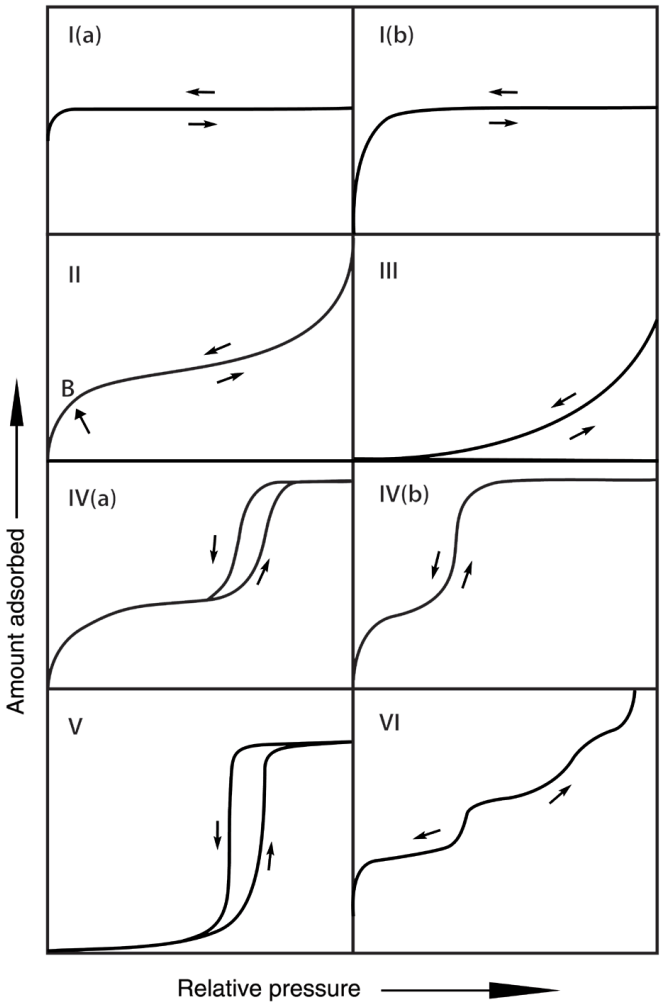

Figure 3.2: Classification of physisorption isotherms [54]

In addition to typical physisorption isotherms, a hysteresis loops were identified for the multilayer range of physisorption that normally is associated with the capillary condensation. Such hysteresis is attributed to the adsorption metastability, network effects, and pore blockage. Basically, it occurs when external surface accessibility for the wide pore only takes place through narrow necks.

Hysteresis had been classified into five types shown in (Figure 3.3) and demonstrated as follows:

1. **Type H1 loop**: narrow loops are signs of delayed condensation on adsorption branch, and usually associated with materials that have a narrow range of uniform mesopores.
2. **Type H2 loop**: observed on materials with complex pore structure that have an important networks effect. H2(a) hysteresis is regarded to the pore blocking in narrow pore necks that is given by some ordered mesopores materials, while H2(b) is associated with the same pore blocking but wider pore necks mesopores materials.
3. **Type H3 loop**: it has and adsorption branch that simulate isotherms Type II, this hysteresis is given by non-rigid aggregates of plate-like particles and macropores pore network as well.
4. **Type H4 loop**: it contains and adsorption branch that is a composite if isotherms types I and II, it's found in some mesopores zeolites and micro-mesopores carbons.
5. **Type H5 loop**: it's an unusual loop associated with open and partially blocked mesopores.

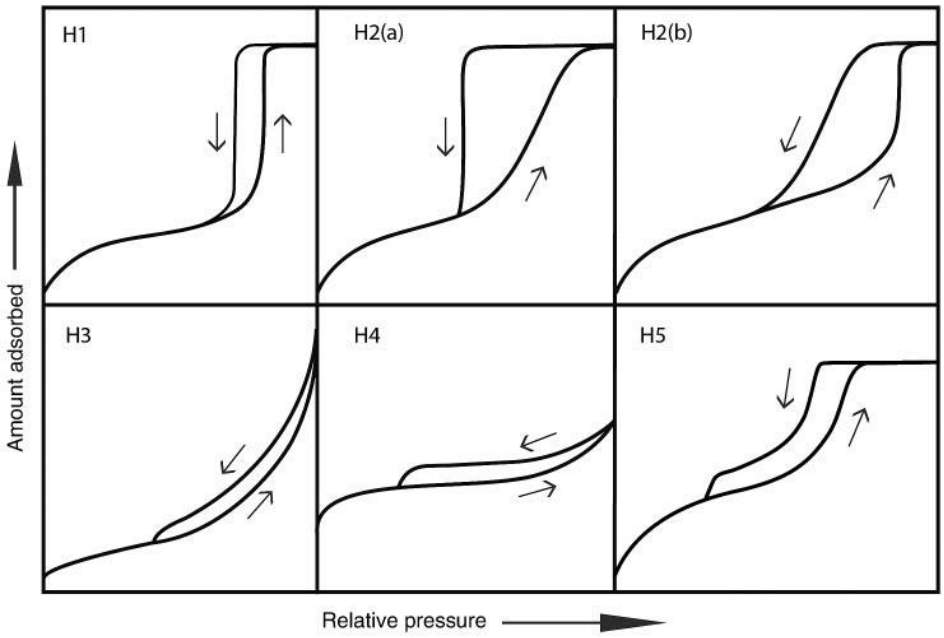

Figure 3.3: Classification of Hysteresis loops [54]

The equipment used was the Micrometrics ASAP 2010 (Figure 3.4). The setting of the apparatus required a preliminary degasifying process to ensure there was no gases or other impurities that might be adsorbed on sorbent's surface or pores. This process was conducted under vacuum condition which consist of two steps, the first step was performed at 90 °C for 1 hour while the second step was performed at 120 °C or 350 °C for fresh or used sorbent, respectively, for 3 hours. The measurement process of nitrogen adsorption was performed under a temperature of -196 °C (~77 K).

Figure 3.4: Micrometrics ASAP 2010

For result analysis the MicroActive software was used to illustrate the results. Where BET method was used to determine the sorbent's specific surface area, and the BJH desorption model was used for determining the pore size distribution, and finally the Nitrogen isotherm was used to determine the total pore volume (V_p) at a relative pressure (p/p_0) of 0.97.

3.4 X-RAY POWDER DIFFRACTION

X-ray diffraction (XRD) can be defined as an analytical technique through which a crystalline material's phase is identified and as well as information on unit cell dimension can be provided. The fundamental principle states that '' X-ray diffraction is based on constructive interference of monochromatic X-rays and a crystalline sample. These X-rays are generated by a cathode ray tube, filtered to produce monochromatic radiation, collimated to concentrate, and directed toward the sample. The interaction of the incident rays with the sample produces constructive interference (and a diffracted ray) when conditions satisfy Bragg's Law'' [55].

$$n\lambda = 2d \sin\theta \qquad \text{(Eq. 3.1)}$$

where n is the order of reflection (usually 1), λ is the wavelength of incident wave, d is the lattice spacing of the crystalline material, θ is the angle of diffraction.

XRD measurements were used to identify the different components phases and crystallite size of fresh and used sorbents. The device used for this was Bruker D8 Advance Powder X-Ray Diffractometer (Figure 3.5). The Diffractometer used Cu Kα radiation (λ = 0.15406 nm), operated at 40 kV and 40 mA, angle (2θ) range used was between 15° and 70° with 3 seconds as step time and 3° as step size.

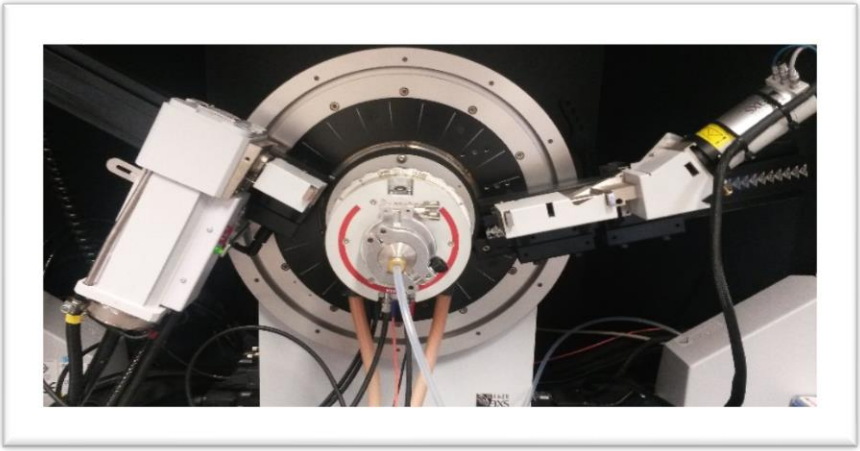

Figure 3.5: Bruker D8 Advance Powder X-Ray Diffractometer

Later with results obtained from these measurements the Crystallography Open Database (COD) was used to identify crystalline phases of sorbents. For the crystallite size of sorbents determination, Scherrer's equation was used based on obtained XRD data.

$$t = \frac{K\lambda}{(b\cos\theta)} \quad \text{(Eq. 3.2)}$$

where t is the average dimension of crystallites (nm), K is the Scherrer constant, falls in the range 0.87-1.0 (k = 0.9, assuming that particles are spherical), λ is the wavelength of X-ray (0.15406 nm), and b is the full width at half maximum of the XRD peak considered (in radians 2θ) located at 2θ [56].

3.5 SCANNING ELECTRON MICROSCOPY (SEM)

The scanning electron microcopy (SEM) analysis is generated by exposing the surface of solid substance to a focused beam of high-energy electrons where a variety of signals is generated at the substance surface. These signals which are known to be a result of the interaction that occurs between the high energy electrons and the sample reveal information about sample's morphology, orientation, crystalline structure, and its chemical composition [57]. Obtained data include a 2-dimensional image of different area sizes and a variety of magnification ranges. It also can perform a chemical composition analysis using the Energy-Dispersive X-Ray Spectroscopy (EDS), with a small withdraw of it can only give analysis for a very small predefined volumetric space of the introduced sample.

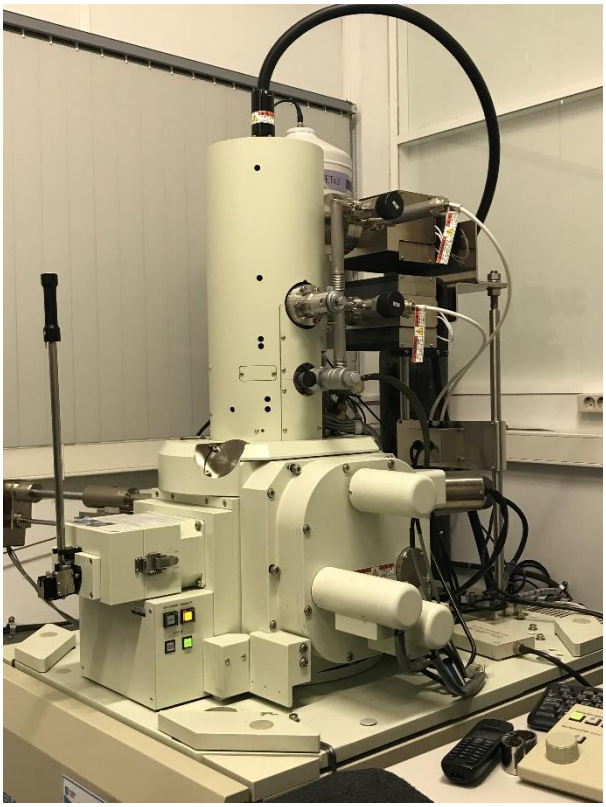

Figure 3.6: JOEL model 7001 field emission gun microscope

The SEM measurement unit used was the JOEL model 7001 field emission gun microscope (Figure 3.6). Sorbent sample were coated in a conductive adhesive containing Au-Pt in a form of a thin film which help improving electron conductivity as the nature of the samples makes them less conductive and subsequently improving the quality of images obtained.

4. CALCIUM LOOPING EXPERIMENTAL SETUP

4.1 SORBENTS PREPARATION

The preparation of the 18 sorbents mixture with waste derived supports involved three CaO precursor sorbents and two waste supports, presented in section 3.1. Mixing ratios appearing in Table 4.1, where sorbents' stability and capture capacity along the carbonation and calcination cycles were evaluated.

Table 4.1: Mixing ratios of sorbents and waste derived support

Material		**CaO Precursor**		
		Commercial $CaCO_3$ / Natural $CaCO_3$ / $Ca(NO_3)_2.4H_2O$		
support	**CFA / SFCC**	**90 %** / **10 %**	**75 %** / **25 %**	**60 %** / **40 %**

Content of CaO (%) in each precursor was the defining factor for the mass used in the mixture preparation. Loss on ignition (LOI) test were made on waste support materials at 900 °C (thermal activation temperature) to determine their mass loss up to this temperature, and subsequently to define the exact mass in which the sorbent/waste support mixture would be prepared. Natural $CaCO_3$ was crushed, sieved and fractions utilized in the experimental tests was between 125-355 μm. For moisture elimination, sorbents and waste support were kept in an oven at 120 °C.

Two methods were used to prepare the sorbents mixtures. The first was used to prepare all 18 samples, by physically dry mixing, where CaO precursor and the support were introduced into a ball mill (Retsch) under a frequency of 70 Hz for 30 minutes. The samples were dried in an oven at 120 °C before the mixing, and after mixing the samples were sealed using a laboratory film to reduce humidity capture which can affect the required weight measurement used for the experiment. The second method; a wet-impregnation, was only applied on $Ca(NO_3)_2.4H_2O$ due to its better solubility in water (1290 g/L at 20 °C) compared to the $CaCO_3$ (14 mg/L at 20 °C). The solvent was distilled water, first the $Ca(NO_3)_2.4H_2O$ was solved in 129 g/ 100 ml at 20 °C using a magnetic stirring bar and then poured onto the waste derived support. And the sample was let to dry inside an oven at 40 °C for 24 hours and at 60 °C for another 24 hours, then it was calcined at 700 °C (10 °C/min) for 3 hours to release the nitrate. A regeneration process was conducted on SFCC before the wet-impregnation by calcining at 600 °C (10 °C/min) for 6 hours to release coke particles. For this method a different setting of wet-impregnation ratio was used, to be specific only two, 90 % and 40 % of CaO precursor.

4.2 THERMOGRAVIMETRIC ANALYSIS

The TGA apparatus shown in Figure 3.1 was used to conduct preliminary experiments on all sorbent samples prepared to give an overview about its CO_2 capture capacity performance and select the sorbent that should be tested later on the fixed-bed, since the TGA apparatus was fully automated and present a relatively quick experiment tool when compared to the fixed-bed unit which will be explained later. The data acquisition necessary for the performed study includes temperature and mass change of the sample with time.

4.2.1 Experimental procedure

TGA apparatus consist of a sample holder enclosed in a chamber on which a crucible containing the sample was placed. A primary gas (air), Secondary gas (CO_2) were supplied to the TGA, which also had a protective gas (Ar) and cooling water supplies.

The weight of the sample introduced to the experiment equipment was calculated based on the final weight intended to undergo for the capture process, to give comparative results, which was 5 mg of Calcium Oxide (CaO). The weight of sample introduced was calculated based on the following equation:

$$m_{sample} = \frac{m_{CaO} * Mr_{\ CaO\ precursor}}{Mr_{\ CaO} * w_{CaO}} \quad \text{(Eq. 4.1)}$$

where m_{sample} is the sample mass (g), M_r is the molecular weight (g/mol) (even for natural $CaCO_3$ it was considered only for $CaCO_3$), w_{CaO} is the mass fraction of CaO on the mixed sorbent

The experimental procedure is explained in the following steps:

1. Sample weight is entered in milligrams, which was calculated after subtracting the weight of the empty crucible from the weight of the crucible containing the sorbent sample.
2. Activate the cooling water and protective gas supplies while making sure that the protective gas (Ar) valve is open and the pressure was set at 2 bars.
3. The specific experiment setup (Figure 4.1) was set as follows:
    - Pre-calcination of the sample at 900 °C for 20 minutes.
    - 10 cycles of carbonation of CaO to $CaCO_3$ and calcination of $CaCO_3$ to CaO.
    - Carbonation process was set for 60 minutes at 700 °C, with an air flow that consisted of 75 % of air and 25 % of CO_2.
    - Calcination process was set for 10 minutes at 800 °C, with atmosphere contained 100 % of air.
    - Air flow was set to 40 ml which corresponds to the 100 % of air flow, when CO_2 was used during the carbonation reaction, 10 ml of total flow was CO_2.
4. This experiment setup was then saved and repeated for all the sorbent samples, the only change was in the weight of the sample being introduced to the equipment.

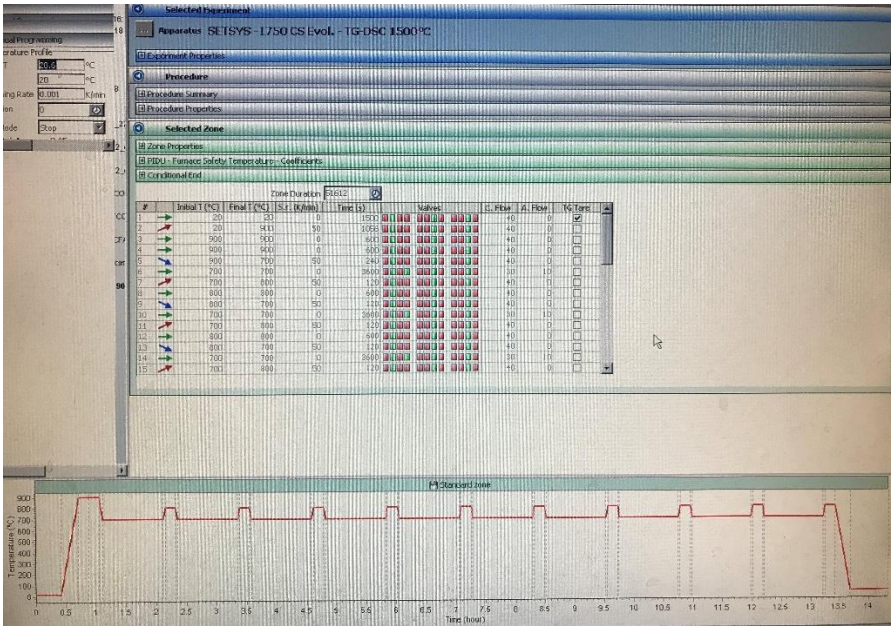

Figure 4.1: TGA experiment setup

An initial setup with 20 cycle and 20 minutes per carbonation cycle was carried out. However, it was less representative of the maximum capture capacity of the sorbent due to short carbonation cycle time. So, the number of cycles had been reduced to allow the possibility of increasing carbonation time as the whole experiment took relatively long time (around 15 hours for 10 cycles).

A 'Blank Experiment' in which the TGA apparatus runs a test with an empty crucible; that doesn't contain a sample, was carried out primarily to eliminate the apparatus atmosphere density change with temperature that influences measured mass from the actual sample's mass change. Before data export for treatment and analysis, the 'blank experiment' measures would be subtracted from the sample's measurements through a built-in feature within the SETSYS-1750 CS Evolution – TG-DSC 1500 °C software.

4.2.2 Assessment of CO_2 capture during calcination-carbonation cycles

Acquired data from the TGA experiment was exported and then treated in a Microsoft Excel spreadsheet. Data imported included the time in a step of 1.5 seconds, sample's temperature (°C) and mass change (mg). A software named Origin was used to plot acquired data (Figure 4.2) from which the maximum mass gain and loss during carbonation and calcination reactions respectively, for each cycle were extracted. The mass variation during the carbonation and calcination of each cycle comes from the CO_2 that was captured and released along the cycles. These data were used to calculate the mass of CO_2 captured by calcined sorbent, carrying capacity (CC), and CaO conversion.

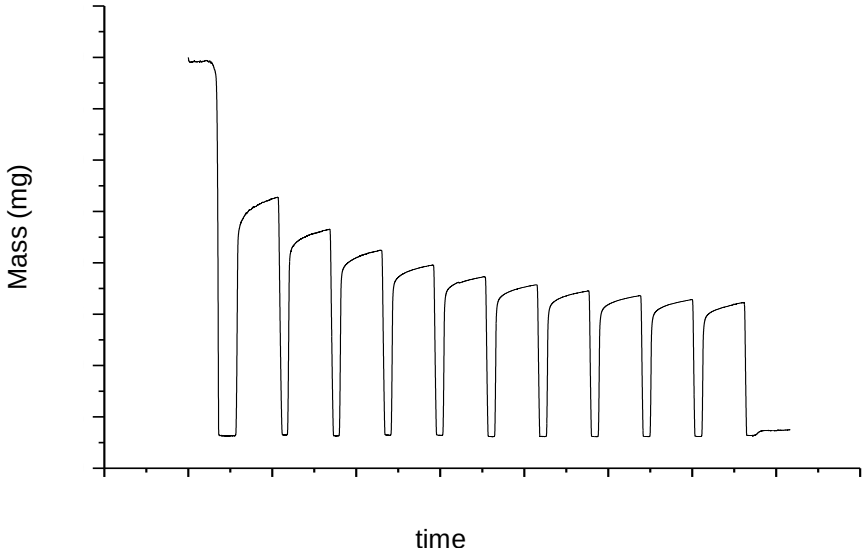

Figure 4.2: Plotted TGA acquired Data

Carrying capacity (CC) of the sorbent can be defined as the mass of CO_2 captured by a unit mass of calcined sorbent (g CO_2 / g calcined sorbent). Also, CaO conversion can be defined as the percentage of carrying capacity of the calcined sorbent when compared to the theoretical carrying capacity of a calcined sorbent constituted only of CaO which is 0.785 (44 g/mol of CO_2 / 56 g/mol of CaO). This value is recalculated for CaO-mixed sorbents considering the CaO mass fraction on the calcined sorbent. These measurements were calculated using the following set of equations:

$$(m_{CO_2})_{capt} = (m_{carb.} - m_{calc.}) \quad \text{(Eq. 4.2)}$$

$$CC = \frac{(m_{CO_2})capt}{m_{calcined\ sorbent}} \quad \text{(Eq. 4.3)}$$

$$CaO_{conversion} = \frac{CC}{CC_{theoretical} * w_{CaO}} * 100\ (\%) \quad \text{(Eq. 4.4)}$$

$$CC_{theoretical} = \frac{Mr_{CO_2}}{Mr_{CaO}} \quad \text{(Eq. 4.5)}$$

Where $(m_{CO_2})_{capt}$ is the amount of CO_2 captured in each cycle, $m_{carb.}$ is the sample mass after carbonation reaction, $m_{calc.}$ is the sample mass after calcination reaction, $m_{calcined\ sorbent}$ is the sample mass of calcined sorbent, $CC_{theoretical}$ is the theoretical carrying capacity of the calcined sorbent sample, Mr_{CO_2} and Mr_{CaO} are the molecular weights of CO_2 and CaO, respectively, w_{CaO} is the mass fraction of the CaO on the calcined sorbent

Results from CaO conversions will be showed on results and discussion chapter.

4.3 FIXED-BED UNIT

A lab-scale fixed-bed reactor was used to carry out tests on sorbent samples, and assess their CO_2 carrying capacities and stability over 20 carbonation-calcination cycles.

4.3.1 Unit description

The fixed-bed unit used consists of a high temperature resistant quartz reactor (3 cm in internal diameter and 10 cm in height) with a porous plate that has a 1.7 mbar of pressure drop for a flow rate of 600 $ml.min^{-1}$ (P = 1 bar; T = 20 °C). This quartz reactor was placed in an oven which make the main body of the fixed-bed unit, the oven has 10 cm in diameter and 30 cm in height with interior coated in high temperature ceramic for heat conduction to the quartz reactor, connected to a temperature controller device; the Eurotherm® 2000 series. Sorbents samples then introduced into the quartz reactor which had its temperature monitored by another thermocouple type K, that was fitted to keep track of sample's temperature. Carbonation temperature was always fixed at 700 °C, meanwhile calcination temperature was alternating between 800 °C and 900 °C for air and CO_2 atmospheres, respectively.

The experiments were carried out with three different atmospheric conditions settings, described as follows:

Firstly, an atmosphere consists of 100 % of air for calcination reaction, and a mixture of 75 % of air with 25 % of CO_2 gases flow for carbonation reaction. Secondly, the calcination atmosphere was changed to 100 % of CO_2 to simulate the ideal conditions of CaO looping, while the carbonation atmosphere retained the same gas mixture of 75 % of air and 25 % of CO_2. Lastly, a 5 % of steam flow was added to improve the sorbent stability and reactivity and to simulate the flow of flue gases of the cement power plant, maintaining the same flow format of the first case, where now the flow rate of calcination reaction would consist of 95 % of air and 5 % of steam, and for carbonation, the same 25 % of CO_2 flow is kept while air is now flowing at 70 % and 5 % for steam.

The gases feed into the reactor unit were controlled by mass flowmeters (Figure 4.3) to ensure a total flow of 1000 ml/min. Each mass flowmeter had to be calibrated as described in 4.3.2.

(a) (b)

Figure 4.3: Gas input flowmeters: a) ALICAT for air flow, b) Brooks for CO_2 flow

Exhaust gas flow was connected to CO_2 gas concentration analyzer to measure the amount of CO_2 in the goutlet gas of the carbonation-calcination reactions. Equipment used for this was the Guardian NG that has a CO_2 concentration range of 0-30 % with ± 2 % of full-scale accuracy (Figure 4.4).

Carbonation-calcination cycles measurement were acquired using a LABVIEW data acquisition software. The recorded data included the fixed-bed temperature, time elapsed, detected signal by the CO_2 equipment on gas outlet, as well as the air flowmeter position.

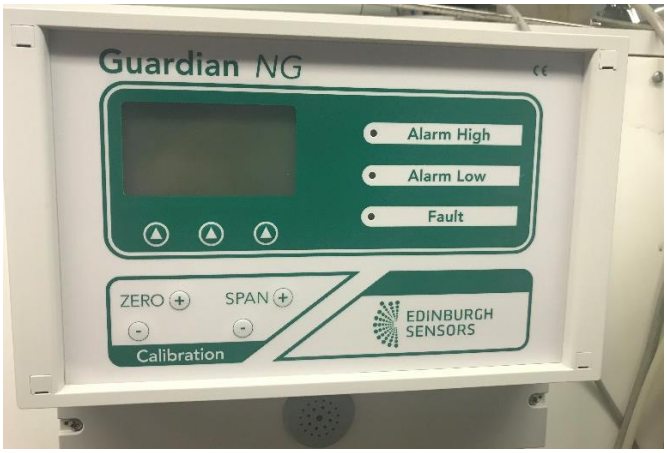

Figure 4.4: Guardian NG CO_2 detector

4.3.2 Mass flowmeters calibration

A calibration for the mass flowmeters was performed before conducting experiments on the fixed-bed reactor. These calibrations are used to determine the set point adjusted on the flowmeters to give the desired flow of gas. The calibrations were made on two flowmeters to define the flow of air and CO_2.

First, Alicat flowmeter for air was calibrated using a bubble flowmeter. Different set points were set on the flowmeter as exemplified in

Table 4.2, the corresponding volumetric flow (Q_v) was calculated using (Eq. 4.6) where the time in seconds required for a bubble to cover a specific volume (V_s) of the bubble flowmeter is measured. The time used for volumetric flow calculation is an average of three measurements.

$$Volumetric\ flow\ (Q_v) = \frac{V_s\ (ml)}{time\ (s)} \qquad \text{(Eq. 4.6)}$$

Figure 4.5 shows that by interpolation it's possible to define the set point for Alicat flowmeter that would allow to obtain the of 750ml/min required flow of air, e.g. for 750 ml/min the set point was 0.73.

Second calibration process was made on the Brooks flowmeter through which the flow of CO_2 was supplied. An air flow of 750 ml/min was maintained, while different set points on the Brooks flowmeter were used following the same procedure as in the Alicat calibration. The Guardian NG CO_2 detector was used to track the change in CO_2 concentration for every set point on the Brooks device. Corresponding CO_2 concentration to the Brooks position is showed in Table 4.2. By interpolation (Figure 4.5) the Brooks set point required to provide a flow of 25 % of CO_2 on the exhaust gases was then defined. Using the same method of bubble flowmeter, this set point was verified using above mentioned equation 4.6.

Table 4.2: Calibration data for Air (Alicat) and CO_2 (Brooks) flowmeters

Alicat Position	Average Q_v (ml/min)
0	0
0.1	119
0.2	220
0.4	420
0.6	625
0.7	726.2
0.8	828.7
0.9	936.1
1	1044.1

Brooks Position	CO_2 (%)	Average Q_v (ml/min)
0	0	750
2	14.95	882
4	17.25	906
6	19.30	929
10	23.00	974
14	26.45	1020
15	27.05	1028

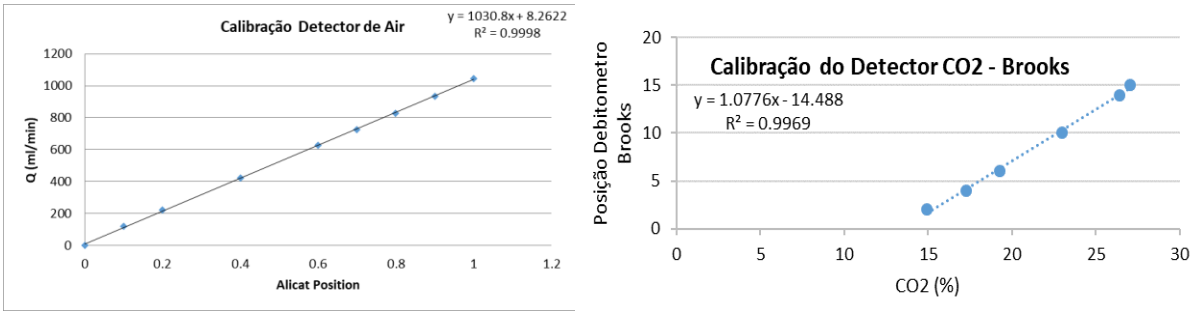

Figure 4.5: Interpolation process used for flowmeters calibration

4.3.3 Experimental procedure

The sorbents' carrying capacity along the carbonation and calcination cycles was tested on a fixed-bed reactor. Samples were reserved in an oven overnight before the test day at a temperature of 120 °C to prevent moisture saturation. Two sample groups containing natural and commercial $CaCO_3$ mixtures were tested for their reactivity and stability.

The experimental procedure follows the respective below order:

1. About 2 grams of sample is introduced into the quartz reactor and were well distributed on the bed. Then the quartz reactor is introduced into the fixed-bed.
2. Inlet and outlet flow tubes are connected into the quartz reactor using clamps to ascertain leakage prevention, and sample temperature thermocouple is inserted in the reactor specific opening.
3. Oven is turned on and the temperature on the Eurotherm® 2000 is set to 900 °C to conduct a pre-calcination process (sorbent activation) on the sample. Two ceramic plates are placed on top of the oven to support the quartz reactor and prevent heat loss, moreover a thermal insulation tape is wrapped around the upper part of the quartz reactor to reduce heat loss from the oven and reactor.

4. Air and CO_2 valves are opened, and the pressure gauge is set to 2 bars, exhaust gases valve is also opened, and the Guardian NG CO_2 detector is plugged in.
5. The set point on Alicat flowmeter is adjusted to allow the desired flow of air. Air flow is always maintained constant during carbonation and calcination cycles.
6. LABVIEW is used to create an experiment data record file to track test measurement. Later this file is exported to a Microsoft excel sheet for calculation of carrying capacity and CaO conversion.
7. The Brooks flowmeter is adjusted to the set point, to allow the defined flow of CO_2 during carbonation cycles and CO_2 atmosphere calcination cycles.
8. Experiments were carried out for 0 cycles during the sorbent activation (only a pre-calcination is made until all the CO_2 is released which is confirmed in the Guardian NG apparatus) and 20 carbonation-calcination cycles at 700 °C for all carbonation cycles and at 800 °C or 900 °C for calcination cycles with air or CO_2 atmospheres, respectively.
9. During experiment, temperature and CO_2 were monitored while gas valves and temperature had to be manually adjusted when swinging between carbonation and calcination reactions. Carbonation is considered complete when CO_2 reading on Guardian NG detector stabilizes (e.g. 25 % of CO_2), and calcination is completed when CO_2 release stops (0% of CO_2). In case of calcination with 100 % of CO_2, it was carried out for 15 min at 900 °C (the flue gas was disconnected from the detector during this time), followed by the total CO_2 release from sorbent under air atmosphere for a few minutes.
10. At the end of experiment, LABVIEW data acquisition is stopped, oven is turned off, Guardian Plus CO_2 detector is unplugged, flowmeters and valves are closed along with the flue gas valve.
11. When quartz reactor temperature falls below 400 °C, it's removed from the oven carefully using insulating gloves. Sample is retrieved and weighted then it's preserved in a container sealed with a laboratory sealing film and analyzed as soon as possible.

An alteration to the setting of gas flow was made when introducing the steam, whereby the dry gas stream (air and/or CO_2) is passed through a bubbler system that has a saturator (gas washing bottle) containing distilled water submerged in a thermostatic bath to generate the steam. Antoine equation was used to define the saturator temperature required for obtaining the desired 5 % volumetric fraction of steam in the total gas flow.

A blank experiment was performed in the fixed bed, without a sample and using the same experimental conditions used for sorbents to define the experiments baseline

It is to be noticed that conducting a 20-cycle experiment on fixed-bed unit requires 2 days of experiments and so during the night the sample was put under a reduced flow of air with the oven turned off.

4.3.4 Assessment of CO_2 capture during calcination-carbonation cycles

At the end of carbonation-calcination cycles, data file acquired from the LABVIEW software was analyzed in Microsoft Excel 2016 spreadsheet developed previously for CO_2 carrying capacity calculations. Calculation methodology used was similar to a previously developed work already published [58].

For CaO conversion rate calculations, molar amount of CO_2 adsorbed during carbonation reaction was calculated based on following equation:

$$\boldsymbol{n_{CO_2,carb}} = \int_{t_1}^{t_2} \left(\boldsymbol{n_{CO_2,i}} - \boldsymbol{n_{CO_2,not\ capt}} \right) \mathbf{d}\boldsymbol{t} \qquad \text{(Eq. 4.7)}$$

Where $\boldsymbol{n_{CO_2,carb}}$ represent the molar amount of CO_2 adsorbed during carbonation, $\boldsymbol{n_{CO_2,i}}$ is the molar amount of CO_2 fed to the reactor, $\boldsymbol{n_{CO_2,not\ capt}}$ is the molar amount of CO_2 that didn't involve in carbonation reaction, t_1 and t_2 are carbonation time interval.

For comparative reasons the amount of CO_2 captured by the CaO sorbent during the carbonation, was also calculated by the CO_2 amount released during calcination reaction, where the molar amount of CO_2 captured is estimated by:

$$\boldsymbol{n_{CO_2,calc}} = \int_{t_1}^{t_2} (\boldsymbol{n_{CO_2,capt}})\ \mathbf{d}\boldsymbol{t} \qquad \text{(Eq. 4.8)}$$

Where $\boldsymbol{n_{CO_2,calc}}$ is the molar amount of CO_2 adsorbed during carbonation and released during calcination, $\boldsymbol{n_{CO_2,capt}}$ is the molar amount of CO_2 released from the sorbent during calcination between time t_1 and t_2.

The CaO conversion of the sorbent was estimated based on equation:

$$CaO_{conversion} = \frac{\mathrm{n_{CO_2,carb}} \times \mathrm{Mr_{CO_2}}}{\mathrm{m_{CaO\_sorbent}}} \Big/ \left(\frac{\mathrm{Mr_{CO_2}}}{\mathrm{Mr_{CaO}}} \times w_{CaO\_sorbent} \right) \times 100\ (\%) \qquad \text{(Eq. 4.9)}$$

Where $\mathbf{Mr_{CO_2}}$ **and** $\mathbf{Mr_{CaO}}$ are the molar mass of CO_2 and CaO, respectively, $\mathbf{m_{CaO\_sorbent}}$ is the mass of CaO present in the calcined sorbent, and $\mathbf{w_{CaO\_sorbent}}$ is the mass fraction of CaO in the calcined sorbent.

Figure 4.6 demonstrate the amount of CO_2 captured and released during carbonation and calcination reactions, respectively. Integration equation explained above calculate the amount of CO_2 by finding the area confined between the baseline and the experiment line.

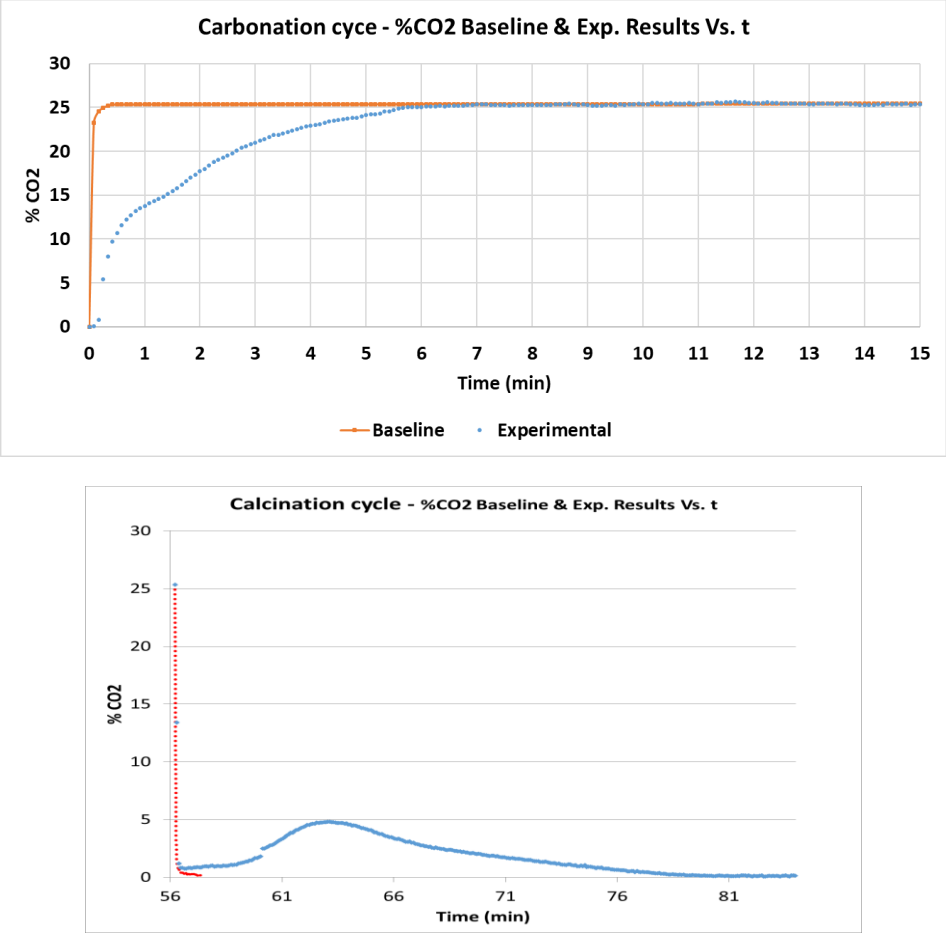

Figure 4.6: CO_2 captured along carbonation and calcination cycles

4.4 IN-SITU X-RAY DIFFRACTION

In-situ X-ray diffraction is often used to investigate a variety of dynamics processes under a non-ambient conditions, such processes include reaction that involve solid state, phase transition, thermal expansion, or crystallite growth [59]. In this work, in-situ XRD is used to track the evolution and formation of CaO and $CaCO_3$ crystallite phase along the several calcination and carbonation cycles. The unit used was the Anton Paar HTK 16N High Temperature Chamber equipped in the Bruker D8 Advance X-Ray diffractometer.

4.4.1 High temperature chamber

The high temperature chamber (Figure 4.7) contains a pre-stressed heating strip that is resistant to elongation upon heating to maximize sample position stability over the experiment temperature range, in this case heating strip are made of platinum. Two thermocouples were used, one is spot-welded to the heating strip to give an accurate temperature measurement of experiment operational condition, the second thermocouple is located right above the sample to track its temperature.

Figure 4.7: In-situ XRD High Temperature Chamber

Th Anton Paar HTK 16N High temperature chamber operates under temperatures up to 1600 °C in air or inert gas. Direct sample heating is applied to the sample that is in direct contact with the heating strip resulting in the minimum temperature gradient across the sample.

4.4.2 Experimental procedure

First, a suspension with sorbent samples and a solvent (ethanol) was prepared and this suspension was deposited on the heating strip with the aid of a pipette. When all the solvent evaporated at room temperature, the high temperature chamber was closed. The calcination-carbonation reactions conducted here are similar in conditions to the fixed bed reaction, thus a calibration for the air and CO_2 flow were made. A gas flow of 100 ml during carbonation was used, consisting of 75 ml of air and 25 ml of CO_2 flow, in correspondence to the 25 v/v % of CO_2. For the 100 % flow of air during calcination a 75 ml of air was used.

The experiment procedure that was programmed for this test was as follows: first, a pre-calcination at 900 °C was carried out to activate the sorbent and a 1st XRD pattern was carried out. It was followed by a second and third patterns after the carbonation and calcination reactions, respectively. A total of 5 carbonation-calcination cycles were carried out. The XRD patterns were carried out in the 2θ angle range between (26 ° - 39 °) with 0.05 ° step size and 6 seconds step time, which targeted the profiles of $CaCO_3$ peaks (29.3 ° and 35.9 °) and CaO peaks (32.3 ° and 37.5 °) which were evaluated later. Both carbonation and calcination reactions lasted for 10 minutes after which the XRD pattern immediately starts. The gradient of heating temperature from the 700 °C carbonation temperature to the 800 °C calcination temperature was 25 °C/min, and the cooling gradient on contrast was 50 °C/min.

The measurement procedure was fully automated and controlled by the software running the equipment, namely the calcination-carbonation temperature adjusting and the XRD patterns achievement. An exception was the CO_2 gas flow, which had been manually controlled through a valve, while air flow was continuous.

4.5 EXPERIMENTAL PLANNING

In this work, experimental tests were conducted on sorbents to check CO_2 capture capacity decay along the cycles and stability of different CaO-precursor sorbents and CaO-mixed sorbents with waste derived support. Additionally, a calcination atmosphere of CO_2 and steam addition effect was evaluated.

Prepared sorbents underwent three consecutive test steps described as follows:

1st test group: all sorbents were analyzed with thermogravimetric (TGA) experiments.

2nd test group: best performing sorbents from TGA experiments were evaluated in the fixed-bed unit under a carbonation atmosphere of 25 % of CO_2 balanced in air and calcination atmosphere of 100 % of air.

3rd test group: a chosen sorbent from experiments carried out in fixed-bed unit were tested under a calcination atmosphere of CO_2, as well test with addition of 5 % of steam.

A summary of fixed-bed experiments is shown in (Table 4.3).

Table 4.3: Summary of Fixed-bed reactor carbonation-calcination experiments

Identification	Pre-calcination atmosphere	Carbonation atmosphere	Calcination atmosphere	Number of carbonation-calcination cycles
Standard conditions	100 % Air	75 % Air 25 % CO_2	100 % Air	0 cycles 20 cycles
CO_2 Calcination	100 % CO_2 (15min) 100 % air		100 % CO_2 (15min) 100 % air	0 cycles 20 cycles
5% of steam	95 % air 5 % steam	70 % Air 25 % CO_2 5 % steam	95 % Air 5 % steam	0 cycles 20 cycles

Characterization was only made on sorbents tested on the fixed-bed reactor, both fresh and used sorbents went through following methods: N_2 sorption for the textural properties, XRD for mineralogical composition, and SEM for morphological properties of sorbents.

On the third group of tests, the aim was to check the effect of different carbonation and calcination atmosphere on the sorbents' capture capacity and stability along cycles. A standard atmosphere where calcination was performed under 100 % of air flow and carbonation under 75 % of air and 25 % of CO_2, was changed and during the calcination the air is replaced by 100 % of CO_2 flow, meanwhile carbonation atmosphere was maintained. The second change was with the addition of 5 % of steam to

both carbonation and calcination atmospheres, where now the calcination atmosphere consists of 95 % of air and 5 % of steam, and carbonation atmosphere consist of 70 % of air, 25 % of CO_2, and 5 % of steam. These atmosphere changes were intended to simulate the flue gas stream composition from cement plant exhaust and the ideal operation conditions of Ca-looping to achieve a pure stream of CO_2 during the calcination.

After finishing the initially planned experimental work, the in-situ XRD technique was used to evaluate the CaO and $CaCO_3$ formation along the carbonation and calcination cycles of the natural $CaCO_3$ because it is the most useful sorbent for industrial application and for a mixed sorbent (75 % CaO with 25 % of CFA) because it was the CaO-mixed sorbent that presented the highest stability on the TGA experiments.

5. RESULTS AND DISCUSSION

Experiment carried out for this work were foremost to test the reactivity decay and stability of a local natural limestone ($CaCO_3$) and to evaluate the effect of supporting this natural sorbent with waste-derived material (CFA and SFCC) by physical dry mixing on the sorbents' performance. For comparison, a commercial $CaCO_3$ was used as a high-purity CaO precursor that can give reference results. The $Ca(NO_3)_2.4H_2O$ was used for the evaluation of sorbent/waste-support using a dry mixing and wet-impregnation method. Due to low solubility of limestone the application of wet impregnation method isn't feasible.

A total of 20 samples were tested in TGA (prepared by dry physical mixing or wet impregnation), under the conditions described on 4.2.1 for 10 cycles. For fixed bed reactor experiments, 8 samples were tested for 0 and 20 cycles, including pure commercial and natural limestone, and again both when mixed with 10 % of CFA and 10 % of SFCC under the standard conditions (Table 4.3). The other two experiments were performed with natural limestone ($CaCO_3$) tested under CO_2 calcination and 5 % of steam as described in Table 4.3.

5.1 FRESH SORBENTS AND WASTE DERIVED SUPPORTS CHARACTERIZATION

A chemical and mineralogical analysis was performed to assess the chemical and mineralogical composition of the CaO-precursors and waste support materials. Characterization for morphological and textural properties were also performed on the fresh samples tested.

5.1.1 Chemical and mineralogical composition

Table 5.1 present the elemental composition of the sorbents and waste derived supports. The natural limestone ($CaCO_3$) and waste-derived supports elemental composition were determined at Laboratory of Analysis of Instituto Superior Tecnico (LAIST) using ICP (Inductively Coupled Plasma) for elemental analysis, except for carbon which was quantified by an internal method (accredited by Portuguese Institute of Accreditation).

Table 5.1: Elemental composition of fresh CaO sorbents precursors (Commercial and Natural $CaCO_3$, $Ca(NO_3)_2.4H_2O$) and waste derived supports (CFA and SFCC)

CaO-precursors/	**Elemental content (wt. %)**									
Waste-derived supports	**Ca**	**Mg**	**Si**	**Al**	**Fe**	**Na**	**K**	**Ti**	**S**	**C**
Commercial $CaCO_3$	39.9	-	-	-	≤0.02	-	≤0.01	-	-	-
Natural $CaCO_3$	39	0.13	2.5	0.17	0.4	-	-	-	-	11.1
$Ca(NO_3)_2.4H_2O$	16.9	-	-	-	-	-	-	-	-	-
CFA	1.5	0.52	28	2.6	2.3	0.26	0.26	0.07	0.21	2.6
SFCC	0.03	0.01	19	12	0.22	0.32	0.05	0.02	< 0.05	<0.7

As seen in Table 5.1, calcium content (weight %) of commercial and natural limestone is more than double of the content of calcium nitrate which justifies the differences in the amounts of CaO precursors required to prepare each sorbent. The calcium content in the CFA is not involved in capture process of CO_2 as presented on a study [48] and also verified experimentally on the TGA analysis experiments that shown that the amount captured by CFA can be neglected. XRD analysis (Figure 5.1) shows the mineralogical composition of the fresh and calcined sorbents in a muffle at 900 °C (10 °C/min) and kept at this temperature for 3 hours. As observed on XRD pattern, the SiO_2 is present in the natural $CaCO_3$ unlike the high purity of commercial $CaCO_3$ and $Ca(NO_3)_2.4H_2O$ that after calcination only contains CaO. It's also observed that at such calcination temperature, as expected all the CO_2 was released from the fresh sorbent, as no traces for $CaCO_3$ peaks were identified for calcined sorbents. It was not possible to perform an XRD pattern for $Ca(NO_3)_2.4H_2O$ because it was a hydrated sample and not a powder. XRD for CFA and SFCC were difficult to analyze due to the amorphous nature and low crystallinity, where according to elemental composition they mostly consisted of Si and Al. Loss on Ignition (LOI) for CFA and SFCC at 900 °C were 3.49 % and 2.27 % respectively. This means that their composition is not completely constant, and during the sorbent activation at 900 °C, the waste-derived supports underwent change that can enhance their thermal stability as indicated by a study made on different types of fly ashes [60].

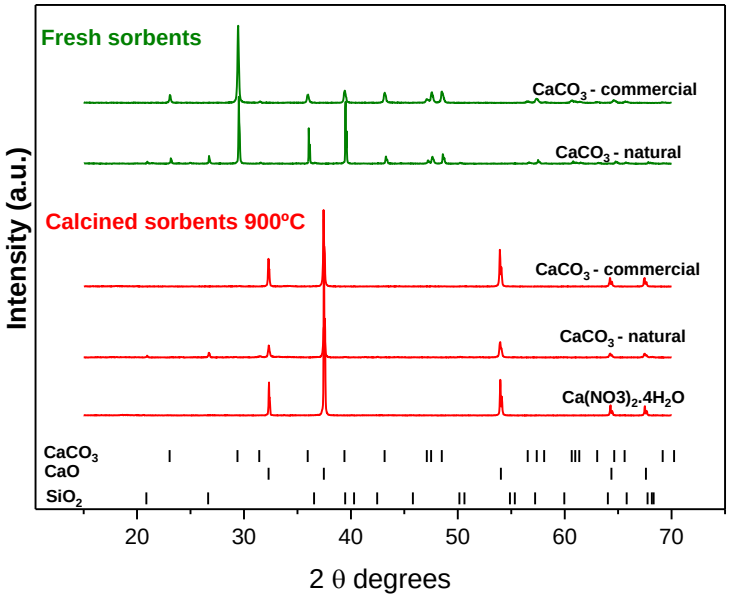

Figure 5.1: XRD patterns of fresh and calcined CaO precursors

5.1.2 Textural and morphological properties

Textural properties of fresh sorbents and waste-derived supports were evaluated through the N_2 sorption technique and expressed as the specific surface area (S_{BET}) and total pore volume (V_p) presented in Table 5.2. The calcined sorbents exhibited an increase in V_p and S_{BET} due to release of CO_2 by calcination, also due to the voids generated as explained in a previous study with WMP sorbents [58]. The commercial $CaCO_3$ sorbent has a higher S_{BET} and V_p, so it is expected that it presents higher carrying capacity along the carbonation-calcination cycles. Compared to SFCC, the CFA has a lower S_{BET} and V_p because SFCC is a microporous zeolite-based catalyst.

The strong effect of calcination temperature on the SFCC textural properties is evident when the S_{BET} and V_p of sorbent calcined at 600 °C and 900 °C is compared. The calcination temperature (900 °C) causes a kind of melting effect that lead to amorphous structure of SFCC obtained in XRD patterns.

Table 5.2: CaO precursors and waste derived support textural properties

CaO sorbents precursors/ Waste derived supports		S_{BET} (m^2/g)	V_p (cm^3/g)
Commercial $CaCO_3$	Dry, 120 ºC	8.4	0.02
	Calcined at 900 ºC, 3h	16.4	0.03
Natural $CaCO_3$	Dry, 120 ºC	1.8	0
	Calcined at 900 ºC, 3h	6.7	0.01
$Ca(NO_3)_2.4H_2O$	As received	n.a.	n.a.
	Calcined at 900 ºC, 3h	5.2	0.01
CFA	Calcined at 900 ºC, 3h	2	0
SFCC	Calcined at 600 ºC, 6h	92.3	0.10
	Calcined at 900 ºC, 3h	19.8	0.05

*n.a: not applicable

The N_2 adsorption isotherms (Figure 5.2), for fresh commercial and natural $CaCO_3$ shows that the isotherms are type II typical of a nonporous or a macroporous sorbent. The N_2 adsorption test was not possible for $Ca(NO_3)_2.4H_2O$ because it's not in powder form. Calcined sorbents exhibited the same non-porous and macropores structures (type II isotherm) where the higher S_{BET} is due to the release of CO_2. In the case of calcined commercial $CaCO_3$ some mesopores can be identified due to the hysteresis presence. Calcined waste-derived supports isotherms (Figure 5.2), where CFA isotherm shows almost a horizontal line adjacent to the abscissa, can be considered to have a negligible N_2 adsorption also in agreement to a presented work [61]. The SFCC isotherm is a type II with a type H3 hysteresis which is evidence of macropores and mesopores presence that is reflected in a higher S_{BET} and V_p given in (Table 5.2).

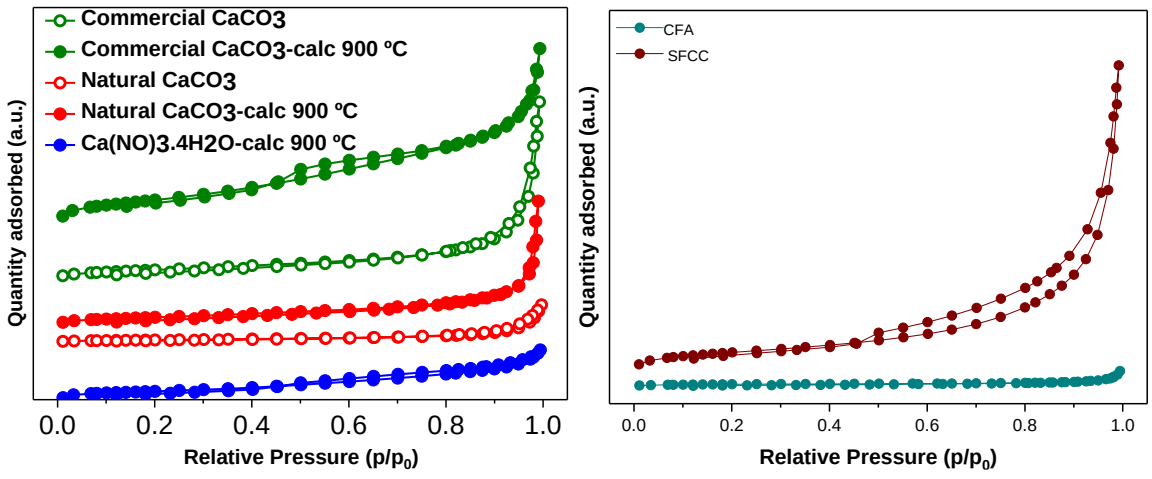

Figure 5.2: N2 sorption isotherms of fresh and calcined CaO sorbents precursors, and waste-derived supports

Figure 5.3a and c shows two magnifications for natural $CaCO_3$ obtained from SEM. Natural $CaCO_3$ exhibited agglomerated semi-cubic non-uniform particles that are nonporous, that agrees with the low S_{BET} shown in Table 5.2, which is similar to some extent with a commercial $CaCO_3$ shown on a previous study [58]. Commercial $CaCO_3$ (Figure 5.3b) shows smaller uniform particles which appear to be organized in stacked plates form (Figure 5.3d). This agrees with the high S_{BET} presented in Table 5.2. SEM images (Figure 5.4) for CFA and SFCC show an expected spherical shape for both sorbent particles due to the high temperature process that they went through [62]. Figure 5.4c and d present differences between CFA and SFCC, i.e. the smaller CFA particles appear to be more compacted containing no pores which correlates with S_{BET} presented (Table 5.2), while SFCC particles are bigger in size and have more porous surface that justify its higher S_{BET} (Table 5.2).

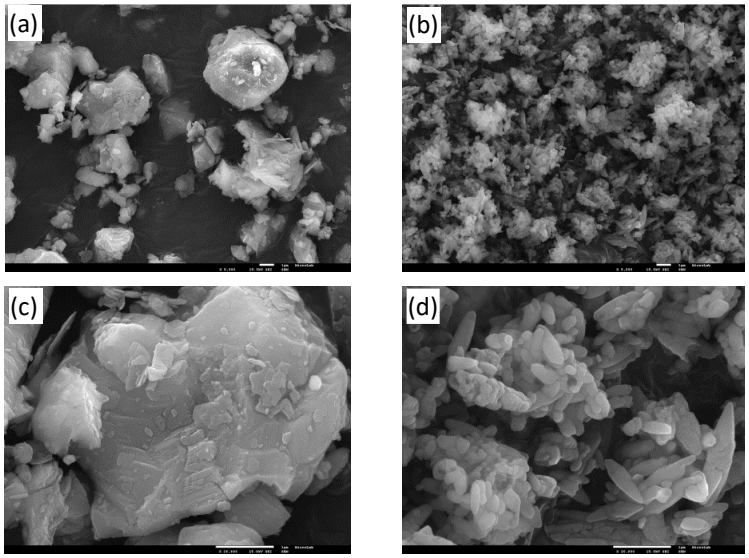

Figure 5.3: SEM micrographs of CaO sorbents precursors: (a) Natural CaCO3 (b) Commercial CaCO3 (magnification: 5000 and scale: 1 µm) and (c) Natural CaCO3, (d) commercial CaCO3 (magnification: 20000 and scale: 1 µm)

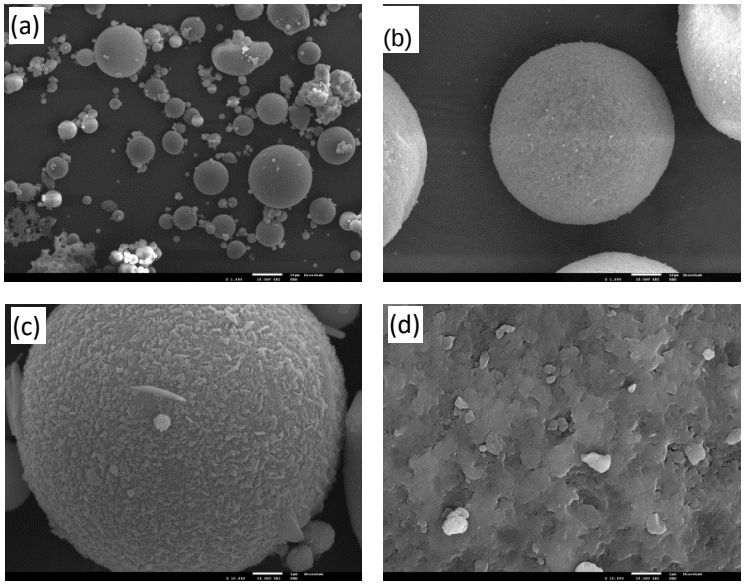

Figure 5.4: SEM micrographs for waste derived supports: (a) CFA and (b) SFCC (magnification: 1000 and scale: 10 µm); (c) CFA and (d) SFCC (magnification: 10000 and scale: 1 µm)

5.2 INFLUENCE OF CaO-PRECURSOR TO SUPPORT RATIO ON CaO CONVERSION

5.2.1 Reactivity test carried out on TGA

An explanation for the arrangement and presentation of results in this section is important. In the case of natural $CaCO_3$ a dry mixed sorbent was prepared with 90 % of CaO and 10 % of CFA or 10 % of SFCC for a total mass of 10 g of CaO with waste-derived support sample, i.e. 9 g of CaO plus 1 g of waste support. However, due to sample shortage the 75 % and 60 % of CaO mixed sorbents were prepared with a total mass of 2 g of CaO with waste-derived support . Later, an inconsistency was observed, and with further experiments the problem was identified to be from the milling process of different mass of sorbents. So, additional samples with 90 % of CaO were mixed with 10 % of CFA or 10 % of SFCC were prepared with 2 g (CaO basis).

Since CaO-precursors have different molecular weights, the CaO content was used as a calculation base (CaO basis), based on which the precursor masses were defined (e.g. to prepare a 10 g of a blend with 90% of CaO and 10% of CFA, a 16.1 g of commercial $CaCO_3$ and 37.9 g of $Ca(NO_3)_2.4H_2O$ were used). The waste derived support LOI value at 900 °C was also considered on the mixing blends calculus.

a. TGA reactivity test: dry physically mixing

Both commercial $CaCO_3$ and $Ca(NO_3)_2.4H_2O$ were prepared only with 10 g (CaO basis) and the natural $CaCO_3$ was prepared in both 10 g and 2 g (CaO basis). When using the mixed sorbent, the commercial $CaCO_3$ (Figure 5.5) shows an improvement of CaO conversion on the first cycle, from 88 % for 100 % of CaO sorbent to around 91 % and 96 % with 10 % of CFA and 10 % of SFCC, respectively. The change in the capture capacity on 1st cycle can be referred to the structural support provided to the sorbent by the waste derived materials, which reduces the sintering effect of pre-calcination applied to sorbents. On the 10th cycle the decay of sorbent reactivity was lower for the supported sorbents as the reduction in CaO conversion was 6 % and 5 % for the mixed sorbents with 10 % of CFA and 10 % of SFCC, respectively, compared to the 8 % reactivity decay for 100 % of CaO sorbent. The increase of the stability provided by waste-derived materials is also observed for the 75 % of CaO sorbent with 25 % of support that shows a final CaO conversion higher than the pure CaO sorbent. The CaO conversion for $Ca(NO_3)_2.4H_2O$, shown on the same figure, had a behavior similar to the commercial $CaCO_3$ from a performance enhancement point of view, yet it had much lower CaO conversion. As mentioned on [63] the $Ca(NO_3)_2.4H_2O$ melts at very low temperature, possibly hindering the formation of pores during CaO-precursor decomposition. The CaO conversion profile for the case of $Ca(NO_3)_2.4H_2O$ behavior along the cycles shows a continuous increase in conversion, a similar behavior using a different sorbent was reported on a study [48] that attributed this to self-reactivation effect. This effect is explained by the pore-skeleton model, in which the reaction is slower in first cycle due to lower reactivity and ion diffusion restrictive effect of the inward (hard) skeleton, and then in subsequent cycles the outward (soft) skeleton that accelerates the carbonation rate is formed and grows continuously.

Natural $CaCO_3$ exhibited a CaO conversion for 100 % of CaO sorbent similar to one reported [58] for a WMP which is also a natural sorbent, only the 90 % of CaO with 10 % of CFA sorbent exhibited a better

CaO conversion as the waste support improved sintering resistance. However, all mixtures presented a lower reactivity decay when compared to the 100 % of CaO sorbents, the 75 % of CaO with 25 % of CFA and 60 % of CaO with 40 % of CFA presented the lowest decay rate of only ~7 % for both cases. This result is attributed to the high amount of CFA present in the composition of the sorbent mixture. Regarding lower CaO conversion it was reported in literature [48] that increasing CFA share above 10 % of total weight can result in formation of gehlenite ($Ca_2Al_2SiO_3$) which consumes active CaO in the process. A possible explanation for the lower CaO conversion in the case of SFCC addition will be presented on the subsection 5.2.2.

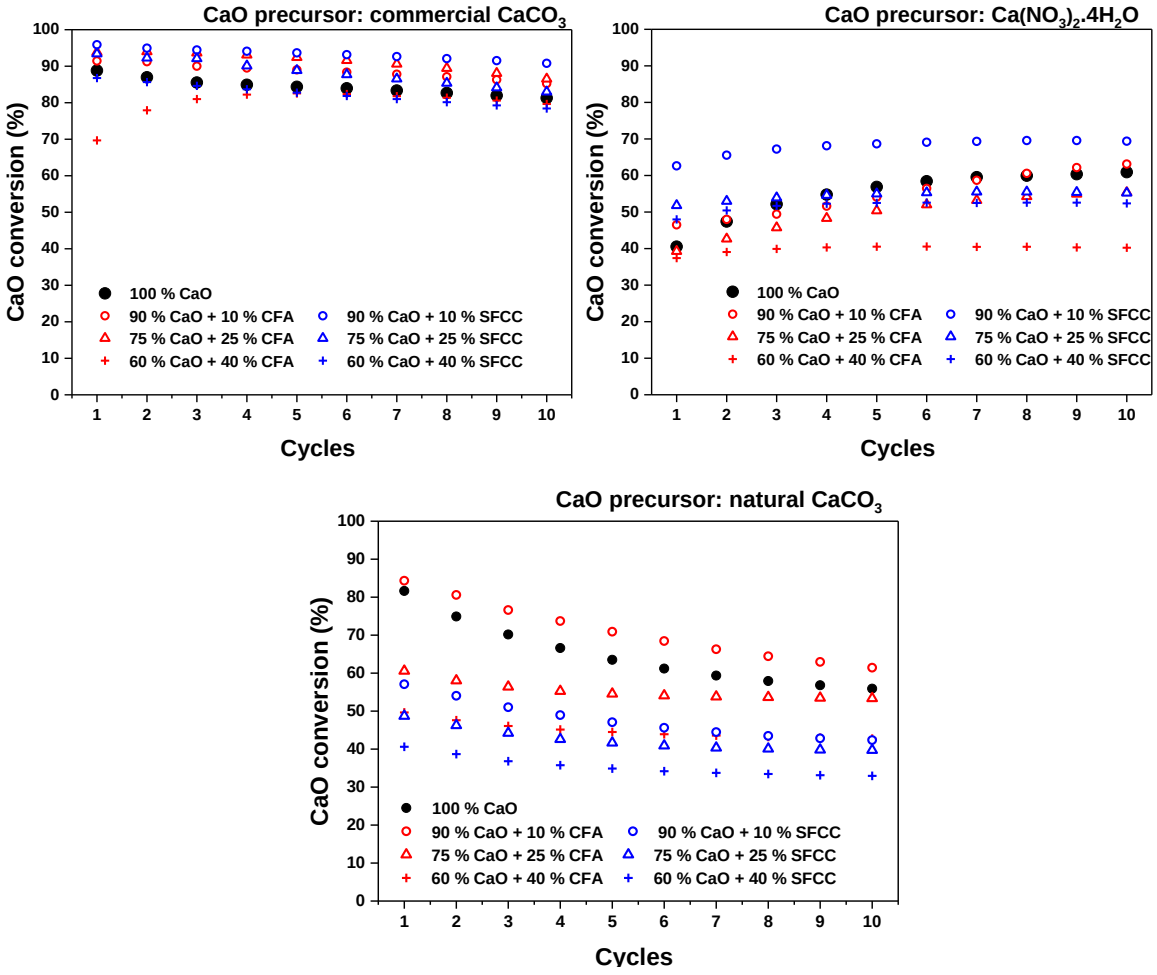

Figure 5.5: CaO conversion (%) of commercial $CaCO_3$, $Ca(NO_3)_2.4H_2O$, natural $CaCO_3$ sorbents

A comparison between performance of 100 % of CaO and 90 % of CaO with 10 % of waste-supported sorbents prepared with 10 g (CaO basis) is illustrated in Figure 5.6. The commercial $CaCO_3$ sorbent had a decay behavior which was much milder than the natural $CaCO_3$, but all their waste-supported sorbents showed an enhancement of the CaO conversion. The high CaO conversion and stability of commercial $CaCO_3$ sorbents is attributed to their smaller and well distributed particles (Figure 5.3b) with their coral shape with higher surface area than natural $CaCO_3$ which particles are larger and less porous. There is no significant effect of adding the 10 % CFA to the $Ca(NO_3)_2.4H_2O$ but an improved CaO conversion was observed when 10 % of SFCC was added. This can be explained through a research that concluded that blockage of pores below 3 nm can happen due to deposition of CFA [64],

which is in agreement with the relative smaller CFA particles obtained in Figure 5.4. The same research added that different CaO conversions with blended sorbents were obtained depending on the type of the CaO precursor (natural or synthetic sorbent) [64], as observed in Figure 5.6, the synthetic sorbents had better performance with SFCC than with CFA. The higher CaO conversion improvement observed for the 90 % of CaO with 10 % of SFCC mixture is probably due to the larger size of SFCC particles compared with the CFA (Figure 5.4), which increase the physical barrier action for this support and preventing the CaO agglomeration and pore blockage.

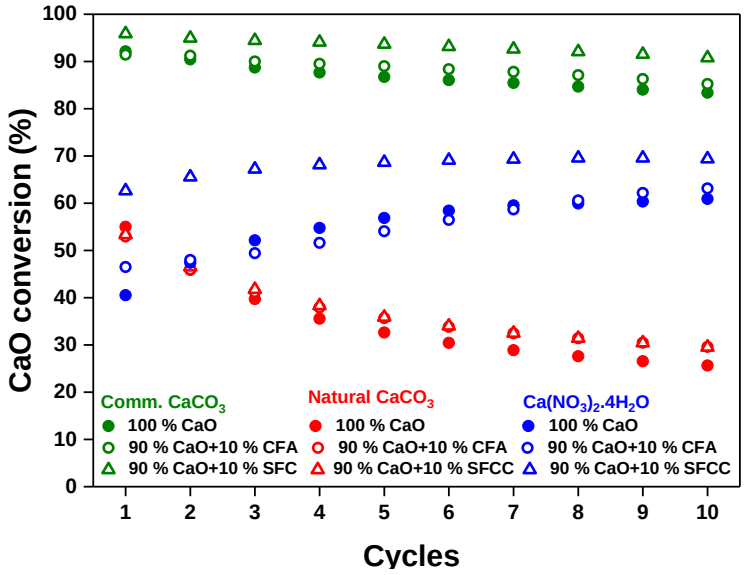

Figure 5.6: CaO conversion of 100 % CaO sorbents and 90 % CaO with 10 % waste-support sorbents

The findings about the inconsistency of results explained above were interesting, i.e. the different sorbent's mass introduced to the ball milling affects the mixing efficiency. Figure 5.7 compares the CaO conversion between 2 g and 10 g (CaO basis) sample blends for natural $CaCO_3$, and a higher CaO conversion was observed with the sample prepared with 2 g (CaO basis). The natural $CaCO_3$ with 10 % of CFA performed better than the mixture with 10 % of SFCC for the 2 g samples, this can be attributed to the smaller particles of CFA generated during milling process when compared to the SFCC as seen in (Figure 5.4). For the 10 g set the mixture with both CFA and SFCC performed similar yet better than the 100 % of CaO sorbent. It had lower CaO conversion on first cycle but achieved a higher reactivity stability along the cycles expressed in lower reactivity decay. The sorbent CO_2 capture deactivation (relative difference between the 1st and 10th cycle's CaO conversion) was evaluated for both set of samples, considering CaO conversion of the 1st cycle as the reference value. For samples prepared with 10 g (CaO basis) the deactivation varies between 44 % - 53 % and for samples prepared with 2 g the deactivation varies between 26 % - 32 % where the highest deactivation values occur with the 100 % of CaO in both sets.

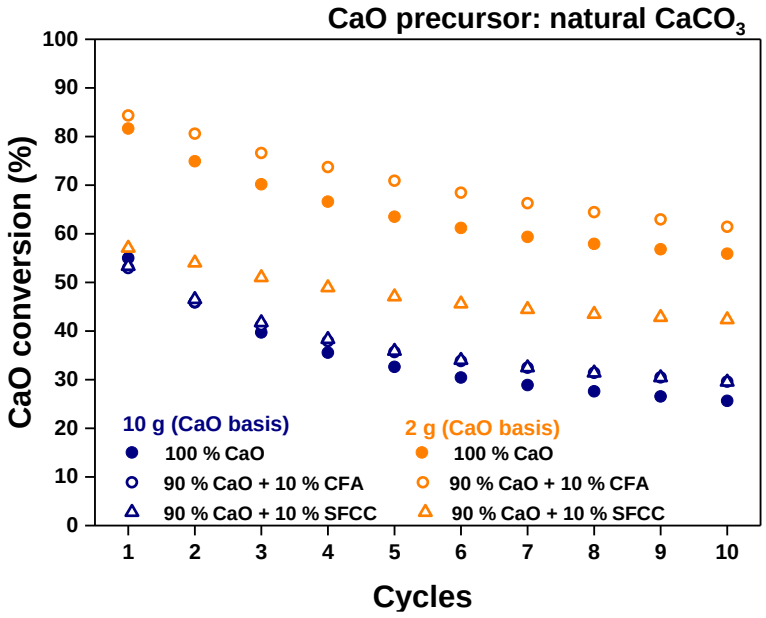

Figure 5.7: CaO conversion for 2 g and 10 g of natural $CaCO_3$ (CaO basis)

b. TGA reactivity test: impregnated SFCC sorbents

Impregnation of $Ca(NO_3)_2.4H_2O$ sorbent was carried out with the SFCC as it demonstrated better performance for dry physically mixing reactivity experiments than CFA. The goal of this experiment was not to perform an exhaustive evaluation of the wet impregnation technique for CO_2 capture using CaO based sorbents, yet in fact, it was an exploratory study. Figure 5.8 illustrates the performance of impregnated sorbents. Both the 90 % of CaO impregnated in 10 % of SFCC and 40 % of CaO in 60 % of SFCC had a lower CaO conversion as compared to the 100 % of CaO sorbent, which appears to be a very low conversion compared to the dry physically mixed sorbents. The sample impregnated with 90 % of CaO exhibited a higher CaO conversion than the sample prepared with 40 % of CaO. The CaO conversion increase along the cycles is usually attributed to the sorbent self-reactivation effect [48], as explained on 5.2.1a. The lower amount of CaO on the sample prepared only with 40 % of CaO justify its lower CaO conversion. Besides, the $Ca(NO_3)_2.4H_2O$ is not the most suitable CaO precursor due to its very low melting point (~45 °C) that promotes sintering, also it's consisted of a coarse and heterogenous morphology (Figure 5.10) and a lower pore volume (Table 5.3) after calcination [63].

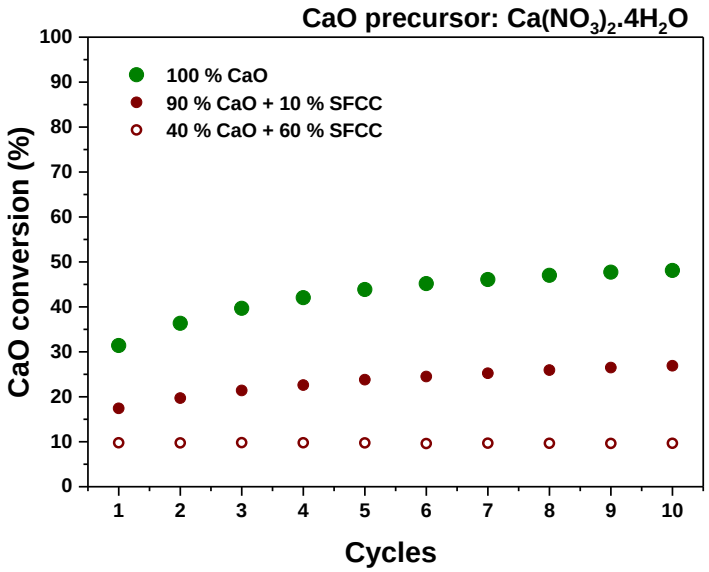

Figure 5.8: CaO conversion of $Ca(NO_3)_2.4H_2O$ precursor impregnated with different ratios in (SFCC)

Although the 40 % CaO with 60 % SFCC sample has a higher S_{BET} (Table 5.3), not much contribution was granted for increasing CaO conversion, because this S_{BET} increase is essentially due to the SFCC fraction as confirmed by its isotherm (Figure 5.9) profile following the SFCC isotherm presented in Figure 5.2. All the isotherms presented in Figure 5.9 are Type II (non-porous or macroporous materials), however, it was observed that the addition of SFCC as support provided some degree of mesoporosity which is proven by the hysteresis present in the case of supported sorbents.

The cubic, coarse, and heterogenous structure of the $Ca(NO_3)_2.4H_2O$ particles calcined sorbent can be observed in Figure 5.10a and b. After impregnation, in both cases the CaO particles seem deposited on the surface of SFCC. Apparently, when less CaO was used, the CaO particles were better spread on the SFCC surface and particles size appears to be more homogenous. In case of impregnation with 90 % of CaO it can be observed that several particles are dispersed without contacting the SFCC particles surface, and like the CaO sample without a support, larger and heterogenous particles are found. The higher S_{BET} observed on the sorbent supported with 60 % of SFCC is also in agreement with the formation of small particles, and of course, the high S_{BET} of SFCC.

At this moment this impregnation technique does not look very promising, but additional studies can be performed in future with another CaO precursor (e.g. $Ca(CH_3OO)_2$ or $Ca(C_5H_7O_2)_2$) that usually have better carrying capacity performance [63].

Table 5.3: Specific surface area (S_{BET}, m^2/g) and total pore volume (V_p, cm^3/g) of CaO sorbent precursor ($Ca(NO_3)_2.4H_2O$) impregnated in SFCC

CaO sorbent precursor ($Ca(NO_3)_2.4H_2O$) impregnated in SFCC	S_{BET} (m^2/g)	V_p (cm^3/g)
90 % CaO + 10 % SFCC	4.04	0.01
40 % CaO + 60 % SFCC	5.44	0.01

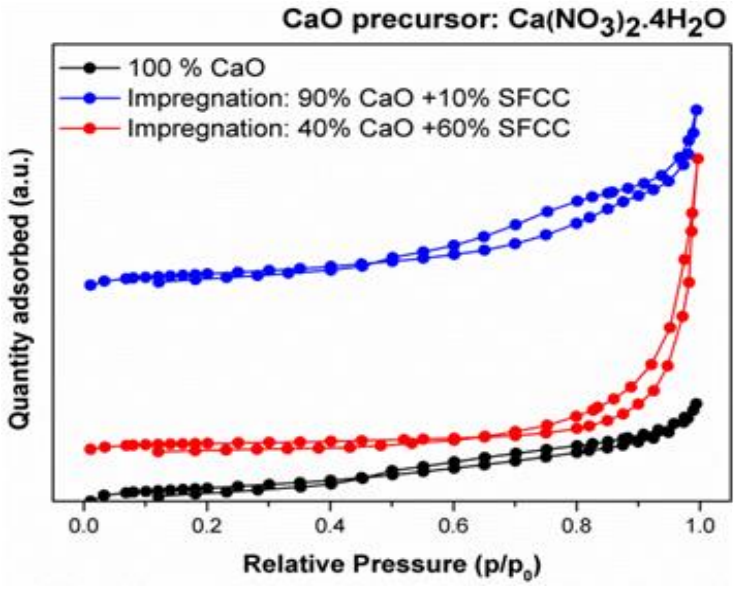

Figure 5.9: Isotherms obtained from N2 sorption technique of impregnated CaO on SFCC

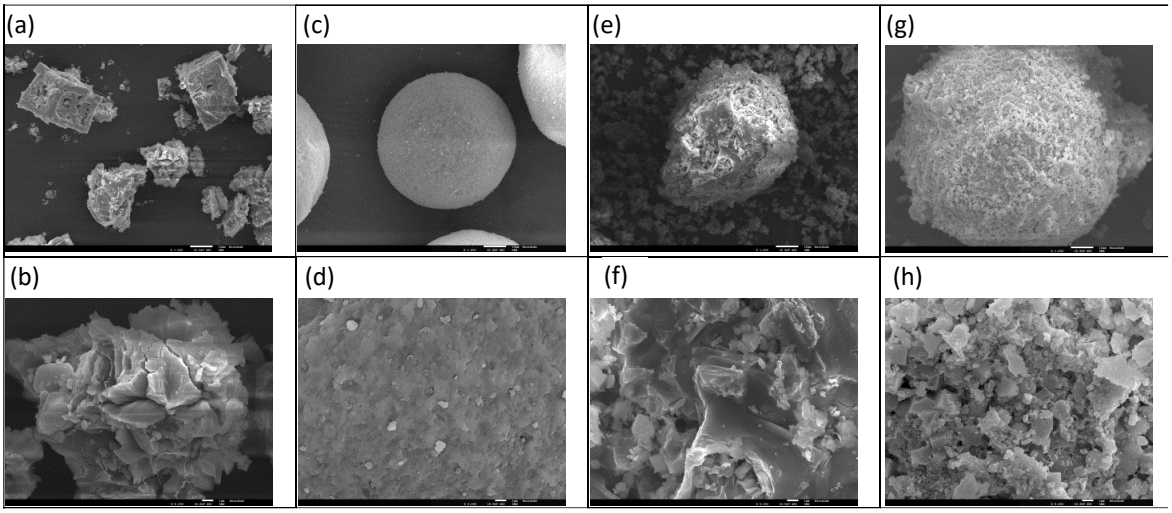

Figure 5.10: SEM micrographs of sorbent and support samples calcined at 900ºC: (a) and (b) $Ca(NO_3)_2.4H_2O$, (c) and (d) SFCC, (e) and (f) impregnation: 90 % CaO + 10 % SFCC, (g) and (h) impregnation: 40 % CaO + 60 % SFCC. The scale of micrographs in first row is 10 µm and in second row is 1 µm.

5.2.2 Reactivity test carried out on fixed-bed unit

The CaO carrying capacity experiments conducted on the fixed bed unit were tailored according to the TGA experiments results demonstrated in section 5.2.1, where the best performing supported sorbents; i.e. 90 % of CaO precursor with 10 % of waste support, were tested on the fixed bed unit. Figure 5.11 illustrate the CaO conversion of pure natural and commercial $CaCO_3$, as well as the mixtures performed with 10 % of waste-derived supports.

The main highlight that can be taken from Figure 5.11 is that as observed on the TGA experiments, the commercial $CaCO_3$ presents a higher CaO conversion than the natural $CaCO_3$ for the 1st cycle. Besides, the commercial $CaCO_3$ had a lower deactivation rate than the natural $CaCO_3$, i.e. 36 % and 69 %, respectively, after 20 cycles. For both sorbents the addition of waste-derived supports improved the CaO conversion of sorbents.

CFA blends had a slightly better performance along the cycles indicating that their particles produced a favorable mixture with the CaO precursors leading to reduced agglomeration of CaO. The deactivation rate of commercial and natural $CaCO_3$ was respectively, 22 % and 58 % when CFA was used as a support, but this deactivation rate increased to 29 % and 64 % when SFCC was used. Possible explanation for this can be that the lower size of CFA particles, which facilitates their dispersion on the CaO particles or its higher thermal stability. Usually CFA is obtained from a thermal conversion process that occurs at temperatures higher than 850 °C, and the SFCC is obtained from a catalytic process performed at lower temperatures (<600 °C).

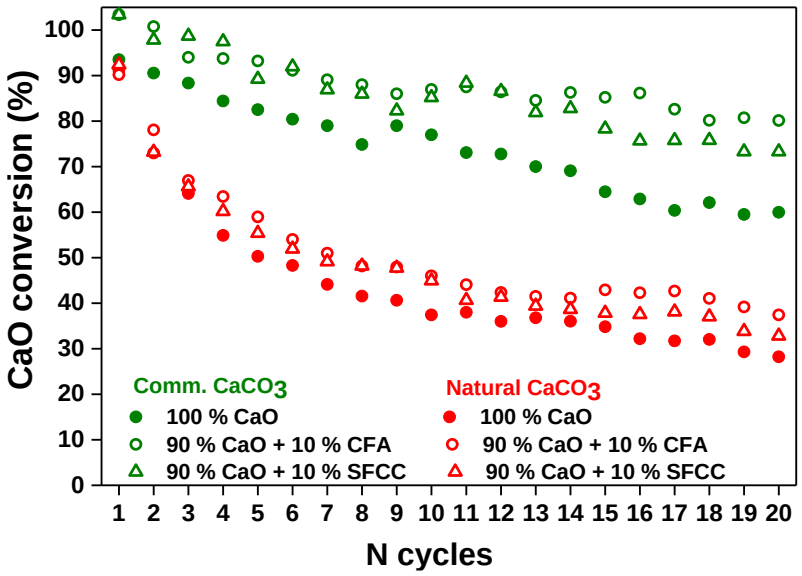

Figure 5.11: CaO conversion of pure sorbents and CaO sorbents supported with 10 % CFA and SFCC over 20 calcination-carbonation cycles carried on fixed bed

The differences observed on CaO conversion, after 10 cycles, of sorbents tested on fixed bed unit when compared to the CaO conversion of the same sorbent resulted from the TGA test can be attributed to two factors; first, the gas flow and second, the time allowed for the carbonation and calcination reactions. On TGA tests, the gas flow is reaching from the top of the sample inside a crucible, which cause a diffusional limitation of gas flow through the CaO sorbent, meanwhile on the fixed bed it's completely different, because the gases flow through the sample allowing for a higher interaction between gases and sorbent. This is especially evident on the first cycles and for samples with lower porosity, as in the case of natural $CaCO_3$. In the TGA the 1st CaO conversion is about 55% but for the experiment carried out on the fixed bed unit is 91%. Along the cycles, due to the development of a skeleton structure (explained on 5.2.1a), which defines the sorbent carrying capacity [26], this effect is not so evident.

The second factor is the time allowed for the carbonation-calcination reactions. In TGA a constant time for the reactions of carbonation and calcination is pre-scheduled, in case of carbonation the reaction is much slower in TGA than in fixed bed, c.a. 60 min vs 15 min for the TGA and fixed bed unit, respectively. Even the 60 min defined for the TGA experiments were insufficient for complete carbonation, but it was not feasible to use higher reaction times for the carbonation due the restrictions of the TGA apparatus availability, as mentioned on subsection 4.2.1. On the fixed bed unit, the carbonation step was only

considered complete when the exhaust gas passing through the CO_2 detector stabilizes around the feed gas CO_2 concentration (e.g. 25% of CO_2) which indicates complete sorbent carbonation. Relatively to the calcination reaction, because it is only considered complete when the concentration on CO_2 on the detector is lower than 0.05 %, often the time required for the total calcination is higher on the fixed bed unit than in the TGA. This means that the sorbent is exposed to high temperatures (800 ºC or 900 ºC) for longer times which contributes for a higher sintering degree and sorbent deactivation.

On the middle calcination-carbonation cycles shown in Figure 5.11 a sudden improvement can be observed on sorbents' performance especially for the commercial $CaCO_3$. This can be justified by the fact mentioned in subsection 4.3.3, when an experimental test was conducted along 2 days and the samples were held under reduced flow of air at ambient temperature during the night, this procedure is seen to be responsible for this small increase in reactivity of the sorbent. The irregularity of data present in above figure in comparison with the TGA CaO conversion results can be related to the methodology used to calculate the sorbents CaO conversion. The quantification of CO_2 captured by the sorbent as described in subsection 4.3.4. and illustrated in Figure 4.6 seems to be very sensitive to small variation of interval times. In present study the data were acquired in each 5 seconds, but lower interval time is proposed for future tests.

Table 5.4: Specific surface area (S_{BET}, m^2/g) and total pore volume (V_p, cm^3/g) of pure and supported CaO sorbents CFA/ SFCC tested in the fixed bed unit for (0 cy) and 20 carbonation-calcination cycles (20 cy)

CaO-based sorbent			S_{BET} (m^2/g)	V_p (cm^3/g)
Commercial $CaCO_3$	**100 % CaO**	0 cycle	24.6	0.09
		20 cycle	14.4	0.06
	90 % CaO + 10 % CFA	0 cycle	25.6	0.1
		20 cycle	16.9	0.09
	90 % CaO + 10 % SFCC	0 cycle	33.4	0.13
		20 cycle	23.8	0.11
Natural CaCO3	**100 % CaO**	0 cycle	31.1	0.21
		20 cycle	10	0.06
	90 % CaO + 10 % CFA	0 cycle	21.1	0.1
		20 cycle	15.2	0.05
	90 % CaO + 10 % SFCC	0 cycle	27.4	0.15
		20 cycle	15.7	0.05

Textural properties shown in Table 5.4 give an insight on the CaO conversion behavior of the sorbents shown in Figure 5.11, the increased S_{BET} of waste-supported commercial sorbents (slightly in case of 90 % of CaO with 10 % of CFA) can justify their initial higher CaO conversion as compared to the 100 % of CaO sorbent. The S_{BET} at 0 cycle (after pre-calcination) increased from 24.6 m^2/g for 100 % of CaO to 25.6 m^2/g and 33.4 m^2/g for CFA and SFCC blends, respectively, a similar proportion increase was observed for the total pore volume. In case of 90 % of CaO with 10 % of SFCC the higher S_{BET} is

also related with the textural characteristics of SFCC that is microporous zeolite-based catalyst. Enhanced CaO conversion can be observed after 20 cycles where the final S_{BET} remained higher for waste blends that for the 100 % of CaO sorbent.

The natural $CaCO_3$ sorbents behaved differently where the S_{BET} after pre-calcination (0cycles) is lower for waste blended sorbents. Previously, it was noticed during characterization of fresh sorbents that the S_{BET} of natural $CaCO_3$ increased 3.8 times and for commercial $CaCO_3$ it increased 2 times after the calcination in the muffle (Table 5.2). This is an evidence that during the first calcination of natural $CaCO_3$, a higher porous material is obtained due to CO_2 release and presence of impurities that contribute for a high S_{BET}. However, the waste addition has a positive effect on the S_{BET} value along the cycles, the lower loss of S_{BET}, was smaller for CFA and SFCC supported sorbents, i.e. only 28 % and 43 % compared to the 68 % for pure sorbents. And with a final S_{BET} of around 15 m^2/g for waste supported sorbents and 10 m^2/g for 100 % of CaO sorbent after 20 cycles. Similarly, the reduction in V_p was greater for the pure sorbent against the waste-supported sorbents.

N_2 adsorption isotherms (Figure 5.12) for the commercial $CaCO_3$ sorbents show that pre-calcined (0 cycle) and spent sorbents have a type II isotherms, which is a characteristic feature of non-porous and macroporous materials. The hysteresis profile means that the sorbent also has some mesopores, that is maintained after 20 cycles. The natural $CaCO_3$ sorbents have a similar type II isotherm, however, unlike what happened for the commercial $CaCO_3$, after 20 cycles, the natural $CaCO_3$ lost the mesoporosity as can be observed on Figure 5.12, where the hysteresis profile disappears. This agrees with the higher deactivation of natural $CaCO_3$ after 20 cycles comparatively with the commercial $CaCO_3$.

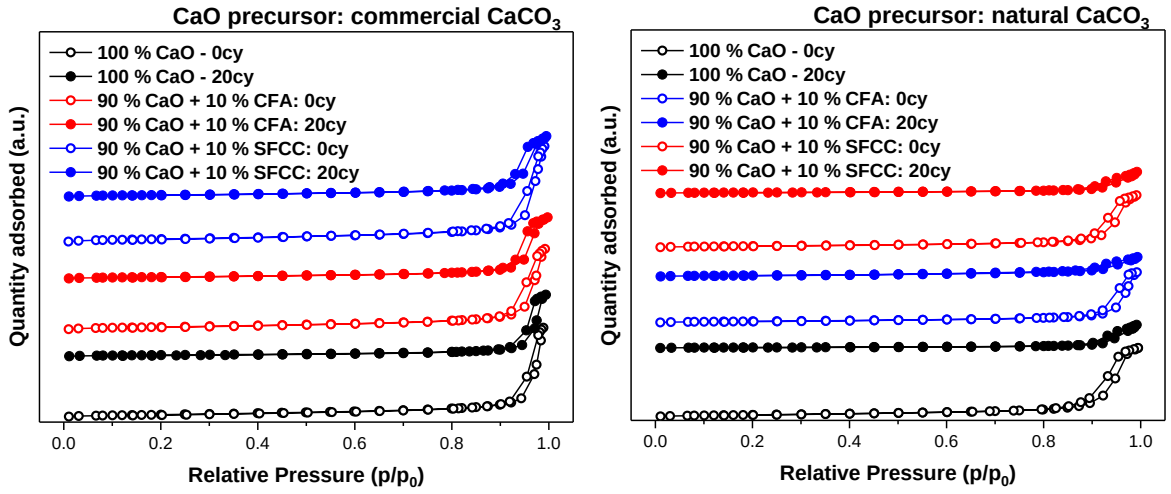

Figure 5.12: N_2 adsorption isotherms for pure and waste supported CaO sorbents tested in the fix bed unit after 0 cycle and 20 calcination-carbonation cycles

BJH desorption was used to determine the PSD of spent CaO sorbents (after 0 and 20 cycles). Figure 5.13 shows that the commercial $CaCO_3$ almost maintained its total pore volume at a constant level with only small reduction as also shown in (Table 5.4), while the pore width was mainly in the range of mesopores (2 nm - 50 nm) with a small share of macropores, namely, in case of sorbent without waste support.

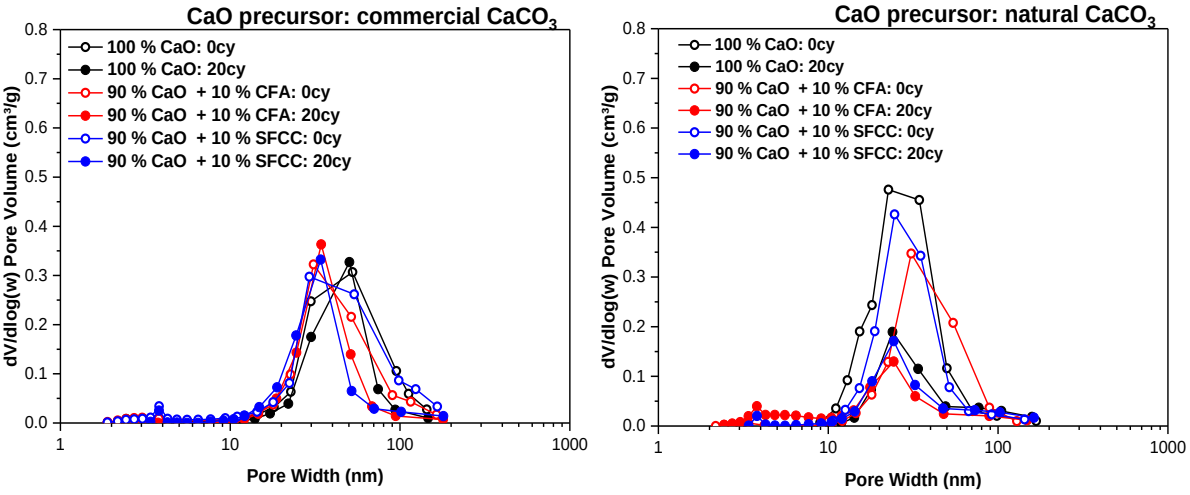

Figure 5.13: BJH desorption pore size distribution of pure and waste supported CaO sorbents tested in the fix bed unit after 0 cycle and 20 calcination-carbonation cycles

For the natural $CaCO_3$ pure and waste-supported sorbents. a reduction in total pore volume after 20 cycles was observed (Table 5.4) where between 0 cycle and 20 cycles the CaO sorbent supported with CFA lost half of its V_p. For the other sorbents the V_p loss was higher, this pore volume reduction is attributed to the sintering and agglomeration of CaO particles followed by macropores formation. The PSD shows that the decrease in V_p is more pronounced for the sorbent without support, however, a significant increase in average pore width is not observed, i.e. the average pore width is always between 20 nm – 30 nm, it's important to remember that N_2 sorption only allows observing pore width up to around 100 nm. For identification of macropores (> 100 nm) the Hg porosimetry technique should be used.

Figure 5.14 shows the SEM images for the pure and the waste blends of commercial $CaCO_3$ after 20 cycles. The sorbent with 100 % of CaO (Figure 5.14a) has grown in particle size compared to fresh sorbent shown in (Figure 5.3b), this increase in particles size resulted in loss of S_{BET} that is shown above. No much difference can be seen between Figure 5.14b and c, except for the presence of CFA (Figure 5.14b) particle while for SFCC (Figure 5.14c) it appears to be completely covered by the CaO. On x20000 magnification, i.e. (Figure 5.14d, e, and f) a clear sintering of 100 % of CaO sorbent particles is observed with loss of stacked particle-shape look which is substituted by a more rounded swollen one. Waste support apparently prevented the CaO particles agglomeration, i.e. the particles of CaO looks smaller and less compact. This structure and texture of commercial $CaCO_3$ mixed with wastes were involved in stability behavior of sorbent by reducing the loss of total pore volume obtained from the pure sorbent. Also, it contributes to the reserving of the S_{BET}, which is higher for waste-supported sorbents than that for the 100 % of CaO sorbent.

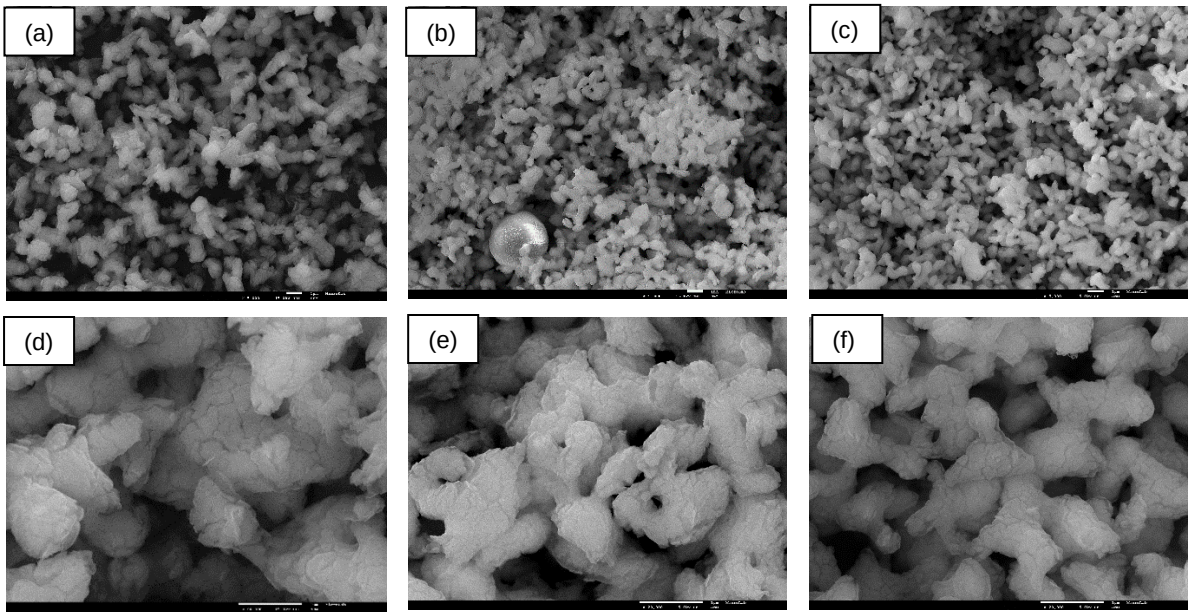

Figure 5.14: SEM micrographs for Commercial $CaCO_3$ sorbents after 20 Calcination-carbonation cycles, a) 100 % CaO, b) 90 % CaO with 10 % CFA, c) 90 % CaO with 10 % SFCC (all at x5000 magnification and scale: 1 µm). d) 100 % CaO, e) 90 % CaO with 10 % CFA, f) 90 % CaO with 10 % SFCC (all at x20000 magnification and scale: 1 µm)

For the natural $CaCO_3$ sorbents SEM micrographs showed that for the 100 % of CaO sorbent, the particles found before on Figure 5.3a are now as CaO particles, more rounded and cracked (Figure 5.15a and d) due to the sintering occurring during the $CaCO_3$ decomposition and CO_2 release at temperature. SEM micrographs for 90 % of CaO with 10 % of CFA show the presence of some CFA particles that hold CaO particles on its surface and thus reducing agglomeration and particles size growth, since these CFA particles actuate as a physical barrier between CaO particles. The larger SFCC particles seen in the SEM images (Figure 5.4) are not found in the SEM micrographs of used sorbent with 90 % of CaO with 10 % of SFCC, except for very small spherical particles that may be SFCC. This disappearance of SFCC particles can be explained by: first, at such high calcination temperature (i.e. 900 °C) the SFCC particles melt down and lose their rounded shape, second, milling is responsible for demolition of rounded shape as presented in a work [65] which aim to improve SFCC activity by grinding. The SEM images presented for grinded SFCC [65] didn't show rounded particles that existed before grinding, yet they looked a bit similar to the blend with the CaO precursor.

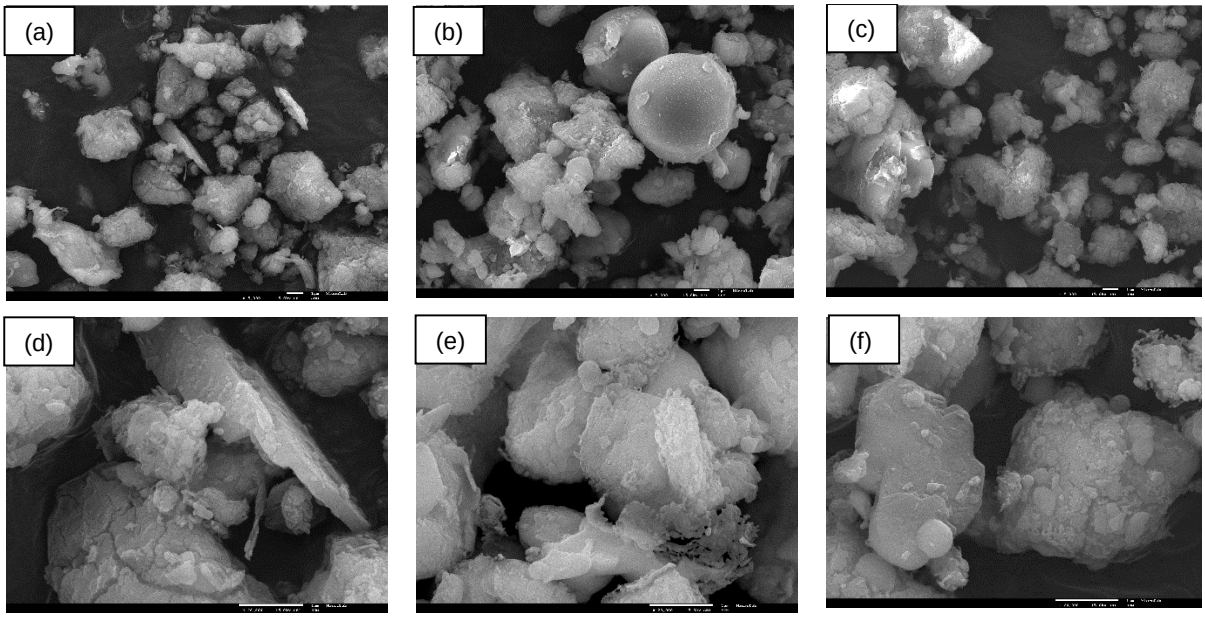

Figure 5.15: SEM micrographs for natural $CaCO_3$ sorbents after 20 Calcination-carbonation cycles, a) 100 % CaO, b) 90 % CaO with 10 % CFA, c) 90 % CaO with 10 % SFCC (all at x5000 magnification and scale: 1 µm). d) 100 % CaO, e) 90 % CaO with 10 % CFA, f) 90 % CaO with 10 % SFCC (all at x20000 magnification and scale: 1 µm)

In agreement with the data illustrated above, Figure 5.16 shows the average crystallite size of CaO on the sorbents, either pure or blended with waste support. The blend between commercial $CaCO_3$ and 10 % of CFA appears to very slightly inhibit the increase of average crystallite size of sorbent where after 20 cycles it had an average size of c.a. 37 nm, which is lower than the value observed for 100 % of CaO sorbent i.e. c.a. 39 nm. The blend with SFCC had the highest average crystallite size, i.e. c.a. 43 nm. For the natural $CaCO_3$ blends the crystallite size was almost similar, stabilizing at a value of c.a. 41 nm for the 100 % of CaO sorbent and c.a. 42 nm for both CFA and SFCC blends. So, in the case of commercial $CaCO_3$ the addition of waste-derived supports had a small effect on the size of crystallite, and, for the natural $CaCO_3$ no considerable decrease was observed.

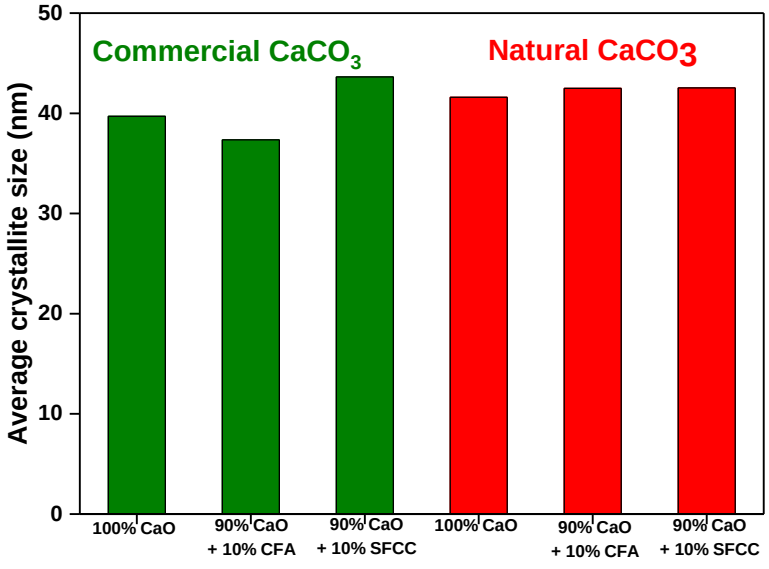

Figure 5.16: CaO crystallite size of commercial and natural $CaCO_3$ and their blends

5.2.3 Reactivity test carried out on in-situ XRD

Experiments performed on the in-situ XRD unit aimed to give an additional insight about the mineralogical change of the sorbent, namely $CaCO_3$ and CaO compositions during each carbonation and calcination cycle, respectively. The great advantage of this technique is the possibility of observing in real time and at the temperatures used for the carbonation-calcination reactions the behavior of sorbent, helping in the understanding of the deactivation process. Figure 5.17 and Figure 5.18 show the mineralogical composition of the natural $CaCO_3$ sorbent without support and with 25% of CFA, during each carbonation and calcination cycle obtained from the XRD pattern.

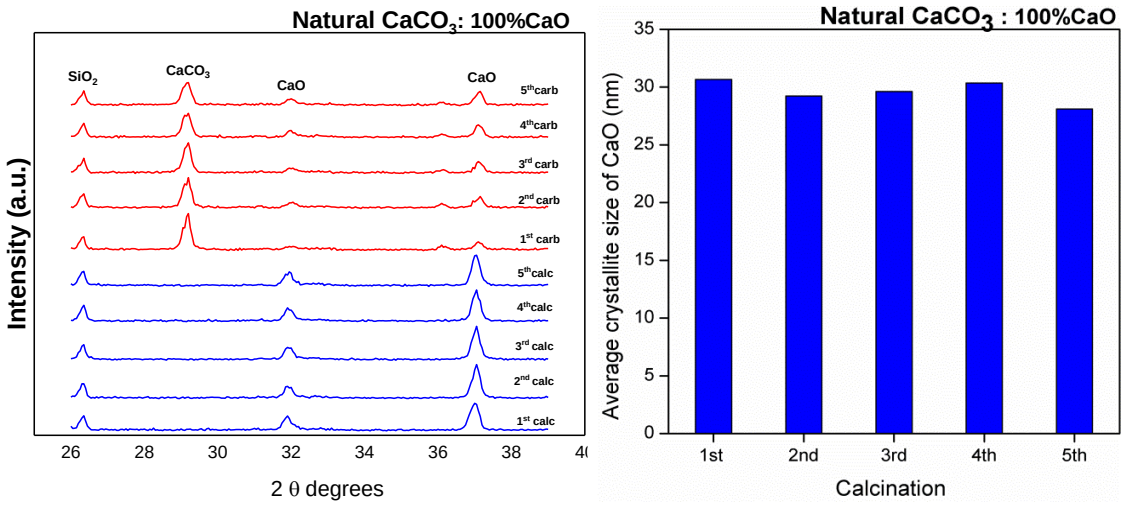

Figure 5.17: XRD and CaO average crystallite size of 5 calcination-carbonation cycles for 100 % natural $CaCO_3$

Along the carbonation cycles it's clear that the intensity of $CaCO_3$ (29° in 2θ) is decreasing, which indicates a reduction in the CaO carbonation, which means that with increasing number of cycles some of the CaO formed during the calcination doesn't take part in next cycle carbonation, as confirmed by the increment of CaO peak (37 º in 2θ) during the carbonation along the cycles. The presence of unreacted CaO during the carbonation looks more pronounced in case of sorbent only with CaO than in sorbent with 25 % of CFA.

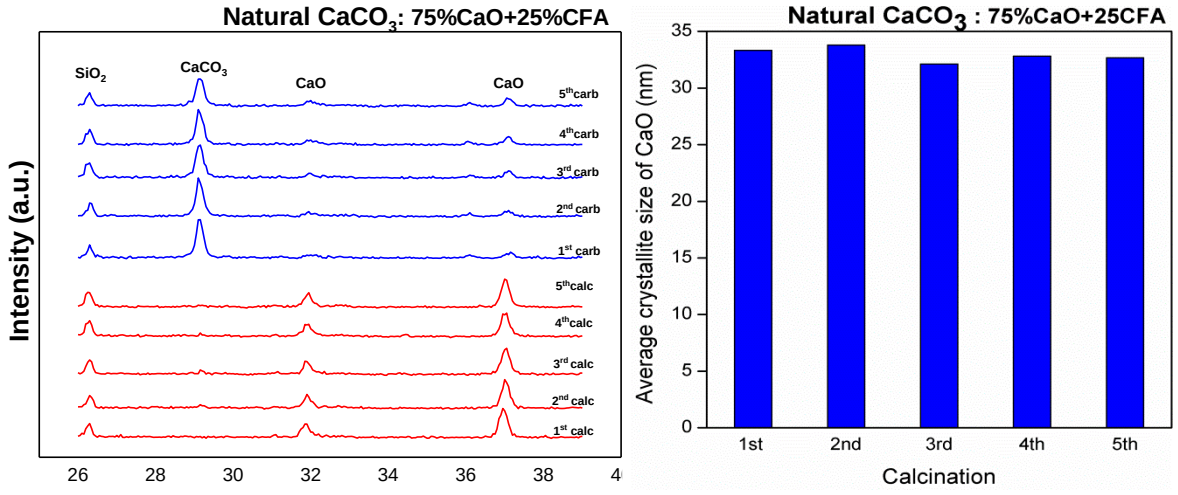

Figure 5.18: XRD and CaO average crystallite size of 5 calcination-carbonation cycles for 75% Natural $CaCO_3$ with 25% CFA

On the calcination cycles, very small changes can be traced on the XRD patterns. The absence of $CaCO_3$ during the calcination cycles confirms that the calcination of sorbent was complete. The peak observed in all cases near 26º in 2θ, is from SiO_2 present on natural $CaCO_3$ that maintains the same appearance along the cycles.

Scherrer's equation mentioned in section 3.4 was used to estimate the CaO average crystallite size during the calcination step for both samples tested. As can be observed on Figure 5.17 and Figure 5.18, for both sorbents the average crystallites size remained almost constant along these 5 cycles, which means that at least during the first cycles, the growth of CaO crystallites should not be the main reason for the sorbents deactivation. So, these results suggest that the deactivation observed during the experimental tests performed in the TGA and fixed bed unit, for the first five cycles, it should be more related with the pores blockage during the carbonation than with the sintering and agglomeration of CaO crystallites.

5.3 INFLUENCE OF CO_2 CALCINATION ATMOSPHERE AND STEAM ADDITION DURING CALCINATION ON THE CaO CONVERSION

This section illustrates the effect of carrying out experiments under different calcination-carbonation reaction atmosphere, namely on the CO_2 carrying capacity performance of the natural $CaCO_3$. These atmospheres are: (1) calcination under 100 % of air and carbonation under 75 % of air plus 25 % of CO_2, this atmosphere is denoted by standard conditions; (2) calcination at 100 % of CO_2 and carbonation at 75 % of air plus 25 % of CO_2 denoted by CO_2 calcination; (3) calcination at 95 % of air plus 5 % of steam and carbonation at 70 % of air plus 5 % of steam and 25 % of CO_2 denoted by 5 % of steam, pre-calcination conditions where similar to the calcination. These experiments were conducted in the fixed bed unit for 0 and 20 cycles, and sorbents were then characterized by the above-mentioned techniques (section 3).

Figure 5.19 shows that the presence of steam during calcination had a significant negative effect on the initial CaO conversion. Meanwhile, a 100% of CO_2 calcination atmosphere had a small negative effect on the initial CaO conversion, but it kept on affecting negatively the CaO conversion, and a final conversion of c.a. 17 % was achieved. On the other hand, the steam presence stabilized the CaO conversion along the cycles resulting in a CaO conversion of 36 % after 20 cycles, i.e. higher than the 28 % achieved for standard conditions. Extensive sintering of CaO tested under CO_2 calcination atmosphere appears to start after the 5th cycle. A possible explanation is presented by [48], i.e. when the CO_2 calcination starts at 900 °C, the $CaCO_3$ phase is still present and due to its low Tammann temperature (524 °C) comparatively with the CaO Tammann temperature (1170 °C), the sintering of sorbent is promoted. This is mitigated in calcination atmospheres without CO_2, like air or N_2, when the calcination temperature (900 °C) is reached, the CaO phase would already exist due to the $CaCO_3$ decarbonation (Figure 2.3).

Steam addition apparently seems to produce two different effects on CaO conversion of natural $CaCO_3$, an adverse at the initial cycles which can be attributed to the conclusions presented on [42], i.e. steam presence during calcination enhances sintering due to the higher thermal conductivity and heat capacity of steam compared to air, which explains the reduced initial conversion with steam. The second effect was observed after the 10^{th} cycle, where an improvement in sorbent stability was obtained during steam addition, which is attributed to the reduction of diffusion resistance through the carbonate layer and the formation of small pores due to the steam addition as stated in [42, 66]. This is consistent with the fact that the carbonation occurs in two stages (Figure 2.2), as already mentioned the second is a slow diffusion-limited stage that becomes dominant with the increasing number of cycles due to the sorbents surface area and pore volume reduction, that benefits with the layer diffusion properties improvement due to steam.

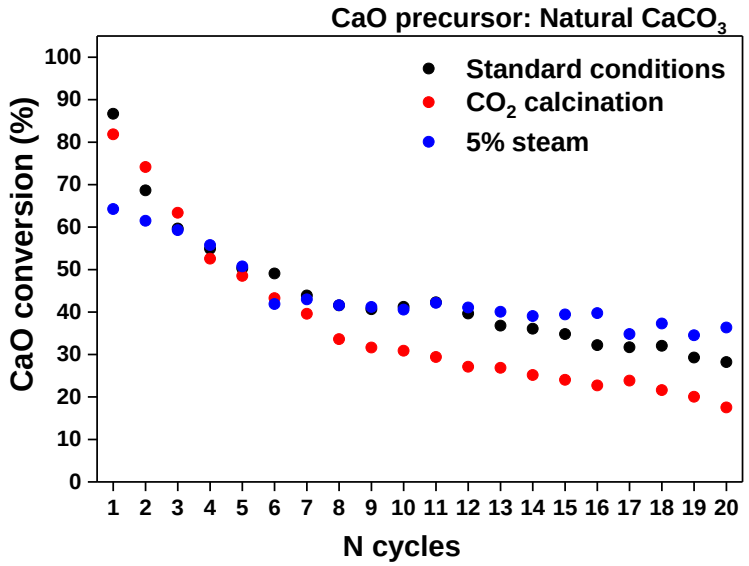

Figure 5.19: CaO conversion of natural $CaCO_3$ sorbent tested in a fixed bed unit under different experimental conditions

The textural properties of the natural $CaCO_3$ tested under different atmospheres (0 and 20 cycles) are presented in Table 5.5. When tested under standard conditions and CO_3 calcination, the textural properties evaluated agree with CaO conversion profile, i.e. after 20 cycles the S_{BET} of the sorbent tested under standard conditions went down from 31 m^2/g to only 10 m^2/g losing c.a. 67 % of its initial value and V_p from 0.2 cm^3/g to 0.06 cm^3/g due to sintering of sorbent. This sintering effect was worse in case of CO_2 calcination atmosphere where sorbent lost c.a. 72 % of its S_{BET} and the V_p went from 0.17 cm3/g to only 0.05 cm3/g after 20 cycles. For 5 % of steam atmosphere test, an improvement in sorbent textural properties was observed. In agreement with the lower CaO conversion values observed in firsts cycles on the fixed bed, an initial lower S_{BET} and V_p were observed, which are justified by the effect of steam in sintering enhancement during the calcination as mentioned above. The enhancement on textural properties observed after 20 cycles, i.e. the S_{BET} and V_p values duplicate, can be explained by the changes on the layer diffusion of CaO based sorbent by the steam.

Table 5.5: Specific surface area (S_{BET}) and total pore volume (V_p) of natural $CaCO_3$ tested in the fixed bed unit after the activation (0 cy) and 20 carbonation-calcination cycles (20 cy), under different experimental conditions

Experimental condition		S_{BET} (m^2/g)	V_p (cm^3/g)
Standard conditions	**0 cycle**	31.1	0.20
	20 cycles	10	0.06
CO_2 calcination	**0 cycle**	25	0.17
	20 cycles	6.9	0.05
5 % steam	**0 cycle**	12.3	0.04
	20 cycles	25	0.08

BJH desorption method to estimate the pore size distribution (Figure 5.20) further shows the porosity change promoted by different atmospheres. It was observed that, independently of the used atmosphere the natural $CaCO_3$ lose pore volume after 20 cycles, which is associated to the sintering process. The natural $CaCO_3$ contains mainly mesopores, between 20-30 nm for standard conditions and CO_2 calcination, and 50 nm for sorbent tested under steam atmosphere. However, under CO_2 calcination and steam addition, some small macropores are also present since the activation of the sorbent (0 cycles). The development of these macropores should be justified by the loss of mesopores due to the CaO sintering, as mentioned previously in this section. In the presence of 5 % of steam, after 20 cycles the initial pore size distribution was split into two different populations. Both populations are in the range of mesopores: a decreasing population with the same average pore width (50 nm) and an increasing population of pores shifted to lower mesopores sizes with pore widths in the range from 2.5 to 11 nm. This explains the increase of S_{BET} and V_p observed on Table 5.5.

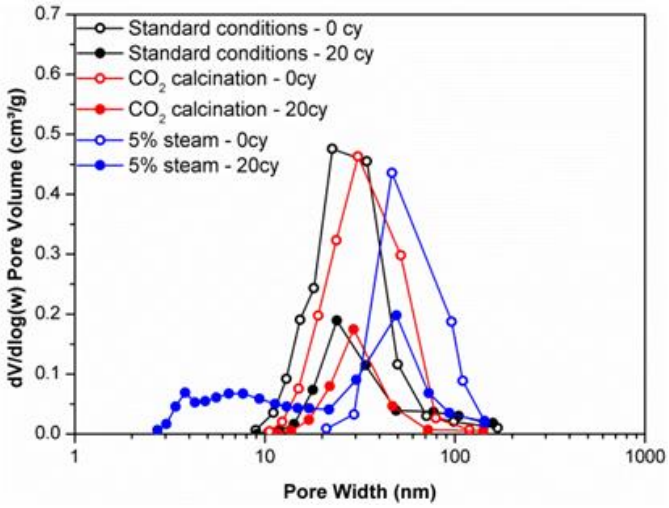

Figure 5.20: Pore size distributions obtained from N_2 adsorption (PSD from BJH desorption branch) of natural $CaCO_3$ tested in the fixed bed unit after the activation (0 cy) and 20 carbonation-calcination cycles (20 cy), under different experimental conditions

The average crystallite size (Figure 5.21) and SEM images (Figure 5.22) performed for the natural $CaCO_3$ tested different atmospheres, support the findings presented above. After the pre-calcination (0 cycles) under standard conditions, an average crystallite size of 24 nm was estimated, much lower than the crystallites sizes estimated for the CO_2 calcination and 5 % of steam atmosphere, respectively, 33 nm and 43 nm. This reinforce the previous explanations about the atmosphere effect on the sintering [42][48]. Under CO_2 calcination the crystallite size grown up 27 nm, between the 0 and 20 cycles, meanwhile, under standard conditions the crystallite grown up only 17nm. These results agree with the CaO conversion obtained on the fixed bed, i.e., higher crystallites usually are related with higher sintering degree and lower CO_2 carrying capacity. This is supported by the SEM images as comparing the large particle size of CaO calcined sorbent (Figure 5.22a and c), which appear to be highly sintered, with the particle size for sorbent tested under standard conditions (Figure 5.15a and d).

The presence of steam contributes for the stabilization of the average crystallite size of sorbent, i.e., after 20 cycles the crystallite maintain the 43 nm. At the beginning, the steam contributes to the sintering and fast grow up of crystallites, but it was followed by the CaO crystallites size stabilization, probably due the S_{BET} and V_p increase in presence of steam (related with diffusional layer changes). The SEM image of 20 cycles test performed with steam (Figure 5.22b) show large and small particles, as well as several cracks within the surface of particles (x5000 magnification). Comparatively with Figure 5.15d, the Figure 5.22d (x20000 magnification) show flatter-more shaped small particles, which is in accordance with the higher S_{BET} of the sorbent after 20 cycles (Table 5.5). The morphology of this sample should be maintained by the steam presence, which contributes for higher S_{BET} values, small pores, access to deeper pore space, and consequently, high and stabilized CaO conversions.

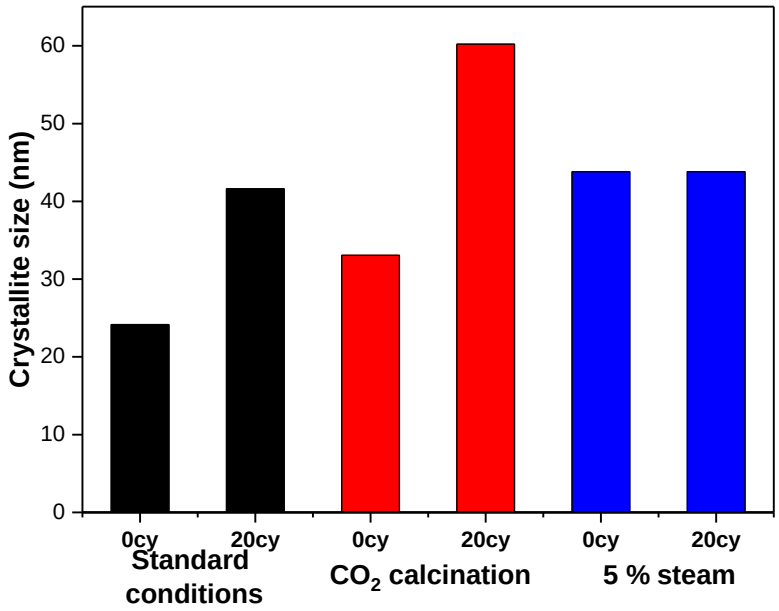

Figure 5.21: Crystallite size (nm) obtained from Scherrer equation of natural $CaCO_3$ tested in the fixed bed unit after the activation (0 cy) and 20 carbonation-calcination cycles (20 cy), under different experimental conditions

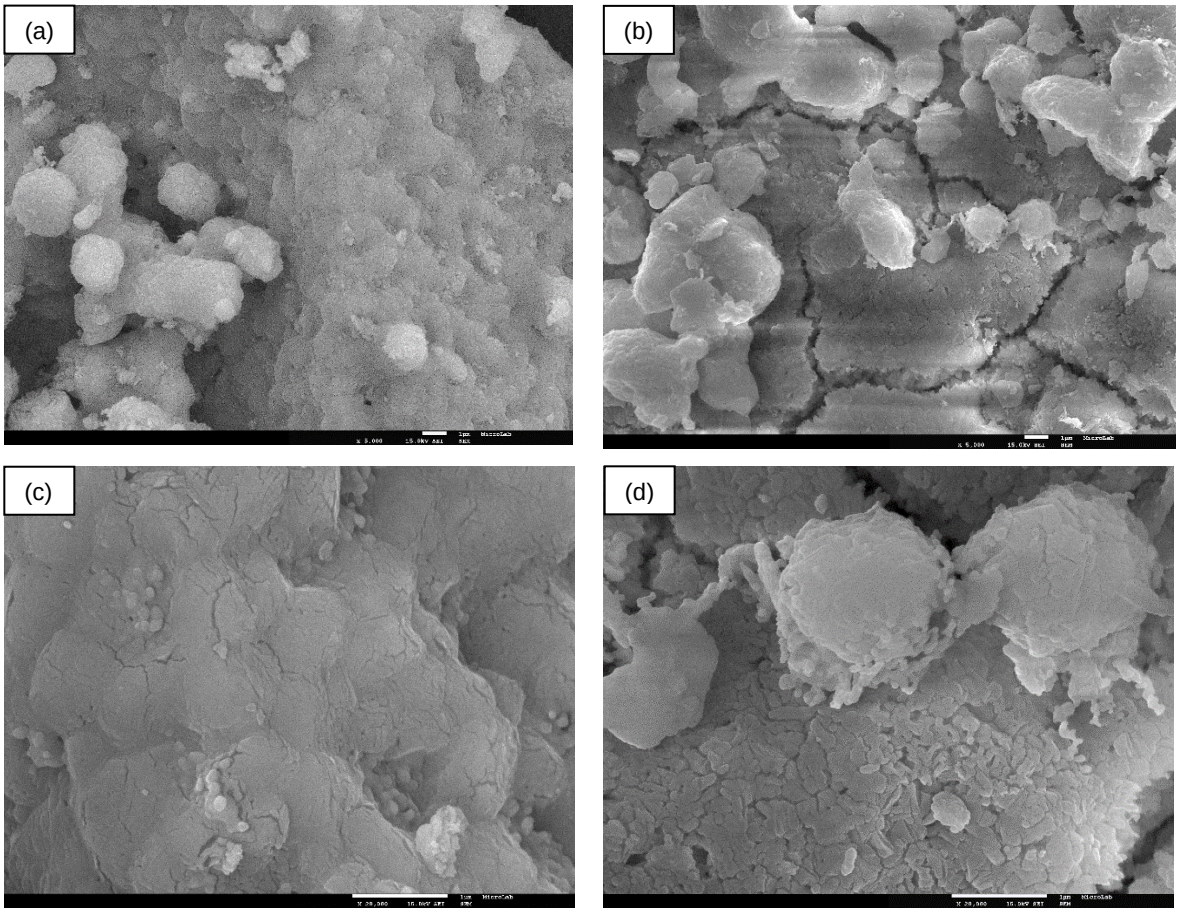

Figure 5.22: SEM micrographs for natural $CaCO_3$ sorbents after 20 Calcination-carbonation cycles, a) CO_2 calcination, b) 5 % steam (at x5000 magnification and scale: 1 µm). c) CO_2 calcination, d) 5 % steam (all at x20000 magnification and scale: 1 µm)

6. CONCLUSION

Calcium looping is an emerging technology for post-combustion CO_2 capture and it is considered as a promising technology that provides two main advantages, a highest capture capacity and a low capture cost when compared to other technologies. However, sintering of CaO-based sorbents emerged to be a huge barrier in calcium looping utilization. In this work, three CaO-precursors and two waste-derived material were used to study the improvement that these waste-derived supports can enforce on CO_2 carrying capacity and stability of CaO sorbents.

This experimental study was conducted on three units, a thermogravimetric analyzer (TGA), a fixed bed reactor unit, and an in-situ XRD equipment. Sorbent samples were prepared with two waste supporting methods, a dry physical mixing in a ball miller with three different CaO-precursor/waste-support mixing ratios, and by wet impregnation of CaO-precursor on a waste-support. TGA test consisted of 10 calcination-carbonation cycles which provided a quick look on sorbent's performance. The natural and commercial $CaCO_3$ sorbents' performance was extensively investigated on a fixed bed unit for 20 calcination-carbonation cycles under standard conditions for the unsupported and supported sorbents, and under different calcination-carbonation conditions for the natural $CaCO_3$. In-situ XRD tests were used to investigate the sintering process through 5 calcination-carbonation cycles.

TGA results showed that addition of CFA and SFCC had a similar enhanced effect on commercial $CaCO_3$, and the 1st and 10th CaO conversion values were always higher for blends with 10 % and 25% of waste derived sorbents. The highest CaO conversion was observed for the blend with 10 % of SFCC, that presented an initial CaO conversion of 96 % and after 10 cycles it was 91 %. The CaO conversion of these sorbents was also very stable, and the blend with lower deactivation was again the sample with 10% of SFCC, namely, 5% of deactivation between the 1st and 10th cycle. The sorbents with 40 % of waste showed the lowest CaO conversion values, this means that for these cases no benefits can be obtained from the anti-sintering physical barrier role of wastes on the CaO deactivation.

The $Ca(NO_3)_2.4H_2O$ sorbent, with and without waste support showed a different CaO conversion profile, i.e., a continuous increase of its reactivity was observed along the cycles, which usually is justified by the formation of a hard and internally stable skeleton. During the first cycles this skeleton hinders the carbonation due to diffusional limitations, however, due to the formation of an external (soft) and stable skeleton along the cycles, an increase of the CaO conversion is observed. This phenomenon is usually defined as thermal stabilization. The blend of $Ca(NO_3)_2.4H_2O$ precursor with 10 % of SFCC presented the highest CaO conversion, meanwhile the blend with 40 % of CFA presented the lower CaO conversion, respectively, 69 % and 40 % after 10 cycles.

In the case of natural $CaCO_3$, it was concluded that introducing an appropriate weight of sorbent and waste-support to the mixing and milling process can affect positively the CaO conversion, as seen in the case of 2 g and 10 g samples (CaO basis) preparation. As a better conversion was observed when 2 g of sorbent sample was prepared, maybe due to the higher efficiency of blend mixing and milling, the effect of adding different amounts of waste derived support was performed with this lower total sample mass. Only the test carried out with 90 % of CaO and 10 % of CFA allowed outperforming the

100 % of CaO sorbent from the first cycle until the 10th cycle, where a final conversion of 61 % was attained. The lower CaO conversion of the other blends with natural $CaCO_3$,when compared to the sorbent without wastes, means that the role of the support wastes on the anti-sintering process is less relevant for the natural sorbent than for the commercial sorbents. This can be probably justified by the presence of impurities on the natural $CaCO_3$ (e.g.SiO_2) and differences on textural and morphological properties of these sorbents.

Summing up, the performance of sorbents can be improved by introducing a waste-support, however, the weight ratio and CaO-precursors are key factors for achieving an enhancement on CO_2 capture decay resistance. On the TGA experiments, the better performance was usually obtained with the addition of 10 % of SFCC, in case of commercial CaO precursors, and 10 % of CFA in case of natural $CaCO_3$.

After 20 calcination-carbonation cycles on a fixed bed reactor, the natural $CaCO_3$ sorbent with 100 % of CaO had a CaO conversion value of 28 %, the addition of 10 % of CFA imposed an enhancement that increased that CaO conversion rate to 37 %, while the addition of 10 % of SFCC had improved the CaO conversion up to 32 %. The commercial $CaCO_3$ showed the highest improvement of CaO conversion with the addition of waste supports. Comparatively with the sorbent without waste support, an enhancement of 21 % and 14 % on CaO conversion values was observed for the 10 % of CFA and 10 % of SFCC blends, respectively, after the 20 carbonation-calcination cycles.

Textural properties characterization also confirmed the positive effect of wastes addition on the S_{BET} values, between the sorbent activation (0 cy) and the 20 cycles, the reduction of the commercial and natural sorbents' S_{BET} was 41 % and 68 % respectively. For the waste blended sorbents, the S_{BET} reduction was decreased, it was respectively, 34 % and 29 % for commercial $CaCO_3$ with 10 % of CFA and 10 % of SFCC, and 28 % and 43 % for the natural $CaCO_3$ with 10 % of CFA and 10 % of SFCC. The lowest reduction on the S_{BET} values was observed for the blend with 90 % of CaO (natural $CaCO_3$ precursor) and 10 % of CFA, namely, from 21.1 m^2/g (0 cy) to 15.2 m^2/g (20 cy).

The use of dry physical mixed sorbents proved to present a better CO_2 capture performance than that obtained in the case of the sorbents prepared by wet impregnation. Possibly wet impregnation requires increasing waste-support to CaO-precursor ratio to have a more effective impregnation, but this reduces the amount of active CaO available for CO_2 capture during the Ca-looping, which can imply the use of high amounts of sorbents during the Ca-looping, with practical and economical negative implications on this technology implementation on industry.

Experiments conducted under different atmospheres were chosen to simulate the flue gas composition of cement industry (e.g. 25 % of CO_2 and steam atmosphere) and obtain a pure CO_2 stream adequate for storage or for practical applications in industry (e.g. CO_2 calcination atmosphere). By changing the calcination atmosphere from pure air to pure CO_2 the sorbent deactivation escalated further as the CO_2 presence in atmosphere will delay the decomposition of $CaCO_3$ until sorbent reaches the calcination temperature (i.e. 900 °C) and thus sintering would further agglomerate the sorbent particles ($CaCO_3$ has a lower Tammann temperature than the CaO). The adverse effect of CO_2 atmosphere started from the pre-calcination were sorbent had lower S_{BET} in comparison with sorbent tested under standard

conditions (31 m^2/g vs 25 m^2/g), this was also confirmed by the higher growth of average crystallite sizes obtained from CO_2 calcined sorbent (24 nm vs 33 nm). After 20 cycles the S_{BET} decrease was 68 % and 72 % for standard conditions and CO_2 calcination, respectively. Meanwhile, the average crystallite size increase was 72 % and 82 % for sorbents tested under standard conditions and calcined with CO_2, respectively.

Addition of steam into calcination and carbonation cycles resulted in a positive stability after 20 cycles, where the CaO conversion of sorbent with steam was higher than the value obtained under standard conditions (36 % vs 28 % of CaO conversion). However, the sorbent tested with steam presented a lower CaO conversion, for the 1st cycle, the conversion was only 64 % and under standard conditions, it was 86 %. The lower initial carrying capacity of sorbents was observed because the steam increases the sintering during calcination, shifting towards larger pores, which is related with the higher thermal conductivity and heat capacity of steam comparatively with air. However, along the cycles the presence of steam on the carbonation reduces the diffusion resistance through the carbonate layer, and small pores are generated, which increase the CaO conversion of sorbent. The textural properties, S_{BET} and the pore size distribution for 0 and 20 cycles confirmed the above explanations. Therefore, the steam atmosphere contributes to waste blended sorbents stabilization, and the deactivation between the 1st and 20th cycle was only 43 % (under standard conditions the deactivation was 67 %).

Due to economic and environmental issues, the natural $CaCO_3$ appears to be the most relevant sorbent for industrial applications. It was verified that the amount of waste derived support added, and the presence of steam are key parameters to increase the sorbent CaO conversion and stability. The possibility of adding CaO spent sorbents; even after the addition of waste derived supports, to the cement production is also an important advantage. The industrial applicability of this study is already promising and should benefit of performing additional studies evaluating the synergetic effects (e.g. steam addition, under CO_2 calcination atmospheres of blended sorbents with waste derived supports).

7. FUTURE WORK

Work conducted in future in the scope of this project may undertake following points into consideration:

- Study behavior of sorbents using different milling and mixing techniques taking into consideration the ball miller to sample weight ratio

- Sorbent blends with waste-derived support should be tested with CO_2 calcination and steam addition

- Other natural sorbents like dolomite and WMP, can be investigated with waste support

8. REFERENCES

[1] H. Ritchie and M. Roser, “Energy Production & Changing Energy Sources,” *OurWorldInData.org*, 2018. [Online]. Available: https://ourworldindata.org/energy-production-and-changing-energy-sources. [Accessed: 12-Sep-2018].

[2] “KP Introduction | UNFCCC.” [Online]. Available: https://unfccc.int/process/the-kyoto-protocol. [Accessed: 12-Sep-2018].

[3] “Kyoto Protocol to the United Nations Framework Convention on Climate Change,” *Rev. Eur. Community Int. Environ. Law*, vol. 7, no. 2, pp. 214–217, 1998.

[4] “International agreements on climate action - Consilium.” [Online]. Available: http://www.consilium.europa.eu/en/policies/climate-change/international-agreements-climate-action/. [Accessed: 12-Sep-2018].

[5] “Paris Agreement on climate change - Consilium.” [Online]. Available: http://www.consilium.europa.eu/en/policies/climate-change/timeline/. [Accessed: 12-Sep-2018].

[6] L. Vinet and A. Zhedanov, “Climate Change 2014: Synthesis Report,” *Nature*, vol. 446, no. 7137, pp. 727–8, 2010.

[7] D. Reay, C. Sabine, P. Smith, and G. Hymus, “Climate Change 2014: Mitigation of Climate Change,” *Nature*, vol. 446, no. 7137, pp. 727–8, 2007.

[8] H. Ritchie and M. Roser, “CO_2 and other Greenhouse Gas Emissions,” *OurWorldInData.org*, 2018. [Online]. Available: http://linkinghub.elsevier.com/retrieve/pii/S0301421511007385. [Accessed: 13-Sep-2018].

[9] J. Gale *et al.*, “Sources of CO_2” *IPCC Spec. Rep. Carbon Dioxide Capture Storage*, pp. 77–103, 2005.

[10] I. E. A. IEA, “Energy Technology Perspectives - Mobilising Innovation to Accelerate Climate Action,” *IEA (International Energy Agency)*, p. 412, 2015.

[11] P. Folger, "*Carbon Capture and Sequestration (CCS) in the United States"*, 2018. [Online]. Available: https://fas.org/sgp/crs/misc/R44902.pdf. [Accessed: 19-Sep-2018].

[12] K. Thambimuthu, M. Soltanieh, and J. C. Abanades, “Capture of CO_2” *IPCC Spec. Rep. Carbon dioxide Capture Storage*, pp. 105–178, 2005.

[13] D. Jansen, M. Gazzani, G. Manzolini, E. van Dijk, and M. Carbo, “Pre-combustion CO_2 capture,” *Int. J. Greenh. Gas Control*, vol. 40, pp. 167–187, 2015.

[14] E. Maron Thorbergsson, “THESIS FOR THE DEGREE OF DOCTOR OF PHILOSOPHY IN THERMO AND FLUID DYNAMICS Oxy-Fuel Combustion Combined Cycles for Carbon Capture”, 2015.

[15] K. Yoro and P. Sekoai, “The Potential of CO_2 Capture and Storage Technology in South Africa’s Coal-Fired Thermal Power Plants,” *Environments*, vol. 3, no. 4, p. 24, 2016.

[16] P. C. Chiang and S. Y. Pan, “Carbon dioxide mineralization and utilization,” in *Carbon Dioxide Mineralization and Utilization*, Singapore: Springer Singapore, pp. 9–34, 2017.

[17] L. Baxter, A. Baxter, and S. Burt, “Cryogenic CO_2 Capture as a Cost-Effective CO_2 Capture Process,” no. c, 2009.

[18] “Separation of gases / liquids | Fujifilm Global.” [Online]. Available: http://www.fujifilm.com/innovation/technologies/separation-of-gases-or-liquids/. [Accessed: 20-Sep-2018].

[19] P. Fennell, “Calcium and chemical looping technology: An introduction,” *Calcium Chem. Looping Technol. Power Gener. Carbon Dioxide Capture*, pp. 3–14, 2015.

[20] M. Erans, V. Manovic, and E. J. Anthony, “Calcium looping sorbents for CO_2 capture,” *Appl. Energy*, vol. 180, pp. 722–742, 2016.

[21] M. Broda, A. M. Kierzkowska, and C. R. Müller, “Synthetic calcium oxide-based carbon dioxide sorbents for calcium looping processes,” in *Calcium and Chemical Looping Technology for Power Generation and Carbon Dioxide (CO_2) Capture*, 2015, pp. 51–72.

[22] A. Bosoaga, O. Masek, and J. E. Oakey, “CO_2 Capture Technologies for Cement Industry,” *Energy Procedia*, vol. 1, no. 1, pp. 133–140, 2009.

[23] S. D. Kenarsari and Y. Zheng, “CO_2 capture using calcium oxide under biomass gasification conditions,” *J. CO_2 Util.*, vol. 9, pp. 1–7, 2015.

[24] M. Broda and C. R. Müller, “Synthesis of highly efficient, Ca-based, Al_2O_3-stabilized, carbon gel-templated CO_2 sorbents,” *Adv. Mater.*, vol. 24, no. 22, pp. 3059–3064, 2012.

[25] E. T. Santos, C. Alfonsín , A.J.S. Chambel, A. Fernandes, A.P. Soares Dias, C.I.C. Pinheiro, M.F. Ribeiro, “Investigation of a stable synthetic sol-gel CaO sorbent for CO_2 capture,” *Fuel*, vol. 94, pp. 624–628, 2012.

[26] P. S. Fennell, R. Pacciani, J. S. Dennis, J. F. Davidson, and A. N. Hayhurst, “The effects of repeated cycles of calcination and carbonation on a variety of different limestones, as measured in a hot fluidized bed of sand,” *Energy and Fuels*, vol. 21, no. 4, pp. 2072–2081, 2007.

[27] A. I. Lysikov, A. N. Salanov, and A. G. Okunev, “Change of CO_2 carrying capacity of CaO in isothermal recarbonation-decomposition cycles,” *Ind. Eng. Chem. Res.*, vol. 46, no. 13, pp. 4633–4638, 2007.

[28] R. Barker, “The reversibility of the reaction $CaCO_3 \rightleftarrows CaO+CO_2$” *J. Appl. Chem. Biotechnol.*, vol. 23, no. 10, pp. 733–742, 2007.

[29] F. C. Yu, N. Phalak, Z. Sun, and L. S. Fan, “Activation strategies for calcium-based sorbents for CO 2 capture: A perspective,” *Ind. Eng. Chem. Res.*, vol. 51, no. 4, pp. 2133–2142, 2012.

[30] R. W. Hughes, D. Lu, E. J. Anthony, and Y. Wu, “Improved Long-Term Conversion of Limestone-Derived Sorbents for In Situ Capture of CO_2 in a Fluidized Bed Combustor,” *Ind. Eng. Chem. Res.*, vol. 43, no. 18, pp. 5529–5539, 2004.

[31] J. Blamey, J. G. Yao, Y. Arai, and P. Fennell, “Enhancement of natural limestone sorbents for calcium looping processes,” in *Calcium and Chemical Looping Technology for Power Generation and Carbon Dioxide (CO_2) Capture*, Elsevier, pp. 73–105, 2015.

[32] L. Jia, J. Wang, and E. J. Anthony, “Reactivation of fluidised bed combustor ash for sulphur capture,” *Chem. Eng. J.*, vol. 94, no. 2, pp. 147–154, 2003.

[33] V. Manovic and E. J. Anthony, “Reactivation and remaking of calcium aluminate pellets for CO_2 capture,” *Fuel*, vol. 90, no. 1, pp. 233–239, 2011.

[34] V. Manovic, Y. Wu, I. He, and E. J. Anthony, “Spray water reactivation/pelletization of spent CaO-based sorbent from calcium looping cycles,” *Environ. Sci. Technol.*, vol. 46, no. 22, pp. 12720–12725, 2012.

[35] C. Salvador, D. Lu, E. J. Anthony, and J. C. Abanades, “Enhancement of CaO for CO_2 capture in an FBC environment,” *Chem. Eng. J.*, vol. 96, no. 1–3, pp. 187–195, 2003.

[36] B. González, J. Blamey, M. McBride-Wright, N. Carter, D. Dugwell, P. Fennell, J. C. Abanades, “Calcium looping for CO_2 capture: Sorbent enhancement through doping,” *Energy Procedia*, vol. 4, pp. 402–409, 2011.

[37] B. González, J. Blamey, M. J. Al-Jeboori, N. H. Florin, P. T. Clough, and P. S. Fennell, “Additive effects of steam addition and HBr doping for CaO-based sorbents for CO_2 capture,” *Chem. Eng. Process. Process Intensif.*, vol. 103, pp. 21–26, 2016.

[38] V. Manovic and E. J. Anthony, “Thermal activation of CaO-based sorbent and self-reactivation during CO2capture looping cycles,” *Environ. Sci. Technol.*, vol. 42, no. 11, pp. 4170–4174, 2008.

[39] V. Manovic and E. J. Anthony, “Lime-based sorbents for high-temperature CO_2 capture - a review of sorbent modification methods,” *Int. J. Environ. Res. Public Health*, vol. 7, no. 8, pp. 3129–3140, 2010.

[40] V. Manovic and E. J. Anthony, “Competition of sulphation and carbonation reactions during looping cycles for CO_2 capture by cao-based sorbents,” *J. Phys. Chem. A*, vol. 114, no. 11, pp. 3997–4002, 2010.

[41] P. Sun, J. R. Grace, C. J. Lim, and E. J. Anthony, “Co-capture of H_2S and CO_2 in a pressurized-gasifier-based process,” *Energy & Fuels*, vol. 21, no. 7, pp. 836–844, 2007.

[42] F. Donat, N. H. Florin, E. J. Anthony, and P. S. Fennell, “Influence of high-temperature steam on the reactivity of CaO sorbent for CO_2 capture,” *Environ. Sci. Technol.*, vol. 46, no. 2, pp. 1262–1269, 2012.

[43] M. H. Chang, W. C. Chen, C. M. Huang, W. H. Liu, Y. C. Chou, W. C. Chang, W. Chen, J. Y. Cheng, K. E. Huang, H. W. Hsu, “Design and Experimental Testing of a 1.9 MWth Calcium Looping Pilot Plant,” *Energy Procedia*, vol. 63, pp. 2100–2108, 2014.

[44] A. Sánchez-Biezma, L. Diaz, J. López, B. Arias, J. Paniagua, M.Lorenzo, J. Álvarez, J.C. Abanades, “CaOling Project-Scope and Overview CaOling Project-First experiences on the 1.7 MWt calcium looping pilot in La Pereda.” [Online]. Available: http://oxyfbc.eu-projects.de/Portals/29/OxyFBC/11_Biezma-2nd International Workshop on OXYCFB Stuttgart-CaOling Project - First experiences on the 1,7MWt calcium looping pilot in La Pereda.pdf. [Accessed: 24-Sep-2018]

[45] “Experimental facilities – FlexiCal.” [Online]. Available: https://www.flexical.eu/experimental-facilities/. [Accessed: 24-Sep-2018].

[46] M. Hornberger, R. Spörl, and G. Scheffknecht, “Calcium Looping for CO_2 Capture in Cement Plants - Pilot Scale Test,” *Energy Procedia*, vol. 114, no. November 2016, pp. 6171–6174, 2017.

[47] M. Ahmaruzzaman, “A review on the utilization of fly ash,” *Prog. Energy Combust. Sci.*, vol. 36, no. 3, pp. 327–363, 2010.

[48] F. Yan, J. Jiang, K. Li, S. Tian, M. Zhao, and X. Chen, “Performance of Coal Fly Ash Stabilized, CaO-based Sorbents under Different Carbonation-Calcination Conditions,” *ACS Sustain. Chem. Eng.*, vol. 3, no. 9, pp. 2092–2099, 2015.

[49] J. Monzó, J; Payá, J; Borrachero, M.V.; Velásquez, S; Soriano, L; Serna, P; Rigueira, “Reusing of Spent FCC Catalyst as a very Reactive Pozzolanic Material: Formulation of High Performance Concretes,” *Int. RILEM Conf. Use Recycl. Mater. Build. Struct.*, no. 3, 2004.

[50] K. Al-Jabri, M. Baawain, R. Taha, Z. S. Al-Kamyani, K. Al-Shamsi, and A. Ishtieh, “Potential use of FCC spent catalyst as partial replacement of cement or sand in cement mortars,” *Constr. Build. Mater.*, vol. 39, pp. 77–81, 2013.

[51] T. Lever, P. Haines, J. Rouquerol, E. L. Charsley, P. V. Eckeren, and D. J. Burlett, “ICTAC nomenclature of thermal analysis (IUPAC Recommendations 2014),” vol. 86, no. 4, pp. 545–553, 2014.

[52] J. G. Dunn, “Thermogravimetry,” in *Characterization of Materials*, John Wiley & Sons, Inc., 2002, pp. 1–21.

[53] K. Sing, “The use of nitrogen adsorption for the characterisation of porous materials,” *Colloids Surfaces A Physicochem. Eng. Asp.*, vol. 187–188, pp. 3–9, 2001.

[54] M. Thommes, K. Kaneko, A. V. Neimark, J. P. Olivier, F. Rodriguez-Reinoso, J. Rouquerol, and K. S.W. Sing, “Physisorption of gases, with special reference to the evaluation of surface area and pore size distribution (IUPAC Technical Report),” *Pure Appl. Chem.*, vol. 87, no. 9–10, pp. 1051–1069, 2015.

[55] B. L. Dutrow, “X-ray Powder Diffraction (XRD).” [Online]. Available: https://serc.carleton.edu/research_education/geochemsheets/techniques/XRD.html. [Accessed: 07-Sep-2018].

[56] “Scherrer equation — EURL ECVAM.” [Online]. Available: https://eurl-ecvam.jrc.ec.europa.eu/glossary/glossary/scherrer-equation. [Accessed: 07-Sep-2018].

[57] S. Swapp, “Scanning Electron Microscopy (SEM).” [Online]. Available: https://serc.carleton.edu/research_education/geochemsheets/techniques/SEM.html. [Accessed: 07-Sep-2018].

[58] C. I. C. Pinheiro, A. Fernandes, C. Freitas, E. T. Santos, and M. F. Ribeiro, “Waste Marble Powders as Promising Inexpensive Natural CaO-Based Sorbents for Post-Combustion CO_2 Capture,” *Ind. Eng. Chem. Res.*, vol. 55, no. 29, pp. 7860–7872, 2016.

[59] M. Dapiaggi, G. Artioli, and L. Petras, “A newly Developed High-Temperature Chamber for in Situ X-Ray Diffraction : Setup and Calibration Procedures,” *Rigaku J.*, vol. 19, no. 1, pp. 35–41, 2002.

[60] J. M. Fox, “Changes in Fly Ash With Thermal Treatment,” *2005 WorldofCoal Ash (WOCA), April 11-15, Lexington, Kentucky,USA*, pp. 1–15, 2005.

[61] N. Koshy and D. N. Singh, “Textural Alterations in Coal Fly Ash due to Alkali Activation,” *J. Mater. Civ. Eng.*, vol. 28, no. 11, p. 04016126-1 - 7, 2016.

[62] Z. T. Ahmed, “the Quantification of the Fly Ash Adsorption Capacity for the Purpose of Characterization and,” 2012.

[63] M. Broda, R. Pacciani, and C. R. Müller, “CO_2 Capture via Cyclic Calcination and Carbonation Reactions,” in *Porous Materials for Carbon Dioxide Capture*, pp. 181–222, 2014.

[64] D. He, C. Qin, V. Manovic, J. Ran, and B. Feng, “Study on the interaction between CaO-based sorbents and coal ash in calcium looping process,” *Fuel Process. Technol.*, vol. 156, pp. 339–347, 2017.

[65] B. Pacewska, I. Wilińska, M. Bukowska, G. Blonkowski, and W. Nocuń-Wczelik, “An attempt to improve the pozzolanic activity of waste aluminosilicate catalyst,” *J. Therm. Anal. Calorim.*, vol. 77, no. 1, pp. 133–142, 2004.

[66] V. Manovic and E. J. Anthony, “Carbonation of CaO-based sorbents enhanced by steam addition,” *Ind. Eng. Chem. Res.*, vol. 49, no. 19, pp. 9105–9110, 2010.